

PUBLISHER

On Behalf of Textile and Apparel Research Application Center
Faruk BOZDOĞAN

EDITOR IN CHIEF

Arif Taner ÖZGÜNEY
arif.taner.ozguney@ege.edu.tr

ASSOCIATE EDITORS

Mehmet KÜÇÜK
mehmet.kucuk@ege.edu.tr
Pelin SEÇİM KARAKAYA
pelinsecim@mail.ege.edu.tr

EDITORIAL BOARD

Ahmet ÇAY
Esen ÖZDOĞAN
Gözde ERTEKİN
Nilgün ÖZDİL

SCIENTIFIC ADVISORY BOARD

Andrej DEMŞAR
Arzu MARMARALI
Bojana VONÇINA
Bülent ÖZİPEK
E. Perrin AKÇAKOCA KUMBASAR
Ender BULGUN
Hüseyin KADOĞLU
Mirela BLAGA
Oktay PAMUK
Ozan AVİNÇ
Peter J. HAUSER
Recep EREN
Rıza ATAV
Savvas G. VASSILIADIS
Turan ATILGAN

ABSTRACTING / INDEXING

Science Citation Index Expanded (SCIE)
Scopus
WOS
EBSCO
TR Dizin
Ulakbilim

TYPESETTING AND PRINTING

Designed by: İ. Buhur ismailbuhur@hotmail.com

META Basım Matbaacılık Hizmetleri
+90 232 343 64 54 / E-mail: metabasim@gmail.com
Printed Date: September, 2019

An Analysis of the Sustainability Disclosures of Textile and Apparel Companies in Turkey

Ebru Saygili, Arikán Tarık Saygili, Seher Goren Yargı 189

Analyzing Some of the Dual-Core Yarn Spinning Parameters on Yarn and Various Fabric Properties

Sevim Hümeyra Çelikkan Aydoğdu, Demet Yılmaz 197

Hazard and Risk Analysis for Ring Spinning Yarn Production Process by Integrated FTA-FMEA Approach

Nazlı Güllüm Mutlu, Serkan Altuntaş 208

Physical, Chemical, Morphological and Thermal Characterisation of Natural Fibers for Sound Absorption

J Niresh, Archana N, Karthik T, Tan Wei Hong 219

Cellulose Monoacetate/Nafion (CMA/N) Hybrid Nanofibers as Interface for Electrochemical DNA Biosensors

Ayse Bostancı, Nilay Aladag Tanik, Yakup Aykut 228

The Performance Analysis of Geotextile Materials Used for Irrigation Water and Weed Control in Stone Garden Landscape Design

Handan Çakar, Özlem Akat Saraçoğlu, Cenk Ceyhun Kılıç, Hülya Akat, Önder Yücel 236

Structural Investigation of UV Aged Tent Fabrics

Emrah Temel, Faruk Bozdoğan, Deniz Mizmizlioğlu 246

Increasing the Process Cycle Efficiency of Men's Trousers Assembly Line

Duygu Selen Kansul, Gülsen Karabay 253

Development of Tubular Woven Preform Reinforced Composite Pipe and Comparison of its Compression Behavior with Filament Wound Composite

Gulsah Pamuk, Ugur Kemiklioglu, Onur Sayman 262

An Image Processing Research Consistent with Standard Photographs to Determine Pilling Grade of Woven Fabrics

Abdurrahman Telli 268

CONTACT

Ege Üniversitesi Tekstil ve Konfeksiyon Araştırma-Uygulama Merkezi
35100 Bornova – İzmir, TÜRKİYE
Tel: +90 232 311 38 89-83

www.dergipark.gov.tr/tekstilvekonfeksiyon
E-mail: teknikonfeksiyon@mail.ege.edu.tr



An Analysis of the Sustainability Disclosures of Textile and Apparel Companies in Turkey

Ebru Saygili¹, Arikán Tarık Saygili², Seher Goren Yargı¹

¹Yasar University, Faculty of Business, Department of International Trade and Finance, 35100 Bornova, Izmir, Turkey

²Izmir University of Economics, Department of Business Administration, 35530 Balcova, Izmir, Turkey

Corresponding Author: Ebru Saygili, ebru.esendemir@yaras.edu.tr

ABSTRACT

The aim of this study is to discuss recent sustainability developments in the textile industry and to explore the disclosures of textile and apparel companies in Turkey. The economic, environmental and social sustainability disclosures of 34 companies were analyzed in relation to Global Reporting Initiative (GRI) standards. The results of the analysis revealed that the most frequently mentioned sustainability issues were related to employees, water, product, market, supplier, education, economic, energy and waste. A majority of companies provided economic disclosures about economic performance and anti-competition; environmental disclosures about water and effluents and energy; and social sustainability disclosures about training, education, employment, health and safety, diversity and equal opportunity, marketing and labeling.

ARTICLE HISTORY

Received: 16.10.2018

Accepted: 30.04.2019

KEYWORDS

Textile and apparel industry, sustainability disclosures, economic sustainability, environmental sustainability, social sustainability, GRI

1. INTRODUCTION

Global warming and other climate changes alongside rising scarcity of natural resources due to increasing population, mass production and consumption needs have promoted more prominent sustainability practices in the textile and apparel industry as it has had in other sectors. Additionally, sensitivity and the demands of an increasing number of environmentally conscious consumers in markets can be expected to significantly affect sustainability applications. Realizing the importance of sustainability Turkish Clothing Manufacturers published Ufuk 2030 in April 2016 in order to inform and guide companies in Turkish textile and apparel industry. Some of these foreseeable effects of sustainability, for textile and apparel manufacturers, can be summarized briefly under five main categories: raw materials, production, supply chain, standards, and regulations and brands [1].

i. Raw Materials: Textile manufacturers prefer natural raw materials, such as cotton and linen, as they are considered healthier. However, obtaining them requires the consumption of precious natural resources, such as water. Global irrigation of cotton fields consumes approximately 2.6% of the Earth's annual water resources, which significantly increases the risk of drought, especially in Central Asia. Additionally, artificial fertilizers and pesticides have long-lasting harmful effects on the environment. Therefore, the Better Cotton Standard has been developed for more responsible farming, including every step in cotton production, from sowing and growing to picking and harvesting [2]. This standard is used by various international brands in their supply chains, including Adidas, H&M, IKEA, Levi Strauss & Co., M&S and Nike. Accordingly, the use of cotton in the textile industry is expected to drop to 18.5% in 2030 from 38% in 2008 whereas the share of polyester is expected to rise to 61% in 2030 from 36.6% in 2008 [1].

To cite this article: Saygili E, Saygili, AT, Yargı SG. 2019. An analysis of the sustainability disclosures of textile and apparel companies in Turkey *Tekstil ve Konfeksiyon* 29(3), 189-196.

ii. Production: Many chemicals are used throughout the textile manufacturing process. Natural raw materials and products require washing before, during and/or at the end of the production cycle, which cause significant unproductive water consumption and significant amounts of effluent water. Manufactured fibers use less water, although they produce greater greenhouse gas emissions [3]. Moreover, manufactured fibers are recyclable, which can reduce the unproductive consumption of natural resources and significantly reduce industrial waste. Sustainability concerns and practices have also shifted scientific studies and technology for the textile and apparel industry [4]. Authorities in the textile and apparel industry globally are striving to create a new foundation by increasing competitiveness and efficiency in operational activities, including resource utilization, as well as by promoting social and environmental consciousness. As a result, changes are expected in consumer preferences towards more environment-friendly renewable and recyclable products. Fibers and fabric recycling can be used in numerous applications, such as soil reinforcement, filtration systems, compositing, acoustics and building insulation [5]. Fashion authorities and society in general are expected to demand a slower pace in fashion trends in the future in order to promote longer use of products and second-hand product consumption. Clothes are being reused in a growing number of ways, such as repurposing as fancy dress or dusters, selling, exchanging and donating [5].

iii. Supply Chain: Working with local suppliers when possible is expected to be one of the most important factors in supplier selection as it offers several benefits. Firstly, it minimizes transportation distances, which decreases carbon emissions. Secondly, it is easier to obtain improved transparency and monitoring practices in supplier relations. Nevertheless, geographical distance is not the only factor to consider while selecting supplies. First, the required supplies may not be available from local suppliers or they may not be sufficiently sensitive about sustainability practices and/or eager to adopt them. Second, the prices offered by local suppliers may not be favorable and compromised solely for the purpose of sustainability. Finally, building sustainable relationships that promote transparency and continuous cooperation may not be possible with local suppliers. However, it is possible to integrate operations through current information technology in order to improve mutual transparency and control applications with suppliers. Thus, the Sustainable Apparel Coalition, a cross-brand initiative, developed its Higg Index for evaluating fiber and fabric efficiency, and improve supply chain performance industry-wide [4, 6]. Applying the most suitable approaches when working with suppliers worldwide, such as preferring rail transportation over alternatives whenever possible, can contribute both to more efficient resource use and to further improvements in operational efficiency and reduced carbon emissions.

iv. Standards and Regulations: The number and scope of standards and regulations aiming to enhance sustainability practices has been increasing continuously. As people become more knowledgeable, they become more sensitive and environmentally conscious while legal authorities, foreseeing the consequences of socially and environmentally irresponsible behavior, continue to set more and stricter standards, and expand the scope of relevant laws and regulations. Standards and regulations, especially in the areas of worker and workplace safety, energy consumption, carbon emissions and waste management, are expected to become critical for sustainability in the textile industry, as in other sectors.

v. Brands: Textile and apparel retailers play very important roles due to their ability to create and improve consumer awareness of sustainability, and to influence their opinions and preferences [7, 8]. In their future sustainability practices, companies aiming at greater brand recognition and customer loyalty are expected to act with great responsibility to promote these practices in the following areas:

- Manufacturing and servicing cycles
- Selection of suppliers and raw materials
- Design of product and production processes
- Worker and work place safety
- Social and environmental consciousness
- Selection of methods for transportation, presentation/ packaging and sale of products
- Monitoring consumption and promoting recycling/ renewing practices of both raw material and products

This study discusses recent sustainability trends in textiles by analyzing the economic, environmental and social sustainability disclosures of textile and apparel companies in Turkey. Specifically, the economic, environmental and social sustainability disclosures of 34 companies were analyzed in relation to the Global Reporting Initiative (GRI) using content analysis.

2. LITERATURE REVIEW

The most widely-used definition of sustainable development is that introduced by the World Commission on Environment and Development (1987) as “development that meets the needs of the present without compromising the ability of future generations to meet their own needs” [9]. Previous studies of the textile industry in Turkey have included sustainable textile production [10], and waste management and recycling [11-13]. According to Eser et al. [12], sustainability practices in fashion should consider product life cycle designs with creative ideas and applications in the areas of product design, production, logistics, retailing, usage and recycling. Accordingly,

product life cycle design is favored in sustainability applications rather than product design. Furthermore, to achieve sustainability in the textile industry, efforts should focus on 3R and 4R concepts, whereby 4R adds *rebuy to reuse, reduce and recycle*, as previously suggested by the 3R approach. 4R emphasizes the importance of rebuying products already produced by reusable and/or recyclable material. Ar and Tokol [14] claim that well-organized and successfully-applied environmental and social sustainability practices generate greater benefits, such as increased operational efficiency and profitability, improved perceptions of company image, corporate trust, brand and customer loyalty in the market, increased ability to recruit better-qualified staff, improved employee satisfaction and organizational commitment, improved shareholder satisfaction, and generating more diverse and favorable financing alternatives. Despite these advantages, Kusku [15] found that Turkish textile companies do not generally seem to have an organizational structure for conducting environmental social sustainability activities. Instead, because they perceive environmental sustainability activities as cost-raising factors, they conduct them through quality coordination departments.

Since the 1990s, a growing number of companies have issued voluntary sustainability disclosures, including those in the textile and apparel industry [16, 17]. These disclosures address issues concerning the economic, environmental and social dimensions of corporate performance [18, 19]. Kamal and Deagan [16], for example, found increasing disclosure of social and environmental governance information in Bangladesh's textile and garment companies' annual reports from 1996 to 2009. They argued that the reason for this increase was to satisfy powerful stakeholders, such as global textile and clothing companies. Kozlowski et al. [17] identified reported indicators in corporate sustainability reports, other documents and web sites of 14 apparel brands belonging to the Sustainable Apparel Coalition (SAC).

The Global Reporting Initiative's (GRI) sustainability reporting guidelines [20], developed through the involvement of multiple stakeholders, appear to be the most widely accepted and influential among companies globally [21]. GRI standards aim to create a common language for organizations and stakeholders regarding economics, environmental and social issues. Various researchers have investigated the GRI sustainability indicators disclosed by different industries [22] across countries including Canada [19], Netherlands [23], Spain [24] and Greece [25]. They found several trends in the results. Overall, for instance, economic indicators focusing on financial issues, environmental indicators focusing on energy and water, social indicators focusing on labor practices were widely reported [19]. Furthermore, the indicators reported, and their frequency varied across industries. The present study provides one of the first analyses of the GRI indicators used

in corporate sustainability reports in the textile and apparel industry in Turkey.

3. MATERIAL AND METHOD

This study analyzes the sustainability performance of the Turkish textile and apparel industry in terms of the GRI sustainability indicators. The research question investigated is: "What GRI sustainability indicators are currently being disclosed by Turkish textile and apparel companies in Turkey?" The disclosures of the companies were analyzed using content analysis, which has been widely used in previous studies investigating sustainability reports [16, 17, 19, 23]. The analysis is based on determining the presence or absence of particular information in a given subject [23, 26]. The intent of the analysis here was to identify all the GRI sustainability indicators reported by companies. The sample was chosen from textile and apparel companies listed in Turkey's Top 500 Industrial Enterprises 2017 Survey [27] and Borsa Istanbul Textile and Leather Index – XTEKS [28]. Among 184 textile and apparel companies, 34 (18%) issued sustainability disclosures. Data was collected from recent disclosures in the companies' sustainability reports, corporate social responsibility (CSR) reports, annual reports and corporate websites, as summarized in Table 1.

Table 1. Distribution of sustainability disclosure types from Turkish textile and apparel companies

Sources of sustainability disclosures	No. of companies
Sustainability reports	9
Corporate social responsibility reports	1
Annual reports	12
Websites	12
Total	34

Table 2 presents the breakdown of the international standards used by the selected companies. A majority use ISO as their quality certificate, followed by GRI and OEKO-TEX, while 16 companies adopted the GRI sustainability standards.

Table 2. International quality certificates and standards adopted by Turkish textile and apparel companies*

International quality certificate and standard	No. of companies
ISO	24
GRI	16
OEKO-TEX	13
OHSAS	11
GOTS	6
USTER	2
BELCORO	2
CERES	1
ISPA	1
LEED	1
GLOBAL GAP CERTIFICATE	1

* Descriptions of the abbreviations are given in Appendix 1.

To provide a basis for the content analysis, keywords were identified from GRI topic-specific standards related to economic, social and environment issues. The frequency counts of keywords and frequency analysis, shown in Table 3, were collected using dictionary-based NVivo software, thereby eliminating errors from multiple inputs of the data [29]. The content analysis was conducted according to issues highlighted by Burla et al. [30] and Elo et al. [31] to improve the reliability of the analysis. The limitation of this study is that it focuses on the sustainability disclosures of the companies. Further studies including surveys and case analysis can be conducted to explore the sustainability practices of textile and apparel companies in Turkey.

4. RESULTS AND DISCUSSION

This section discusses the results from the content analysis of the sustainability disclosures of textile and apparel companies. The first part of the research determined the GRI topic-specific standards, related keywords and phrases. The frequency results of the keywords and phrases are reported in the last column of Table 3. The italicized words represent more general and comprehensive concepts related to GRI standards. There were 6 topic-specific standards related to economic issues, 8 topic-specific standards related to environmental issues and 19 topic-specific standards related to social issues. According to the results, general and comprehensive keywords (italic words) were more frequent than topic-specific keywords. For instance, the frequency of employee was 7, which means it was repeated more than 1,500 times while the frequency of

water was 5 (repeated between 1,000 and 1,249 times). The frequencies of employee right / benefits, and customer and product were 4 (repeated between 750 and 999 times). The frequencies of market, supplier and education were 3 (repeated between 500 and 749 times). The frequencies of economic, energy, waste, community and public were 2 (repeated between 250 and 499 times). The frequencies of other keywords and phrases included in the analysis were 1 (repeated between 0 and 249 times).

The second part of the research analyzed the percentages of companies disclosing GRI economic, environmental and social standards, according to the occurrences of the keywords given above. Figure 1, which presents the percentages of companies disclosing GRI economic standards, shows that a majority of the companies had sustainability disclosures about economic performance (74%) and anti-competition (65%). In contrast, only a few companies made disclosures about anti-corruption (29%). Figure 2, which presents the percentages of companies disclosing GRI environmental standards, shows that a large proportion of the companies made sustainability disclosures about water and effluents (82%) followed by energy (68%) and supplier environmental assessment (62%). However, only 12% made disclosures about environmental compliance. Figure 3, which presents the percentages of companies disclosing GRI social standards, shows that most companies made sustainability disclosures about training and education (88%), and employment (85%) while 74% made disclosures about occupational health and safety, diversity and equal opportunity, marketing and labeling. In contrast, none made disclosures about supplier social assessment and socioeconomic compliance.

Table 3. Frequency of selected issues in the sustainability disclosures of Turkish Textile and Apparel companies*

GRI Code	Topic specific standards	Frequency of GRI topic specific keywords**
GRI 201	Economic performance	<i>economic</i> (2), direct economic (1), climate (1), benefit plan (1), financial assistance (1)
GRI 202	Market presence	<i>market</i> (3), entry level wage (1), local senior manager (1)
GRI 203	Indirect economic impacts	infrastructure (1), indirect economic (1)
GRI 204	Procurement practices	local supplier (1)
GRI 205	Anti-corruption	corruption / bribery (1), anti-corruption policies, (1), incidents of corruption (1)
GRI 206	Anti-competitive behavior	<i>competition</i> (1), anti-competitive behavior (1), trust (1), monopoly (1)
GRI 301	Materials	weight/volume (1), recycled input (1), reclaimed product (1)
GRI 302	Energy	<i>energy</i> (2), internal energy consumption (1), external energy consumption (1), energy intensity (1), energy reduction (1), energy reduction of products (1)
GRI 303	Water and effluents	<i>water</i> (5), water withdrawal (1), water discharge (1), water consumption (1)
GRI 304	Biodiversity	protected area (1), impact of activities and products (1), protected habitat (1), red list species (1)
GRI 305	Emissions	Direct greenhouse gas (GHG) emissions (1), energy indirect GHG emissions (1), other indirect GHG emissions (1), GHG emission intensity (1), reduction of GHG emissions (1), emission of ozone depleting substances (1), nitrogen oxide, sulfur oxide, other airborne emissions (1)
GRI 306	Effluents and waste	<i>effluent</i> (1), <i>waste</i> (2), water discharge quality and destination (1), waste type and disposal method (1), significant spills (1), transport of hazardous waste (1), affected water bodies (1)
GRI 307	Environmental compliance	non-compliance with environmental laws and regulations (1)
GRI 308	Supplier environmental assessment	<i>supplier</i> (3), selecting new suppliers using environmental criteria (1), negative environmental impacts on supply chain (1)

Table 3. Continued

GRI Code	Topic specific standards	Frequency of GRI topic specific keywords**
GRI 401	Employment	<i>employee</i> (7), new employees, employee turnover (1), full-time employee rights and benefits (4), parental leave (1)
GRI 402	Labor/management relations	minimum notice periods (1)
GRI 403	Occupational health and safety	no. of workers covered by occupational health and safety system (1), work related injuries (1), work related ill health (1)
GRI 404	Training and education	<i>education</i> (3), hours of training (1), employee skill programs (1), employee regular performance and career development reviews
GRI 405	Diversity and equal opportunity	diversity of governance bodies and employees (1), ratio of remuneration of women to men
GRI 406	Non-discrimination	incidents of discrimination and corrective actions (1)
GRI 407	Freedom of association and collective bargaining	operations and suppliers in which the right of freedom of association and collective bargaining may be at risk (1)
GRI 408	Child labor	operations and suppliers at significant risk for incidents of child labor (1)
GRI 409	Forced or compulsory labor	operations and suppliers at significant risk for incidents of forced or compulsory labor
GRI 410	Security practices	trained security personnel (1)
GRI 411	Rights of indigenous peoples	incidents of violations involving rights of indigenous people (1)
GRI 412	Human rights assessment	operations subject to human rights reviews (1), employee training on human rights (1), significant investment agreements including human rights (1)
GRI 413	Local communities	<i>community</i> (2), operations with local community (1), operations with potential negative impacts on local communities (1)
GRI 414	Supplier social assessment	selecting new suppliers using social criteria (1), negative social impacts on the supply chain (1)
GRI 415	Public policy	<i>public</i> (2), political contributions (1)
GRI 416	Customer health and safety	<i>customer</i> (4), health and safety impacts of products (1), incidents with non-compliance concerning the health and safety of the products (1)
GRI 417	Marketing and labeling	<i>market</i> (3), <i>product</i> (4), requirements for product information labeling (1), incidents of non-compliance concerning product information labeling (1), incidents of non-compliance concerning marketing communications (1)
GRI 418	Customer privacy	complaints concerning breaches of customer privacy and losses of customer data (1)
GRI 419	Socioeconomic compliance	non-compliance with laws and regulations in the social and economic area (1)

* Each level on the scale represents the total number of words as follows: 0-249=1, 250-499=2, 500-749=3, 750-999=4, 1000-1249=5, 1250-1499=6, 1500 and above=7

** italicized words are represent more general and comprehensive concepts.

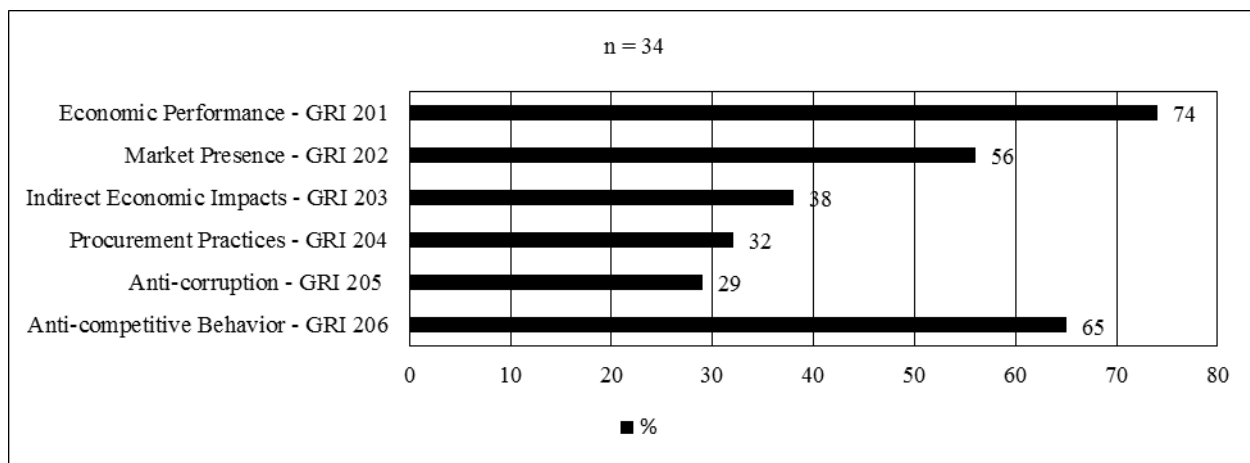


Figure 1. Percentages of companies disclosing GRI Economic Standards

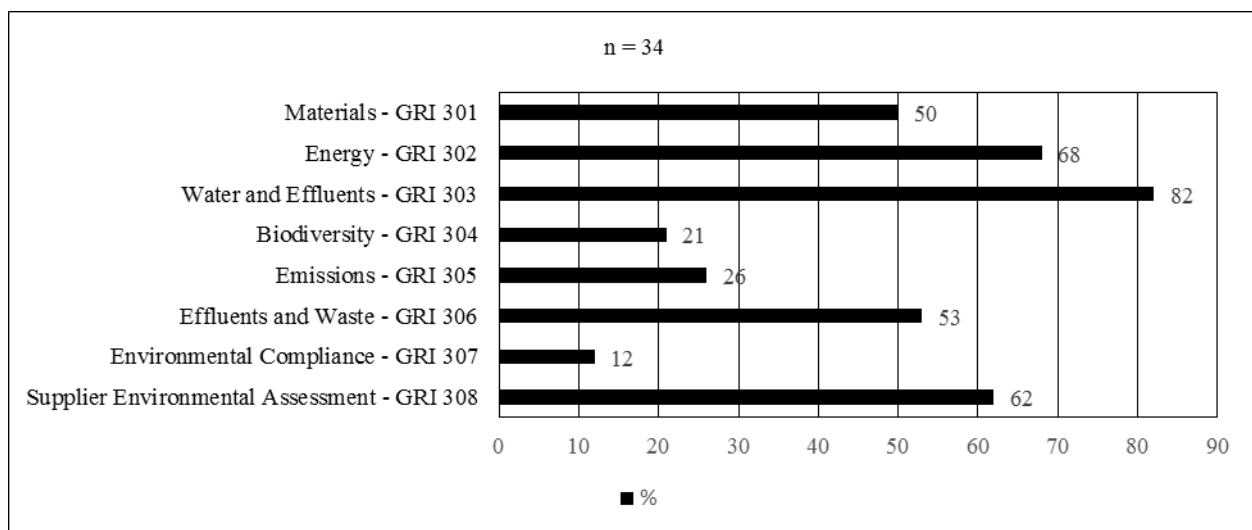


Figure 2. Percentages of companies disclosing GRI Environmental Standards

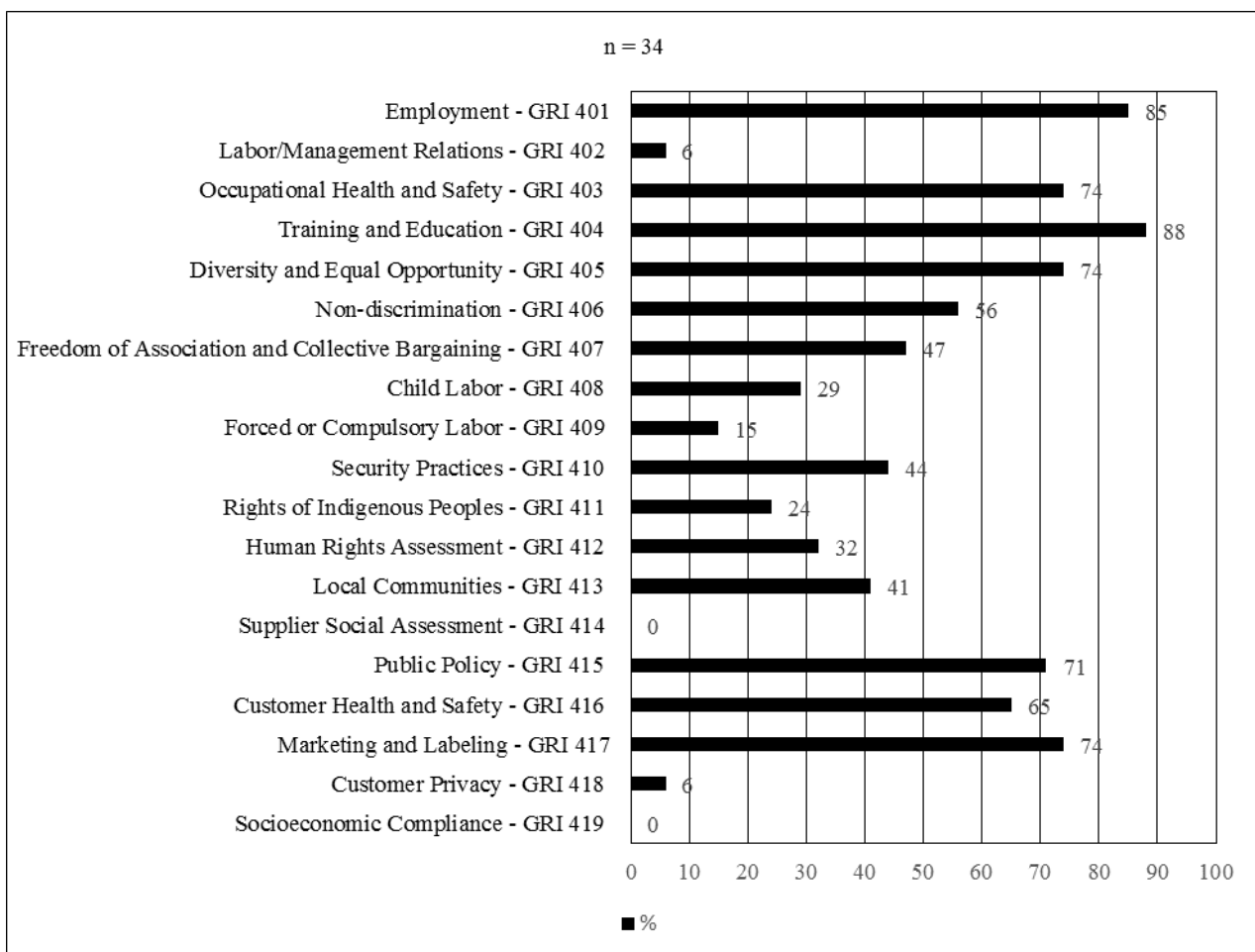


Figure 3. Percentages of companies disclosing GRI Social Standards

5. CONCLUSION

There is a rising trend in discussions about sustainability issues in the textile and apparel industry because environmental and social sustainability applications will inevitably have a significant effect on economic sustainability at both the micro and macro level. More

recyclable and/or renewable as well as health and environment-friendly types of raw materials provided by innovative scientific and technological research, such as manufactured fibers instead of cotton, are expected to be used by textile and apparel companies to promote sustainability. Innovative studies in the textile industry are expected to focus on methods for more efficient production

and use of manufactured fibers due to the factors explained previously. Capital investment and expenditure will most likely shift to focus on modernized, more efficient and fully-automated production systems, enabling the option of customized production through 3D technologies, more effective environmental management and protection systems as well as more efficient resource planning systems with minimized/eliminated usage of harmful chemicals. Innovative technologies are also expected to enable regional and even personalized product lines to be produced through fully automated 3D and similar technologies. The bottom line in supplier selection should be looking for those with lesser footprints and open to mutually beneficial and sustainable relationships through transparency and control. Cost considerations should be treated carefully, yet at a lower level of importance, since additional costs incurred for purpose of sustainability will be offset by increased demand and sales and/or other longer-term benefits. Complying with standards and regulations regarding sustainability, as well as improving them by internal practices, are believed not only to promote sustainability but also to increase operational effectiveness and efficiency. Competitive activities and operational efficiency are concentrated around innovative methods of producing

longer-lasting products requiring fewer washing and cleaning processes.

The results of the analysis reveal that approximately 18% of textile and apparel companies in Turkey currently provide sustainability disclosures. The GRI issues emphasized most concern employees, and water, followed by employee rights, product, market, suppliers, education, the economy, energy, waste, the community and the public. Wide variations were observed in GRI topic-specific disclosures, including economic, environmental and social topics. A majority of the sampled companies disclosed economic issues, including economic performance and anti-competition, although only a few provided disclosures about anti-corruption. A large proportion of the companies provided environmental disclosures about water and effluents, and energy whereas few provided disclosures about environmental compliance. Social sustainability disclosures, including training, education and employment, were provided by most companies. Finally, a number of companies provided disclosures about occupational health and safety, diversity and equal opportunity, marketing and labeling. However, made disclosures about supplier social assessment and socioeconomic compliance.

REFERENCES

- Ufuk 2030. 2016, September 16. Retrieved from <https://tgfd.org.tr/assets/2017/ufuk2030baski26.09.16.pdf> (Accessed July 30, 2018).
- Better Cotton Initiative. 2018. What makes BCI and Better Cotton unique? Retrieved from <https://bettercotton.org/resources/message/> (Accessed July 25, 2018).
- Turley DB, Copeland JE, Horne M, Blackburn RS, Stott E, Laybourn SR, Harwood J, Hughes JK. 2009. The role and business case for existing and emerging fibres in sustainable clothing: Final report to the department for environment, food and rural affairs (Defra), London, UK.
- Fletcher K. 2013. Sustainable fashion and textiles: design journeys. Greenpeace, hazardous chemicals in branded luxury textile products on sale during, 16.
- Morley NJ, Bartlett C, McGill I. 2009. Maximising reuse and recycling of UK clothing and textiles: A report to the department for environment, food and rural affairs. Oakdene Hollins Ltd, London: Defra.
- Scott G. 2018. The higg index. Retrieved from <https://apparelcoalition.org/the-higg-index/> (Accessed June 13, 2018).
- Goworek H, Fisher T, Cooper T, Woodward S, Hiller A. 2012. The sustainable clothing market: An evaluation of potential strategies for UK retailers *International Journal of Retail & Distribution Management* 40(12), 935-955.
- Jones P, Comfort D, Hillier D. 2010. Sustainability in the global shop window *International Journal of Retail & Distribution Management* 33(12), 882-92.
- Weed SWS. 1987. World commission on environment and development. Oxford University Press, Oxford, UK.
- Alkaya E, Demirer GN. 2014. Sustainable textile production: A case study from a woven fabric manufacturing mill in Turkey *Journal of Cleaner Production* 65, 595-603.
- Pulat E, Etemoglu AB, Can M. 2009. Waste-heat recovery potential in Turkish textile industry: Case study for city of Bursa *Renewable and Sustainable Energy Reviews* 13(3), 663-672.
- Eser B, Celik P, Cay A, Akgumus D. 2016. Tekstil ve konfeksiyon sektöründe surdurulabilirlik ve geri dönüşüm olanakları *Tekstil ve Mühendis* 23, 101.
- Guyer GT, Nadeem K, Dizge N. 2016. Recycling of pad-batch washing textile wastewater through advanced oxidation processes and its reusability assessment for Turkish textile industry *Journal of Cleaner Production* 139, 488-494.
- Ar AA, Tokol T. 2010. Tekstil sektöründeki işletmelerin yeşil pazarlamadan kaynaklı kazanımları *Elektronik Sosyal Bilimler Dergisi* 9(31), 148-168.
- Kusku F. 2007. From necessity to responsibility: Evidence for corporate environmental citizenship activities from a developing country perspective *Corporate Social Responsibility and Environmental Management* 14(2), 74-87.
- Kamal Y, Deegan C. 2013. Corporate social and environment - related governance disclosure practices in the textile and garment industry: Evidence from a developing country *Australian Accounting Review* 23(2), 117-134.
- Kozlowski A, Searcy C, Bardecki M. 2015. Corporate sustainability reporting in the apparel industry: An analysis of indicators disclosed *International Journal of Productivity and Performance Management* 64(3), 377-397.
- Steurer R, Langer ME, Konrad A, Martinuzzi A. 2005. Corporations, stakeholders and sustainable development I: A theoretical exploration of business-society relations *Journal of Business Ethics* 61(3), 263-281.
- Roca LC, Searcy C. 2012. An analysis of indicators disclosed in corporate sustainability reports *Journal of Cleaner Production* 20(1), 103-118.
- Empowering Sustainable Decisions. 2018. March 08 GRI Standards. Retrieved from <https://www.globalreporting.org/standards/> (Accessed April 25, 2018).
- Belal AR. 2016. Corporate social responsibility reporting in developing countries: The case of Bangladesh. Routledge.

-
22. Lozano R. 2013. Sustainability inter-linkages in reporting vindicated: A study of European companies *Journal of Cleaner Production* 51, 57-65.
23. Asif M, Searcy C, Santos PD, Kensah D. 2013. A review of Dutch corporate sustainable development reports *Corporate Social Responsibility and Environmental Management* 20(6), 321-339.
24. Gallego I. 2006. The use of economic, social and environmental indicators as a measure of sustainable development in Spain *Corporate Social Responsibility and Environmental Management* 13(2), 78-97.
25. Skouloudis A, Evangelinos KI. 2009. Sustainability reporting in Greece: Are we there yet? *Environmental Quality Management* 19(1), 43-60.
26. Krippendorff K. 2004. Content analysis: An introduction to its methodology. Sage, Thousand Oaks, CA.
27. İstanbul Sanayi Odası. 2017. Türkiye'nin 500 büyük sanayi kuruluşu 2017. Retrieved from <http://www.iso500.org.tr/500-buyuk-sanayi-kurulu/2017/?ara=&year=2017&sayfa=2> (Accessed June 15, 2018).
28. KAP. 2018. Merkezi kayıt istanbul. Retrieved from <https://www.kap.org.tr/en/Endeksler> (Accessed June 15, 2018).
29. White, MD, Marsh, EE. 2006. Content analysis: A flexible methodology *Library Trends* 55(1), 22-45.
30. Burla L, Knierim B, Barth KL, Duetz M, Abel T. 2008. From the text to coding: Intercoder reliability assessment in qualitative content analysis *Nursing Research* 57, 113-117.
31. Elo S, Kääriäinen M, Kanste O, Pölkki T, Utriainen K, Kyngäs H. 2014. Qualitative content analysis: A focus on trustworthiness *SAGE open* 4(1), 1-10.

Appendix 1. Descriptions of Abbreviations

International Organization for Standardization	: ISO
Global Reporting Initiative	: GRI
International Association for Research and Testing in the Field of Textile and Leather Ecology	: OEKO-TEX
Occupational Health and Safety Management Systems	: OHSAS
Global Organic Textile Standard	: GOTS
Uster Textile Quality Control Technologies	: USTER
Autocoro Yarn Quality Certification	: BELCORO
Certification of Environmental Standards	: CERES
International Sleep Products Association	: ISPA
Leadership in Energy and Environmental Design	: LEED



Analyzing Some of the Dual-Core Yarn Spinning Parameters on Yarn and Various Fabric Properties

Sevim Hümeysa Çelikkan Aydoğdu, Demet Yılmaz

Suleyman Demirel University, Engineering Faculty, Textile Engineering Department, West Campus, Isparta, Turkey

Corresponding Author: Demet Yılmaz, demetyilmaz@sdu.edu.tr.

ABSTRACT

Nowadays, in order to improve some of the properties of core-spun yarns, a new type of core-spun yarn called as dual-core has been developed. In literature, there are limited studies and hence findings about dual-core yarns. Therefore, in this study, dual-core yarns were produced with three different sheath fibres (viscose, cotton and cotton/Tencel blended fibres) and two different core filament linear density (50 and 70 denier) having three different yarn counts (12/1 Ne, 16/1 Ne and 20/1 Ne). Woven and knitted fabrics were manufactured and yarn quality parameters and some of the fabric properties such as fabric pilling behaviour, breaking and bursting strength, breaking elongation and bending rigidity were investigated. Therefore, at the end of study, it was possible to investigate the effect of sheath fibre type, yarn count and core filament linear density on yarn and fabric properties of dual-core yarns.

1. INTRODUCTION

In recent years, usage of elastic materials and demands to elastic fabrics and garments have been increased due to their stretch and recovery capability and thus wear comfort and fitness compared to common textile products [1]. Elastic materials under different names such as Lycra, Spandex, T400, PBT etc. are widely used in casual apparel products, denim fabrics, sportswear, medical textiles etc. to provide the stretchability and elasticity. One commonly used method to produce elastic woven or knitted fabrics is core-spun yarn spinning technology. In core-spun yarn spinning method, any type of elastic filament specially placed to centre of the yarn is covered and wrapped by short staple fibres such as cotton, wool or man-made fibres. Produced yarn is called as core-spun and consisting of core filament and sheath parts. Core-spun yarn production method makes possible to optimally benefit the features of two different components in the same structure. In order to improve the properties of core-spun yarns, particularly recovery, stability and dimensional change, a new type of core-spun yarn called as dual-core yarn has been developed.

Core filaments such as soft (Elastane) and hard material (PES, PA etc.) are coated with staple natural or synthetic filaments and hence resultant yarn is composed of dual core filaments such as PET+Elastane or PA+Elastane, and sheath fibres. In particular, elastic-soft and semi elastic-hard core filaments are used in dual-core yarn production to enhance high elasticity obtained by elastic component and high recovering, stability and low shrinkage obtained by semi elastic component to dual-core yarns.

Core-spun yarns have been used for many years and therefore the effects of the elastic core, the sheath fibres for covering the yarn and various spinning parameters on structures and properties of core-spun yarns were investigated in many studies. However, textile producers and researchers have newly focused on dual-core spun yarns and hence there are a few works about the dual-core spun yarns [1-4]. Hua et al. [1] worked on the development of elastic core-spun yarn containing a mix of Spandex and polyethylene terephthalate/polytrimethylene terephthalate (PET/PTT) bi-component filament as a core material to obtain better elastic property. Spandex and PET/PTT bi-

ARTICLE HISTORY

Received: 22.10.2018

Accepted: 13.02.2019

KEYWORDS

Dual-core yarn, core-spun yarn, elastic fabrics, Spandex

To cite this article: Çelikkan Aydoğdu SH, Yılmaz D. 2019. Analyzing some of the dual-core yarn spinning parameters on yarn and various fabric properties *Tekstil ve Konfeksiyon* 29(3), 197-207.

component filaments were covered with cotton fibres on a modified ring-spinning machine with a core spinning attachment. The experimental results indicated that dual-core yarns have much lower yarn stress decay as well as lower hairiness, CV_m and higher elongation values compared to the core-spun yarns using only Spandex core filament. In addition, it was found that Spandex count significantly affects the breaking elongation and stress decay of dual-core yarns and elongation of the yarns increases with the increase of the draw ratio of Spandex. Kılıç [2] and Tantawy et al. [3], in their studies, fed dual-core filaments in two different ways to the yarn centre. Kılıç [2] welded PET and Spandex filaments by intermingling process and positioned the combined filaments in front roller nip in terms of a standard V-grooved guide roller under certain tension (3.5). In second part of the study, PET and Spandex filaments were fed separately by similar guide roller under certain tension (for 3.5 for PET, 1.08 for Spandex). Intermingled and separately fed PET and Spandex core filaments were covered by cotton fibres and multicomponent dual-core yarns were obtained. Kılıç [2] determined that production methods (core-spun and dual-core) have statistically significant influence on yarn properties. In addition, it was indicated that production parameters such as twist, Elastane pre-draft also statistically affect the elasticity and growth values of woven fabrics. Tantawy et al. [3] studied the effect dual-core weft yarns with different yarn counts on the pilling properties of denim fabric (3/1 Z twill) and found that dual-core yarn type and yarn count have influence on fabric pilling property. Ertaş et al. [4] produced 16/1 Ne dual-core yarns for the weft thread using 77 dtex PES and 78 dtex Spandex core filaments and cotton wrapping fibres. In their study, it was determined that the construction has a much more impact on the fabric width and thus on the unit weight properties than the elasticity ratio. As the density increases, the elasticity value, permanent elongation and depth of the colour have been found out to decrease substantially due to more rigidity of the fabric resulted from higher fabric density. It was determined that the ratio between the elasticity and the permanent elongation values is not affected from the density changes, and remains at the same value in almost all the fabrics. In addition, permanent elongation value is superior at the same elasticity value compared to the conventional Elastane core wefts. As reported above, there are a few studies and findings about

the dual-core yarns to understand the structure and features of this yarn type. In this study, we are interested in the identification of the effect of various process parameters on dual-core yarn and some of the fabric properties. Dual-core yarns having three different yarn counts were produced with three different sheath fibres and two different core filament linear densities. This study provides a better understanding the effect of sheath fibres, core filament and yarn finenesses on dual-core yarns. In addition, majority of the studies reported in the literature has focused on the usage of cotton fibre as a sheath fibre for core-spun yarns composed of single [5-24] and dual core filaments [1-4]. Present study was therefore undertaken to investigate the effect of different sheath fibre types on dual-core yarns.

2. MATERIAL AND METHOD

2.1. Material

In the study, it was produced dual-core spun yarns having 12/1 Ne, 16/1 Ne and 20/1 Ne yarn counts on Merlin conventional ring spinning machine. Cotton (100%), viscose (100%) and cotton/Tencel fibre blend (50/50%) were used as a sheath part of the dual-core spun yarns. Fibre properties were given in Table 1. As a core material, X55 and Spandex filaments were used together for dual-core spun yarns. Linear densities of core filaments were 50 and 70 denier for X55, and 70 denier for Spandex. Spandex fibre, one of the most important thermo-plastic elastomeric fibres being commercially produced worldwide, is made with long chain synthetic polymers comprised of mostly segmented polyurethanes [25]. X55 is a Spandex fibre commercialized by Xanadu firm to provide crimp and stretch properties to material.

Similar to core-spun yarn, during the dual-core spun yarn production, X55 and Spandex (X55+Spandex) core filaments were supplied separately under control of a positive feed roller system and sent to the V-grooved guide roller. And both core materials composed of X55+Spandex filaments were wrapped by cotton, viscose and cotton/Tencel covering fibres. During dual-core yarn production, core filaments were given to the drafting system under specific tension (draft), and the values were 1.1 for first type of core filament (X55) and 3.63 for second type of core filament (Spandex). Production parameters for dual-core yarns were that roving count was about 0.81-0.87 Ne, ae was 4.0, spindle speed was 10500-11000 rpm [26].

Table 1. Fibre properties

Properties	Cotton	Viscose	Tencel
Fibre length	28.62 mm	38 mm	38 mm
Fineness	Mic 4.22	1.3 dtex	1.3 dtex
Maturity	97.2 %	-	-
Tenacity	30.58 g/tex	-	-
Colour grade	33-44	-	-

2.2. Method

Dual-core spun yarn samples were conditioned under standard atmospheric conditions of $20\pm1^{\circ}\text{C}$ and $65\pm2\%$ R.H. for 24 h. Seven cops were tested for each yarn properties and one test was done on each cops. Yarn evenness and imperfections was tested on Uster Tester 5 at 400 m/min test speed. Mechanical properties of the yarns were measured on Uster Tensorapid 4. To analyse the fabric properties, yarn samples were used as a weft yarn and woven fabrics were produced having plain weave and 30 cm*150 cm dimensions. Fabric density values were 39 warp/cm*18 weft/cm for 12/1 Ne, 33 warp/cm*19 weft/cm for 16/1 Ne, and 33 warp/cm*21 weft/cm for 20/1 Ne yarn counts. Pilling behaviour of all fabrics was tested on the Nu-Martindale Abrasion Tester according to TS EN ISO 12945-2 test method. Fabric strength and breaking elongation was tested according to TS EN ISO 13934-1/1999 on Lloyd LR5K Plus electronic tensile strength machine. Due to limited fabric sample, tensile properties of woven fabrics were tested for only weft direction. In the study, it was also obtained knitted samples from the dual-core spun yarns and fabric density values varied as 110-113 loop/cm² for 12/1 Ne, 121-125 loop/cm² for 16/1 Ne, 124-128 loop/cm² for 20/1 Ne yarn counts. Bursting strength of the fabrics was tested according to ISO 13938-2. Three samples were tested for tensile properties of woven and knitted fabrics. Bending rigidity of the woven fabric samples was also analysed according to ASTM D 1388-96 test method by WIRA bending rigidity tester. Three samples of both of warp and weft direction were tested for each fabric and the average values were determined.

All the tests were carried out on the same testers and test results were analysed statistically by SPSS 16.0 statistical software to determine any significant differences. ANOVA tests were used for two-way analysis of variance for the analysis of the production parameters, multiple-range test LSD method for the comparison of sheath fibre types (Table 2) and t-test for the comparison of yarn counts (Table 3-4) and ANOVA analyses were performed for $\alpha=0.05$ significance level [26]. In the tables, yarn counts of 12 Ne, 16/1 Ne and 20/1 Ne were indicated by 12, 16 and 20, respectively.

3. RESULTS AND DISCUSSIONS

3.1. Yarn Properties

In this part, it was given the properties of dual-core spun yarns produced with 50/70 and 70/70 X55+Spandex core filaments and cotton, viscose and cotton/Tencel sheath fibres. The results were coded depending on production

parameters and viscose, cotton, cotton/Tencel sheath fibres were shown by V, C and C/T while 12 Ne, 16/1 Ne and 20/1 Ne yarn counts were displayed by 12, 16 and 20, respectively. The results of ANOVA tests were shown in Tables 2-3.

Yarn unevenness

Yarn unevenness results are shown in Figure 1. According to CVm values, dual-core yarns having viscose and cotton/Tencel fibre sheath fibres have significantly lower mass variation values than the yarns having cotton sheath fibres (Table 2). Higher yarn unevenness of cotton sheath fibres corresponds to the results in the core-spun yarns having single elastic core filament [26] and other yarn types. Erdumlu et al. [27] and Kılıç and Okur [28] studied the effect of cotton fibres, viscose rayon fibres and its blends on ring, compact and vortex yarn properties and it was indicated that an increasing ratio of regenerated cellulosic fibre content in the blend decreases unevenness and the lowest CVm value was found for 33/67% cotton-regenerated cellulosic fibre blend [28]. Therefore, findings for the effect of different sheath fibre types on CVm values of dual-core yarns are in agreement with that of the other yarn types. The reason for CVm results may be attributed to fibre length and high variation in cotton fibre length compared to viscose and cotton/Tencel fibres. When the yarn becomes finer, unevenness values of the yarns tend to increase as a result of decreasing the number of fibres in yarn structure as reported in other yarn types. Erdumlu et al. [27] reported that mass variation of conventional ring, OE-rotor and vortex increases with finer yarn counts. Örtlek and Ülkü [29] also indicated higher unevenness of finer core-spun vortex yarns than that of the coarser ones. As far as the effect of X55 core filament linear density is concerned, yarn unevenness results change depending on yarn count and sheath fibre types. CVm values mostly decrease with coarser core filament for 12 Ne and 16 Ne yarn counts. However, there is a different trend in 20 Ne dual-core yarns sheathed with viscose and cotton/Tencel fibres and unevenness of the yarns increases with coarser core filament. This trend is consistent with the results of core-spun yarns and unevenness of core-spun yarns having viscose and cotton/Tencel wrapping fibres increases with coarser core filament in 30 Ne and 40 Ne yarn counts [26]. As the core filament is getting coarser, for finer yarn counts in core-spun yarns having single or dual core filaments, core filament can be not covered uniformly with less number of sheath fibres and this case may lead to higher CVm values.

Table 2. ANOVA LSD test results for dual-core yarn and fabric properties produced with different sheath fibres and yarn counts

Property	Sheath fibres		Sig.	Property	Sheath fibres		Sig.
CVm12	Viscose	Cotton	0.000*	Woven-Strength12	Viscose	Cotton	0.028*
		Cotton/Tencel	0.419		Cotton	Cotton/Tencel	0.000*
	Cotton	Cotton/Tencel	0.000*			Cotton	0.057
CVm16	Viscose	Cotton	0.000*	Woven-Strength 16	Viscose	Cotton	0.000*
		Cotton/Tencel	0.933		Cotton	Cotton/Tencel	0.000*
	Cotton	Cotton/Tencel	0.000*			Cotton	0.095
CVm20	Viscose	Cotton	0.000*	Woven-Strength20	Viscose	Cotton	0.115
		Cotton/Tencel	0.001*		Cotton	Cotton/Tencel	0.009*
	Cotton	Cotton/Tencel	0.000*			Cotton	0.000*
Thick12	Viscose	Cotton	0.000*	Woven-Elongation12	Viscose	Cotton	0.002*
		Cotton/Tencel	0.840		Cotton	Cotton/Tencel	0.001*
	Cotton	Cotton/Tencel	0.000*			Cotton	0.009*
Thick16	Viscose	Cotton	0.000*	Woven-Elongation16	Viscose	Cotton	0.095
		Cotton/Tencel	0.904		Cotton	Cotton/Tencel	0.001*
	Cotton	Cotton/Tencel	0.000*			Cotton	0.008*
Thick20	Viscose	Cotton	0.000*	Woven-Elongation20	Viscose	Cotton	0.059
		Cotton/Tencel	0.658		Cotton	Cotton/Tencel	0.163
	Cotton	Cotton/Tencel	0.000*			Cotton	0.009*
Neps12	Viscose	Cotton	0.000*	Knitted-Bursting12	Viscose	Cotton	0.002*
		Cotton/Tencel	0.868		Cotton	Cotton/Tencel	0.160
	Cotton	Cotton/Tencel	0.000*			Cotton	0.000*
Neps16	Viscose	Cotton	0.000*	Knitted-Bursting16	Viscose	Cotton	0.000*
		Cotton/Tencel	0.729		Cotton	Cotton/Tencel	0.000*
	Cotton	Cotton/Tencel	0.000*			Cotton	0.175
Neps20	Viscose	Cotton	0.000*	Knitted-Bursting20	Viscose	Cotton	0.006*
		Cotton/Tencel	0.667		Cotton	Cotton/Tencel	0.001*
	Cotton	Cotton/Tencel	0.000*			Cotton	0.000*
H12	Viscose	Cotton	0.000*				
		Cotton/Tencel	0.487				
	Cotton	Cotton/Tencel	0.001*				
H16	Viscose	Cotton	0.001*				
		Cotton/Tencel	0.520				
	Cotton	Cotton/Tencel	0.003*				
H20	Viscose	Cotton	0.000*				
		Cotton/Tencel	0.073				
	Cotton	Cotton/Tencel	0.015*				
Tenacity12	Viscose	Cotton	0.773				
		Cotton/Tencel	0.006*				
	Cotton	Cotton/Tencel	0.013*				
Tenacity16	Viscose	Cotton	0.049*				
		Cotton/Tencel	0.001*				
	Cotton	Cotton/Tencel	0.000*				
Tenacity20	Viscose	Cotton	0.000*				
		Cotton/Tencel	0.842				
	Cotton	Cotton/Tencel	0.000*				
Elogantion12	Viscose	Cotton	0.000*				
		Cotton/Tencel	0.787				
	Cotton	Cotton/Tencel	0.000*				
Elogantion16	Viscose	Cotton	0.000*				
		Cotton/Tencel	0.717				
	Cotton	Cotton/Tencel	0.000*				
Elogantion20	Viscose	Cotton	0.000*				
		Cotton/Tencel	0.000*				
	Cotton	Cotton/Tencel	0.000*				

*The mean difference is significant at the 0.05 level.

Table 3. t-test results of dual-core yarns produced with different sheath fibres and yarn counts for yarn properties

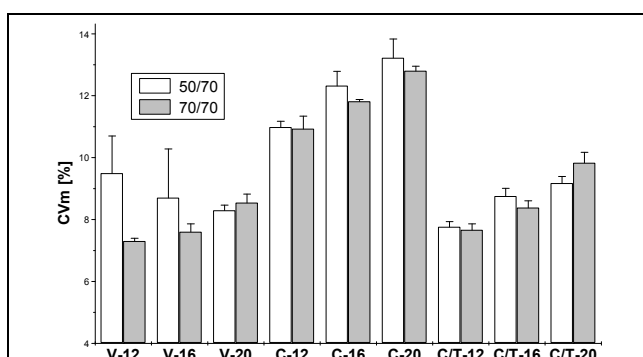
Production parameters		CVm	Thick places	Neps	H	Tenacity	Elongation
Viscose	12 Ne	0.000*	0.111	0.006*	0.000*	0.000*	0.000*
	16 Ne	0.000*	0.001*	0.001*	0.000*	0.000*	0.000*
	20 Ne	0.000*	0.082	0.000*	0.000*	0.000*	0.000*
Cotton	12 Ne	0.000*	0.000*	0.000*	0.000*	0.000*	0.000*
	16 Ne	0.000*	0.000*	0.000*	0.000*	0.000*	0.000*
	20 Ne	0.000*	0.000*	0.000*	0.000*	0.000*	0.000*
Cotton/Tencel	12 Ne	0.000*	0.000*	0.000*	0.000*	0.000*	0.000*
	16 Ne	0.000*	0.000*	0.000*	0.000*	0.000*	0.000*
	20 Ne	0.000*	0.000*	0.000*	0.000*	0.000*	0.000*

*The mean difference is significant at the 0.05 level.

Table 4. t-test results of dual-core yarns produced with different sheath fibres and yarn counts for fabric properties

Production parameters		Strength	Elongation	Bursting strength
Viscose	12 Ne	0.000*	0.000*	0.000*
	16 Ne	0.000*	0.000*	0.000*
	20 Ne	0.000*	0.000*	0.000*
Cotton	12 Ne	0.000*	0.000*	0.000*
	16 Ne	0.000*	0.000*	0.000*
	20 Ne	0.000*	0.000*	0.000*
Cotton/Tencel	12 Ne	0.000*	0.000*	0.000*
	16 Ne	0.000*	0.000*	0.000*
	20 Ne	0.000*	0.000*	0.000*

*The mean difference is significant at the 0.05 level.

**Figure 1.** Yarn unevenness results

ANOVA results indicate that the effects of sheath fibre ($p=0.000$) and yarn count ($p=0.000$) are statistically significant at 5% level. However, sheath fibre*yarn count ($p=0.193$), core filament linear density ($p=0.273$) and its interactive effects with sheath fibre ($p=0.639$), yarn count ($p=0.424$) and sheath fibre*yarn count ($p=0.921$) do not have statistically significant effect on the yarn irregularity values. Therefore, these results suggest that sheath fibre type due to its effect on fibre properties and yarn count related from its effect on number of fibres in yarn structure

have a relatively higher significant influence on yarn unevenness in comparison to core filament linear density.

Yarn imperfections

In the study, it was not determined any thin places for all yarn types. However, thick places and neps values are given in Figures 2-3 and statistical test results are given in Tables 2-3. According to the results, dual-core yarns produced with cotton sheath fibres have significantly higher thick places and neps values than the yarns with viscose and cotton/Tencel wrapping fibres. As in yarn unevenness results, yarn imperfections are getting higher with the finer yarn counts. Regarding the core filament linear density, there is no clear trend in the results of thick places of all dual-core yarns. However, neps values seem to be increased as the core filament becomes coarser. This result is also in harmony with the findings determined for core-spun yarns having single core filament at the yarn centre [26].

When the thick places of dual-core spun yarns are analysed statistically, ANOVA results indicate that effects of sheath fibre ($p=0.000$), yarn count ($p=0.000$) and sheath fibre*yarn count ($p=0.000$) are statistically significant at 5% level. However, core filament linear density ($p=0.222$) and its

interactive effects with sheath fibre ($p=0.223$), yarn count ($p=0.379$) and sheath fibre*yarn count ($p=0.310$) do not have considerably affect on thick places values of the yarns. As to neps faults, similar trend is observed and sheath fibre ($p=0.000$), yarn count ($p=0.000$) and sheath fibre*yarn count ($p=0.000$) have statistically more important influence while the effect of core filament linear density ($p=0.364$) and its interactive effects with sheath fibre ($p=0.124$), yarn count ($p=0.110$) and sheath fibre*yarn count ($p=0.287$) are not statistically significant level on the neps values. As in yarn unevenness, the results reveal that sheath fibre type and yarn count are the considerably important production parameters for lower thick places and neps faults and both core filament linear density values lead to similar yarn faults at the same sheath fibres and yarn counts.

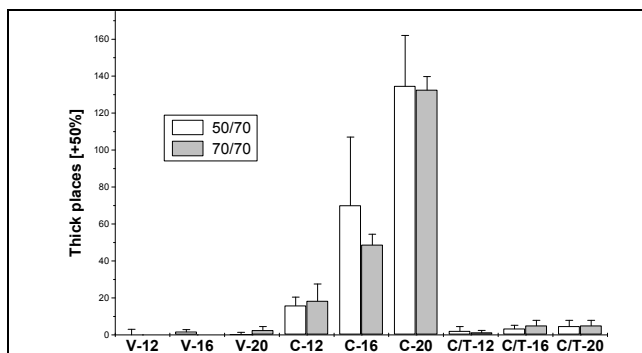


Figure 2. Thick places results

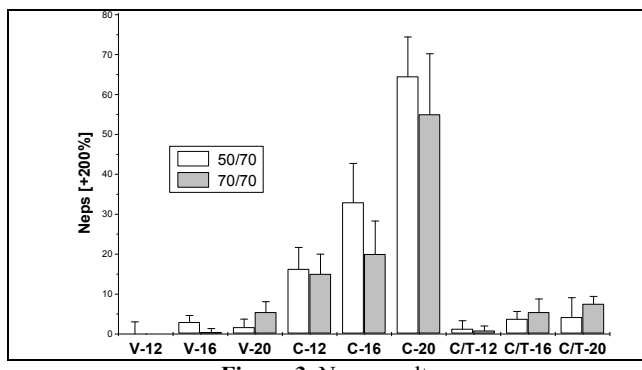


Figure 3. Neps results

Yarn hairiness

Hairiness properties of dual-core yarns were evaluated by Uster hairiness index (H) and the yarns containing cotton sheath fibres have been found to be more hairy while the yarns having viscose covering fibres have significantly lower hairiness values (Figure 4). In particular, H values of cotton fibres are significantly different from other sheath fibres while viscose and cotton/Tencel sheath fibres give statistically similar yarn hairiness. Erdumlu et al. [27] also reported for different yarn types like ring, rotor and vortex and longer length of viscose rayon fibre, when compared with cotton, provided fewer protruding fibres and lower H values. Hence, fibre length of sheath fibres plays an important role in the hairiness values for spun yarns.

Hairiness index of all dual-core yarns decreases with a reduction in the yarn count and less number of fibres in yarn cross-section gives lower hairiness index, as in other yarn types. On the other hand, for the effect of core filament linear density, different trends have been observed depending on the sheath type and yarn count. As the core filament become coarser, hairiness values increase in 16/1 Ne and 20/1 Ne cotton, and 12/1 Ne and 16/1 Ne cotton/Tencel sheathed dual-core yarns. For dual-core yarns with cotton/Tencel wrapping fibres, coarser core filament may decrease the yarn hairiness due to lower percentage of cotton sheath fibres. For cotton sheath fibres, in contrast to our expectations, coarser core filament causes higher yarn hairiness in 20 Ne yarn count. In another part of this study, this trend was observed for 30 and 40 Ne cotton sheathed core-spun yarns while 20 Ne, 30 Ne and 40 Ne viscose and cotton/Tencel wrapped core-spun yarns, and hairiness of core-spun yarns increased with coarser core filament usage [26]. Hence, one may think that yarn hairiness starts to increase beyond the certain yarn count because of the coarser core filament and the limit for yarn count changes depending on sheath fibre type.

When ANOVA results are analysed, it is determined that sheath fibre ($p=0.000$), yarn count ($p=0.000$) and yarn count*core filament linear density ($p=0.006$) have statistically significant effect on H hairiness values of dual-core yarns. However, core filament linear density ($p=0.447$) and interactive effects of sheath fibre*yarn count ($p=0.103$), sheath fibre*core filament linear density ($p=0.319$) and sheath fibre*yarn count*core filament linear density ($p=0.112$) are found statistically insignificant at 5% level. Therefore, as in ring spun and other yarn types, staple fibre properties, particularly fibre length, and changes in number of sheath fibres in yarn structure resulted from yarn count and linear density of core filament have a relatively higher significant influence on hairiness of dual-core yarns. Vuruşkan [24] also stated that yarn count is the most effective parameter on yarn hairiness in comparison to yarn twist and elastane draft for core-spun yarns comprising core filament.

The findings regarding the effect of core filament linear density on yarn hairiness is also consistent with the literature [12-13, 29] and explained by the more possibility of displacement of the core filament and disrupting the sheath fibres orientation because of higher percentage of elastic core filament in the yarn structure [13]. Another explanation may be insufficiently and improperly coating of coarser core filament due to less number of fibres in finer yarn counts. If the results are concluded in a general expression, core-spun yarns comprising single and dual core filaments with cotton sheath fibres become more hairy with finer yarn counts and coarser core filament linear densities. As to viscose and cotton/Tencel covering fibres, coarser yarn count and core filament linear density lead to higher yarn hairiness.

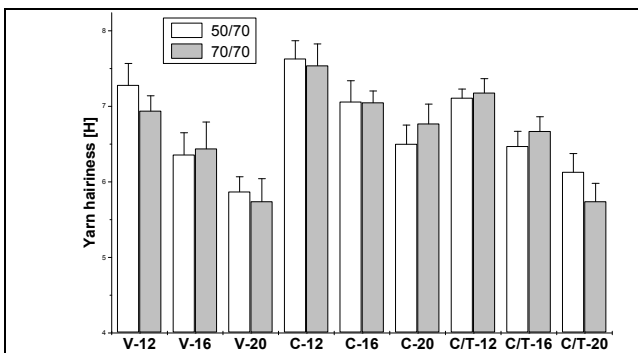


Figure 4. Yarn hairiness results

Yarn tenacity

Differences in tenacity results are given in Figure 5. When the effect of sheath fibre type on tenacity values of dual-core yarns are examined, the findings are similarly determined in core-spun yarns comprising single elastic component. Dual-core yarns obtained by cotton/Tencel sheath fibres give the highest tenacity values while tenacity of the yarns covered by cotton sheath fibres is the lowest. As the dual-core yarns become finer, as expected, tenacity of the yarns decreases. As far as core filament linear density is concerned, tenacity values of the dual-core yarns reduce with coarser core filament usage except 16 Ne viscose sheathed dual-core yarns. This result is consistent with the findings for core-spun yarns having single elastic core filament [12-13, 26, 30-31], which reported that most of the loading stress is mainly taken up by relatively lesser extensible sheath component in core spun yarns. Therefore, strength of sheath or wrapping fibres mainly determines the overall yarn tenacity of core-spun yarns. As the core filament is getting finer, number of sheath fibres and thus contribution to yarn tenacity increases. This case provides more resistance to applied load and higher tenacity values are achieved [13, 22, 24, 29]. In present study, the findings of lower tenacity values of coarser core filaments confirm these statements and strength of sheath fibres appears to have significant affect on tenacity of dual-core yarns than yarn and core filament linear densities.

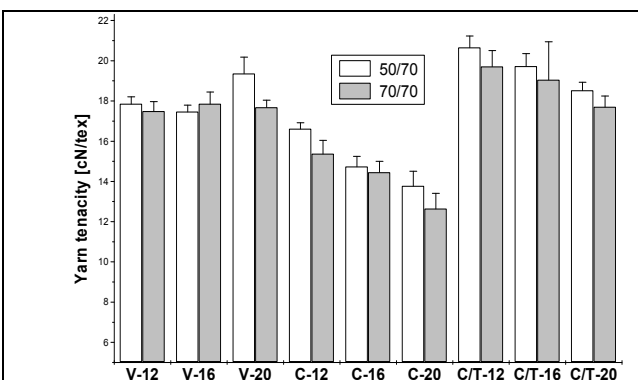


Figure 5. Yarn tenacity results

On the other hand, ANOVA results indicate that the effect of sheath fibre ($p=0.000$), yarn count ($p=0.000$) and core

filament linear density ($p=0.000$) and interactive effects of these parameters ($p=0.000$) except sheath fibre*core filament linear density ($p=0.000$) are found statistically significant level on yarn tenacity values. Therefore, all production parameters of dual-core yarns have a relatively higher significant influence on tenacity of the dual-core yarns.

Yarn breaking elongation

The results are indicated in Figure 6. For the effect of sheath fibre type, dual-core yarns produced with viscose sheath fibres have the highest values while the yarns having cotton wrapping fibres have the lowest breaking elongation values for all yarn counts and core filament linear densities. Since the elongation of viscose and Tencel fibres are greater than cotton, an increase in yarn elongation is also inevitable [28]. On the other hand, mostly, there are not statistically significant differences in the results of viscose and cotton/Tencel sheath fibres and hence both sheath fibres lead to considerably higher breaking elongation values than the dual-core yarns produced from cotton sheath fibres. Breaking elongation values of the dual-core yarns significantly decrease as the yarn becomes finer for all sheath fibre types. An examination of the effect of core filament linear density on yarn breaking elongation indicates that the increasing ratio of core filament content in the yarn structure with the usage coarser core filament leads to an increase on yarn elongation.

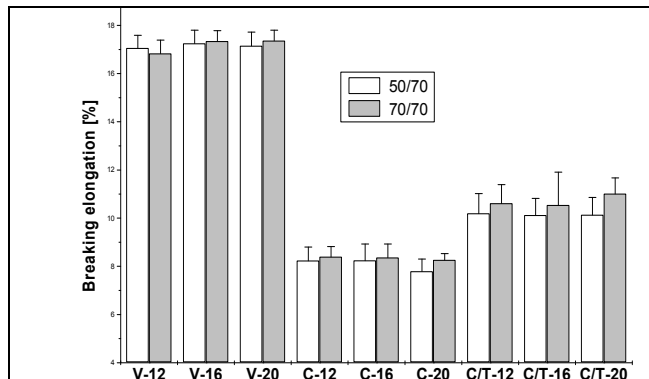


Figure 6. Yarn breaking elongation results

According to ANOVA results, the effects of all parameters and their interactions on breaking elongation are generally statistically significant at 5% level. Therefore, not only the sheath fibre and yarn count but also core filament linear density is the parameters determining the breaking elongation of dual-core yarns.

3.2. Fabric Properties

In this part, it was given some of the woven and knitted fabric properties of 12/1 Ne, 16/1 Ne and 20/1 Ne dual-core spun yarns produced with X55 (50 and 70 denier) and Spandex (70 denier) core filaments and cotton, viscose and cotton/Tencel sheath fibres. ANOVA results were summarized in Table 2 and Table 4.

Pilling behaviour

Pilling is a very serious problem for the fabrics that arises after the usage of the fabric. Pilling behaviour of all fabrics was tested and Table 5 displays the pilling rates of the woven fabrics produced from dual-core yarns having different sheath fibres, yarn counts and core filament linear densities. A general assessment shows that the fabrics woven from dual-core yarns comprising viscose and cotton/Tencel sheath fibres have almost similar pilling rates for all yarn counts. However, the fabrics produced from the dual-core yarns with cotton sheath fibres have a bit higher pilling tendency than the other fabrics. This trend may result from higher yarn Uster H hairiness values of cotton sheathed dual-core yarns. Upon a general evaluation of pilling results of the dual-core yarns indicates that the sheath fibre properties is more effective on yarn hairiness and thus pilling behaviour of the fabrics is affected from sheath fibre characteristics in comparison to the effect of the yarn count and core filament linear density.

Tensile properties of the woven fabrics

As reported, dual-core yarns were used as weft yarn during the woven fabric production and fabric strength and breaking elongation was tested for only weft direction because of the inadequate fabric sample. When the tensile properties of the fabrics are analysed, different trend is observed depending on yarn count. In the fabrics woven from 12 Ne and 20 Ne dual-core yarns, fabric breaking strength values are higher for the fabrics having cotton/Tencel sheathed fibres while lower for the fabrics

having cotton fibres (Figure 7). The possible reason for this result could be the tenacity values of these yarns. Furthermore, in 12 Ne yarn count, finer core filament provides higher fabric strength while an inverse tendency becomes in 16 Ne and 20 Ne yarn counts and lower fabric strength is obtained for all sheath fibre types. According to statistical results, as determined in yarn tensile properties, the effect of sheath fibre ($p=0.000$), yarn count ($p=0.000$) and its interactive effects of sheath fibre*yarn count ($p=0.000$) are found statistically significant level on fabric strength. The effect of core filament linear density is seen to be statistically important depending on sheath fibre type and yarn count and interactive effects of core filament linear density with sheath fibre ($p=0.003$), yarn count ($p=0.000$) and sheath fibre*yarn count ($p=0.000$) are statistically significant level on fabric strength.

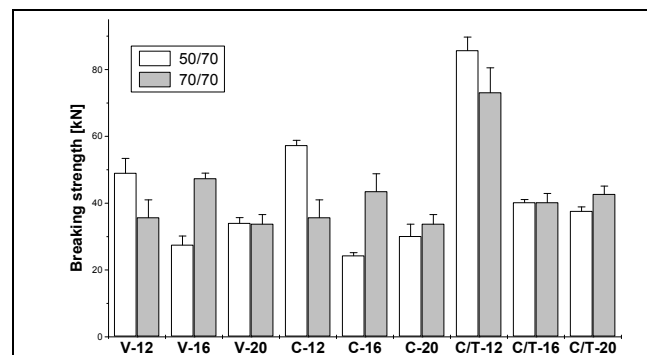


Figure 7. Breaking strength values of woven fabrics

Table 5. Pilling property of the fabrics

Yarn type	500 cycle	1000 cycle	2000 cycle	3000 cycle	5000 cycle	7000 cycle
12 Ne	Viscose-50/70 denier	4-5	4-5	3-4	3-4	3-4
	Viscose-70 /70denier	4-5	4-5	4-5	3-4	3-4
	Cotton-50/70 denier	4-5	3-4	3-4	3-4	2-3
	Cotton-70/70 denier	4-5	3-4	3-4	3-4	2-3
	Cotton/Tencel-50/70 denier	4-5	4-5	4-5	3-4	3-4
	Cotton/Tencel-70/70 denier	4-5	4-5	4-5	3-4	3-4
16 Ne	Viscose-50/70 denier	4-5	4-5	4-5	3-4	3-4
	Viscose-70 /70denier	4-5	4-5	4-5	3-4	3-4
	Cotton-50/70 denier	4-5	3-4	3-4	3-4	2-3
	Cotton-70/70 denier	4-5	3-4	3-4	3-4	3-4
	Cotton/Tencel-50/70 denier	4-5	4-5	4-5	3-4	3-4
	Cotton/Tencel-70/70 denier	4-5	4-5	4-5	3-4	3-4
20 Ne	Viscose-50/70 denier	4-5	4-5	4-5	3-4	3-4
	Viscose-70 /70denier	4-5	4-5	4-5	3-4	2-3
	Cotton-50/70 denier	4-5	4-5	4-5	3-4	3-4
	Cotton-70/70 denier	4-5	4-5	4-5	3-4	3-4
	Cotton/Tencel-50/70 denier	4-5	4-5	4-5	3-4	3-4
	Cotton/Tencel-70/70 denier	4-5	4-5	4-5	3-4	3-4

When the breaking elongation results of the woven fabrics are studied, it is seen that the dual-core yarns having viscose sheath fibres give significantly higher fabric breaking elongation values than the other sheath fibres as in yarn breaking elongation (Figure 8). On the other hand, there are no clear trend regarding the effect of core filament linear density on fabric breaking elongation and elongation values of the fabrics change depending on yarn counts and sheath fibre types. According to statistical results, as determined in yarn tensile properties, the effect of sheath fibre ($p=0.000$), yarn count ($p=0.019$) and core filament linear density ($p=0.000$) and interactive effects of yarn count*core filament linear density ($p=0.000$) and sheath fibre*yarn count*core filament linear density ($p=0.000$) except sheath fibre*core filament linear density ($p=0.225$) are found statistically significant level on fabric breaking elongation values. Therefore, yarn count, type of sheath fibre and core filament linear density influences the tensile properties of the woven fabrics significantly.

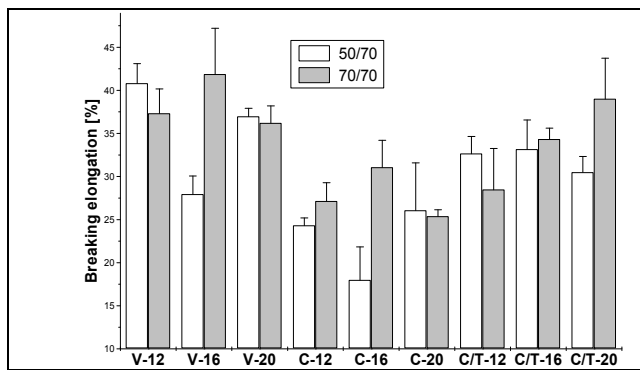


Figure 8. Breaking elongation values of woven fabrics

Bursting strength

Bursting strength is the ability of the fabric to resist rupture by pressure and depends on the tensile strength and extensibility of the material. In this study, the bursting strength of the fabrics knitted from the dual-core yarns produced from different sheath fibres and core filament linear density were measured for three different yarn counts and comparisons were realized. According to the results, bursting strength results of plain knitted fabrics in Figure 9 change depending on sheath fibre and core filament linear densities. Upon the general evaluation of the sheath fibres, dual-core yarns having cotton and cotton/Tencel sheath fibres give higher bursting strength values than that of the viscose sheath fibres due to strength characteristics of the sheath fibres. This result is agreed with findings of [27] in which investigated the yarn and fabric properties of different yarn types produced from various fibre types. On the other hand, ANOVA results indicate that the effect of sheath fibre ($p=0.000$), yarn count ($p=0.000$) and interactive effects of these parameters ($p=0.000$), sheath fibre*core filament linear density ($p=0.027$), sheath fibre*yarn count*core filament linear density ($p=0.000$) are found statistically significant level. However, core filament linear density ($p=0.204$) and sheath fibre*core filament linear

density ($p=0.250$) do not have statistically significant effect on fabric bursting strength. The usage of coarser core filament provides higher bursting strength values in 12 Ne and 16 Ne yarn counts for the fabrics having viscose and cotton sheath fibres while this case is observed in 20 Ne yarn count for cotton/Tencel sheath fibre.

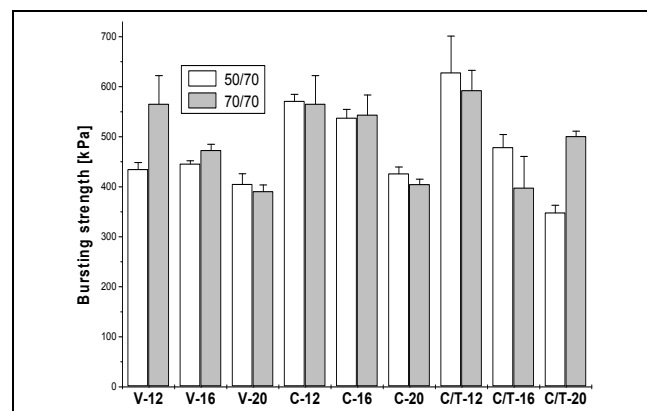


Figure 9. Bursting strength values of knitted fabrics

Bending rigidity

Bending resistance is the resistance of a certain size of textile sample to bend under its own weight and one of the parameter representing the fabric comfort. In the study, bending rigidity of the fabrics was tested for warp and weft direction and calculated for the samples and the results were given Figure 10. As far as the effect of sheath fibre type is concerned, the fabrics woven from dual-core yarns having cotton/Tencel sheath fibres have mostly higher rigidity values compared with that of the cotton and viscose sheathed fibres. However, the effect of the sheath fibre type and also yarn count are not statistically significant on bending rigidity of the fabrics. On the other hand, an investigation of the effect of the core filament linear density shows that bending rigidity of the fabrics change depending on yarn count and sheath fibre type. For viscose and cotton sheath fibres, coarser core filament leads to higher bending rigidity up to certain yarn counts and then rigidity decreases with core filament linear density. However, for cotton/Tencel sheath fibres, coarser core filament leads to lower fabric bending rigidity values.

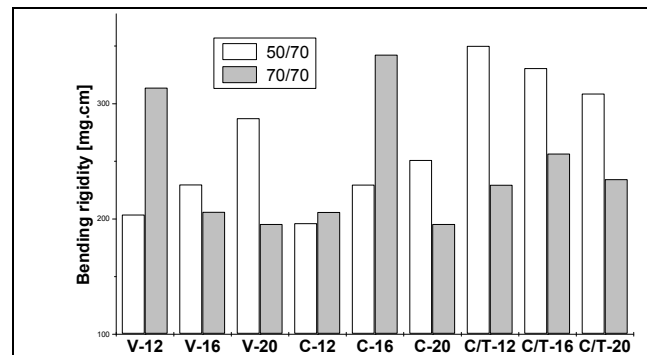


Figure 10. Bending rigidity results of woven fabrics

4. CONCLUSIONS

This study investigated dual-core yarn and fabric properties obtained by different sheath fibre types, yarn counts and core filament linear densities. The outstanding properties of dual-core yarns observed within the scope of this study can be summarized as follows.

- Regarding the effect of sheath fibre type, viscose and cotton/Tencel fibre sheath fibres have significantly lower yarn unevenness, imperfections and hairiness values and pilling behaviour resulted from fibre properties, particularly, fibre length, number of short fibres and low variation in fibre length. On the other hand, yarn and fabric tenacity values of dual-core yarns obtained by cotton/Tencel sheath fibres is better than the other yarns due to positive contribution of sheath fibre strength to the yarn tenacity while viscose sheath fibres give higher yarn and fabric elongation values because of the elongation of viscose fibre. Although its effect is considered insignificant, cotton/Tencel sheath fibres have mostly higher fabric bending rigidity values compared with that of the cotton and viscose sheath fibres.
- When the dual-core yarns become finer, yarn unevenness and imperfections increase while hairiness and tensile properties decrease as a result of decreasing number of sheath fibres in yarn structure.
- On the other hand, effect of core filament linear density on dual-core yarn and fabric properties changes depending on yarn count and sheath fibre types as determined in core-spun yarns having single elastic core filament. In a general expression, the results display an increasing or decreasing trend to a certain yarn count

while an opposite trend occurs beyond this yarn count for each sheath fibre type, particularly cotton and other sheath fibre types. This case is probably due to improperly coating of core filament, more possibility of displacement of the core filament and disrupting the sheath fibres orientation resulted from changes in number of fibres and fibre properties related from sheath fibre characteristics and yarn counts. Additionally, tenacity of dual-core yarns increases with finer core filaments while higher breaking elongation is obtained with coarser ones in dual-core yarns.

- Statistical results also indicates the significant effect of production parameters of the sheath fibre type and yarn count on yarn unevenness, thick places, neps, yarn hairiness and fabric bursting strength. On the other hand, all production parameters of dual-core yarns have a relatively higher significant influence on tensile properties of the dual-core yarns and hence woven fabrics.

At the end of this study, some findings related with the dual-core yarns with limited number of findings are presented to the literature and also obtained some results about the effect of various process parameters on dual-core yarn and some of the fabric properties.

ACKNOWLEDGEMENTS

The authors also wish to express their gratitude to MinaTekstil San. Tic. A.Ş. (Kahramanmaraş/Turkey) for the sample preparation and ADIM Tekstil San. Tic. A.Ş. (İsparta/Turkey), GÖKHAN Tekstil San. Tic. A.Ş. (Denizli/Turkey) and Comfytex (Kayseri/Turkey) for the sample testing.

REFERENCES

1. Hua T, Wong NS, Tang WM. 2018. Study on properties of elastic core-spun yarns containing a mix of Spandex and PET/PTT bi-component filament as core *Textile Research Journal* 88(9), 1065-1076.
2. Kılıç G. 2017. Improving quality in core-spun yarn production. PhD thesis, Erciyes Üniversitesi, Natural and Applied Sciences, Kayseri, Turkey.
3. El-Tantawy S, Sabry M, Bakry M. 2007. The effect of different weft yarn production technique on the pilling property of jeans fabrics *International Design Journal* 7(3), 161-169.
4. Ertas OG, Ünal BZ, Celik N. 2016. Analyzing the effect of the elastane-containing dual-core weft yarn density on the denim fabric performance properties *The Journal of The Textile Institute* 107(1), 116-126.
5. Bizjak M, Kadoğlu H, Kostanjsek K, Çelik P, Bayraktar GB, Duran D, Dimitrovski K. 2017. Properties of elastic fabrics with treated and untreated Co/PBT yarns in weft direction *IOP Conference Series: Materials Science and Engineering* 254(9), 092001.
6. Kaynak HK. 2017. Optimization of stretch and recovery properties of woven stretch fabrics *Textile Research Journal* 87(5), 582-592.
7. Broega AC, Rocha AM, Souto AP, Ferreira F, Oliveira L. 2016. Development and characterization of cotton elastic yarns to improve wear comfort of bi-elastic thin fabrics. *16th Autex World Textile Conference* 2016 June 8–10, Ljubljana, Slovenia.
8. Kadoğlu H, Dimitrovski K, Marmaralı A, Çelik P, Bayraktar G, Bedez Üte T, Ertekin G, Demsar A, Kostanjek K. 2016. Investigation of the characteristics of elasticised woven fabric by using PBT filament yarns *Autex Research Journal* 16(2), 109-117.
9. Maqsood M, Tanveer H, Mumtaz HM, NawabY. 2016. Modeling the effect of elastane linear density, fabric thread density, and weave float on the stretch, recovery, and compression properties of bi-stretch woven fabrics for compression garments *The Journal of The Textile Institute* 107(3), 307-315.
10. Akankwasa NT, Jun W, Yuze Z, Mushtaq M. 2014. Properties of cotton/T-400 and 100% cotton plain knitted fabric made from ring spun yarn *Materialwissenschaft und Werkstofftechnik* 45(11), 1039-1044.
11. Akankwasa NT, Wang J, Zhang Y. 2015. Study of optimum spinning parameters for production of T-400/cotton core spun yarn by ring spinning *The Journal of The Textile Institute* 107(4), 504-511.
12. Qadir MB, Hussain T, Malik M, Fahemm A, Jeong SH. 2014. Effect of elastane linear density and draft ratio on the physical and mechanical properties of core-spun cotton yarns *Journal of Textile Institute* 105(7), 753-759.

-
13. Das A, Chakraborty R. 2013. Studies on elastane-cotton core-spun stretch yarns and fabrics: Part I-Yarn characteristics *Indian Journal of Fibre&Textile Research* 38, 237-243.
14. Helali H, Babay AD, Msahli S. 2012. Influence of dorlastan draft and yarn count on the elastic recovery of the dorlastan core spun yarns *Following Cyclic Test* 103(4), 378-374.
15. Mourad MM, Elshankery MH, Almetwally AA. 2012. Physical and stretch properties of woven cotton fabrics containing different rates of Spandex *Journal of American Science* 8(4), 567-572.
16. Adeli B, Akbar A, Shanbeh GM. 2011. Structural evaluation of elastic core-spun yarns and fabrics under tensile fatigue loading *Textile Research Journal* 81(2), 137-147.
17. Baghaei B, Shanbeh M, Ghareaghaji AA. 2010. Effect of tensile fatigue cyclic loads on bagging deformation of elastic woven fabrics *Indian Journal of Fibre&Textile Research* 35, 298-302.
18. Çelik P, Bedez Üte T, Özden D, Çömlekçi H, Akkale EC. 2009. Öz/manto oranı ve büüküm sayısının filament özlü ipliklerin iplik özelliklerine etkisi *Tekstil Teknolojileri Elektronik Dergisi* 3(2), 29-37.
19. Herath CN, Kang BC 2008. Dimensional stability of core spun cotton/Spandex single jersey fabrics under relaxation *Textile Research Journal* 78(3), 209-216.
20. Özdi N. 2008. Stretch and bagging properties of denim fabrics containing different rates of elastane *Fibres & Textiles in Eastern Europe* 16(1), 66.
21. El-Ghezal S, Babay A, Dhouib S, Cheikhrouhou M. 2009. Study of the impact of elastane's ratio and finishing process on the mechanical properties of stretch denim *The Journal of The Textile Institute* 100(3), 245-253.
22. Dhub AB, El-Ghezal S, Cheikhrouhou M. 2006. A study of the impact of elastane ratio on mechanical properties of cotton wrapped elastane-core spun yarns *The Journal of the Textile Institute* 97(2), 167-172.
23. Demirbaş S. 2005. Farklı elastomerik elyaf çeşitlerinin fiziksel özelliklerinin karşılaştırılması. Yüksek Lisans Tezi, Süleyman Demirel Üniversitesi, Fen Bilimleri Enstitüsü, Isparta.
24. Vuruşkan D. 2010. The Optimization Of Production Variables Of Modified Ring Spinning Machine For Producing Yarn With Elastane And Effect Of Variables On Yarn Quality. PhD thesis, Çukurova University, Natural and Applied Sciences, Adana, Turkey.
25. Hu J, Lu J, Zhu Y. 2008. New developments in elastic fibers *Polymer Reviews* 48(2), 275-301.
26. Celikkann SH. 2018. An Investigation Of The Yarn And Fabric Properties Of Core And Dual Core Elastane Spun Yarns. MSc. Thesis, Süleyman Demirel University, Natural and Applied Sciences, Isparta, Turkey.
27. Erdumlu N, Ozipek B, Oztuna AS, Cetinkaya S. 2009. Investigation of vortex spun yarn properties in comparison with conventional ring and open-end rotor spun yarns *Textile Research Journal* 79(7), 585-595.
28. Kilic M, Okur A. 2011. The properties of cotton-Tencel and cotton-Promodal blended yarns spun in different spinning systems *Textile Research Journal* 81(2), 156-172.
29. Örtlek HG, Ülkü Ş. 2007. Effects of Spandex and yarn counts on the properties of elastic core-spun yarns produced on Murata vortex spinner *Textile Research Journal* 77(6), 432-436.
30. Kim HJ, Yang HW, Zhu CH, Huh Y. 2009. Influence of the core-sheath weight ratio and twist on the tensile strength of the ring core yarns with high tenacity filaments *Fibers And Polymers* 10(4), 546-550.
31. Babaarslan O. 2001. Method of producing a polyester/viscose core-spun yarn containing Spandex using a modified ring spinning frame *Textile Research Journal* 71(4), 367-371.



Hazard and Risk Analysis for Ring Spinning Yarn Production Process by Integrated FTA-FMEA Approach

Nazlı GÜLÜM MUTLU, SERKAN ALTUNAŞ

Department of Industrial Engineering, Yıldız Technical University, Istanbul, Turkey

Corresponding Author: Nazlı GÜLÜM MUTLU, ngmutlu@yildiz.edu.tr

ABSTRACT

The hazard analysis and management is vital in textile industry to avoid losing customers and wasting resources caused by the failures in production systems. Risk analysis is also very significant to decrease possible hazards and to avoid possible damage in production systems. In this study, an approach based on Failure Mode and Effects Analysis (FMEA) and Fault Tree Analysis (FTA) is proposed to analyze the ring spinning yarn production process in a textile industry. First, the possible hazards in the production line, yarn production system, in an integrated company operating in the textile sector are analyzed by FTA method. Then, FMEA is applied to ring spinning yarn production process in a textile industry to rank all possible risks corresponding to hazards in descending order with respect to both occupational health and safety. It is very important to remove all possible hazards in textile industry to decrease the number of risks related to occupational health and safety. Therefore, in total of 57 hazard root causes are determined in the yarn production department. Subsequently, the faults related to the hazard root causes are examined by FTA and then risk corresponding to these hazards are prioritized by FMEA. The results obtained from the proposed FTA-FMEA approach show that decision makers and engineers can easily decrease the number of hazards and risks with respect to both occupational health and safety in practice.

1. INTRODUCTION

Reducing the failures and hazards is crucial for a company to maintain their position on the market, to increase their competitiveness in the market, and to contribute to the country's economic development. The failure and hazard management is known to reduce the defects in the production system, to increase the effective use time of the machines and the equipment, to decrease customer complaints and to increase productivity [1]. Analyzes of production process and improvement of processes efficiency in the textile industry are also important to increase the competitiveness of firms [2, 3]. Güner and İşler [4] examined the effect of equipment conditions on process efficiency. Burdak and Krenczyk [5] pointed out that the potential risks in production systems must be managed to ensure effective management of enterprises. The focus of the risk management is to identify hazards associated with

functional units and their components, to estimate and evaluate the risks, and to carry out activities to prevent risks and their constant control [6]. Peddada [7] and Hiles [8] emphasized that risk management performance is important to ensure business continuity and is an indicator for the success of management. The quality of textile products is directly related to yarn quality. Yarn quality also depends on the production conditions. In order to improve yarn quality in the literature, many number of studies have been conducted to optimize production conditions [9-14]. Küçük and Güner [2] analyzed the efficiency value of firms in the textile industry by using fuzzy logic approach and ranked criteria that have impact on efficiency value. Also, synthetic fiber and cotton are the most basic substances for textile products. However, the life cycle of synthetic fibers and cotton has a negative impact on the environment [15]. Therefore, it is obvious that the present fiber or cotton

To cite this article: Mutlu NG, Altuntaş S. 2019. Hazard and risk analysis for ring spinning yarn production process by integrated FTA-FMEA approach. *Tekstil ve Konfeksiyon* 29(3), 208-218.

should be used in the least-loss manufacturing. Therefore, it is necessary to analyze the production processes, to define hazards and to take necessary measures. One of the leading sectors in Turkey is textile sector. It has an important role in Turkish economy as it creates new job opportunities and contributes to the development of the economy [16, 17]. Analyzing the factors that threaten the sustainability the development of textile sector is very important due to its effect on quality of the products and reduction of production loss [18].

There are also risks that threaten occupational health and safety in the textile industry. Malik et al. [19] pointed out that there are many risks related to workers in the textile industry, such as physical, chemical, biological, and determined the role of hazards control measures in Occupational Health and Safety (OHS) in textile industry. Khan et al. [20] focused on the occupational health and safety in the textile industries of Lahore as well.

In literature, studies, which examined textile production conditions, have basically focused on optimization. But, there are limited number of studies, which has been focused on definition and classification of hazards in the ring spinning yarn process. Therefore, in the present study, the hazards in the ring spinning production facility of an enterprise in the textile sector is analyzed and risks corresponding to these hazards are ranked by using FTA-FMEA approach. It is believed that the results obtained from FTA-FMEA approach provided useful information to reduce losses and prevent failures and hazards.

2. LITERATURE REVIEW

The potential risks in production systems can be mainly caused by failures and hazards due to the material, human, production measurement method and machines/equipment. The risk analysis and evaluation methods with top-down or bottom-up approaches can be evaluated to reduce the risks in the systems. In the literature, hazard and risk analysis methods are used to define undesirable events and their status in production systems. What-If [21], Checklist [21, 22], Preliminary hazard analysis (PHA) [21, 23, 24], Fault tree and Event tree analysis (FTA) [22, 24], Subsystem hazard analysis (SSHA) [24], System hazard analysis (SHA) [24] are some of the methods used for hazard analysis. Furthermore, Failure Mode and Effect Analysis (FMEA) [6, 25, 26], Hazard and Operability (HAZOP) [6, 26], Human reliability analysis (HRA) [22], Probabilistic risk assessment (PRA) [24] are extensively used for risk analysis in production systems.

FMEA method is one of the well-known method and it is used for the identification of possible hazard types in various areas of the textile sector, taking precaution for eliminating hazards or reducing their effects to improve process performance in the literature. Beyene et al. [27] implemented FMEA to identify defects that led to production stoppages in a textile firm, found out that stoppage time can be reduced and the productivity can be

increased. Küçük et al. [28] identified the failure modes in the laying and cutting process in the clothing sector by using FMEA tool. Paired et al. [29] used the FMEA method to detect garment manufacturing defects and to develop a quality control system and then to analyze the optimization of production efficiency using a simulation-based optimization technique. Kumar et al. [30] analyzed the processing failures affecting the process by using FMEA method in addition to value streaming analysis and Kaizen tools to reduce the cycle time of T-shirt production. Kaewsom and Rojanarowan [31] conducted the FMEA study to reduce the failure of the broken filament in the direct spinning process. Özyazgan [32] conducted FMEA analysis and implementation in a textile factory producing woven fabric. Peddada [7] categorized risks as business risk, control risk, opportunity risk and personal risk and stated that they are used in FMEA method in the evaluation of the risks.

In addition, Liu et al. [33] reported the major shortcomings of FMEA based on literature review. They are given in the following [33]:

1. The relative importance among O, S and D is not taken into consideration.
2. Different combinations of O, S and D may produce exactly the same value of RPN, but their hidden risk implications may be totally different.
3. The three risk factors are difficult to be precisely evaluated.
4. The mathematical formula for calculating RPN is questionable and debatable.
5. The conversion of scores is different for the three risk factors.
6. The RPN cannot be used to measure the effectiveness of corrective actions.
7. RPNs are not continuous with many holes.
8. Interdependencies among various failure modes and effects are not taken into account.
9. The mathematical form adopted for calculating the RPN is strongly sensitive to variations in risk factor evaluations.
10. The RPN elements have many duplicate numbers.
11. The RPN considers only three risk factors mainly in terms of safety.

The FMEA may be insufficient to identify hazards due to the fact that it focus on failure mode [24]. In this study, integrated FTA-FMEA approach is used to identify hazards and to focus on failure modes.

There are also studies using FTA and FMEA methods together in the literature [34-37]. Martins and Gorscak [38] deeply analyzed the root causes of the failures by applying the FTA for the critical failures after ranking failure types carrying out an FMEA study for the safety-critical systems.

The literature review revealed that the FMEA and FTA methods have been determined to be a useful method and frequently used for failure analysis for the systems and their components and ranking the risk potentials of the failures. For this reason, the FTA and FMEA methods have been integrated and used in order to analyze the hazards in the ring spinning yarn production of a company operating in the textile sector within the scope of this study.

3. MATERIAL AND METHOD

3.1 Materials

In this study, the FTA-FMEA application has been implemented for a ring spinning yarn production of a company operating in the textile sector. There are 20 ring spinning machines with 1,200 spindles in the ring spinning facility. The annual ring spinning production capacity of the company is 5,000 tons (90% combed cotton and 10% carded). The blow room, foreign matter control, carding, draw-frame, the wadding preparation, wadding transfer, combed cotton, cording, ring, coil, mobile cleaner, fixation, coil winding, bale-opening, needle opening, electromagnet mixer, condenser, feeding unit, and fine opening machines are used in ring spinning facility.

3.2 Methods

3.2.1 Failure Mode and Effect Analysis (FMEA)

The FMEA method is a systematic approach used to identify and prevent failures in the product and the production processes before they occur. It identifies the failures with a bottom-up approach [1]. FMEA uses three important inputs, namely the Occurrence (O), Severity (S) and Detectability (D), related to potential hazards/failures in a system, design, process, or equipment and to provide an input for mitigation measures to mitigate risk [6, 25]. For FMEA application, the information on system structure, defining system boundary for the analysis, and the level of analysis and analysis procedure are available at IEC 61812: 2006. Also, some of the terms used in the method are as follows [25].

- **Item:** Any part, component, device, subsystem, functional unit, equipment or system that can be individually considered.
- **Failure:** Termination of the ability of an item to perform a required function.
- **Failure mode:** Manner in which an item fails.
- **Failure effect:** Consequence of a failure mode in terms

of the operation, function or status of the item.

- **Failure severity:** Failure mode effect severity as related to the defined boundaries of the analyzed system.
- **System:** Set of interrelated or interacting elements.

The Risk Priority Number (RPN) is calculated as shown in Equation 1,

$$RPN = (O)(S)(D) \quad (1)$$

where, O denotes occurrence which implies the probability of occurrence of a failure mode for a predetermined or stated time period, D means detectability, i.e. an estimate of the chance to identify and eliminate the failure before the system or customer is affected and S is a non-dimensional number that stands for severity, i.e. an estimate of how strongly the effects of the failure will affect the system or the user [25]. Classification of RPN is given in Table 1.

FTA method is a hazard analysis and evaluation method using a top-down approach and it also allow showing the diagrams of the logical relationship between the root causes of the possible hazards and the top event due to those root causes [7]. The FTA method is used to describe the multiple hazards conditions that cause two or more events that lead the occurrence of the top event. The logic gate symbols and the event symbols are given in Table 2.

3.2.2 Fault Tree Analysis (FTA)

The logic gate symbols and the event symbols are frequently used in establishing logical relationships between the root causes of the hazards. Also, some of the terms used in the method are as follows [39].

Table 1. Classification of RPN

Classification	RPN
Intolerable	>201
High	101-200
Moderate	51-100
Tolerable	1-50

3.2.3 Integration of FTA and FMEA Methods

In this study, the FTA and FMEA methods have been integrated and used to analyze the failures in the production system, to determine the root causes, and to rank them. The proposed FTA-FMEA approach is given in Figure 1. As can be seen from Table 2, there are 2 logic gates and 4 event symbols. Step 6 and Step 7 are related to FTA. Furthermore, the remaining steps except for Step 6 and Step

Table 2. Logic gate symbols and event symbols [7]

Gate Symbol	Gate Name	Causal Relation	Event Symbol	Event Name	Meaning
	AND	Output event occurs if all input events occur simultaneously		CIRCLE	Basic event with sufficient data
	OR	Output event occurs if any one of the input events occurs		DIAMOND	Undeveloped event
				RECTANGLE	Event represented by a gate
				TRIANGLE	Transfer symbol

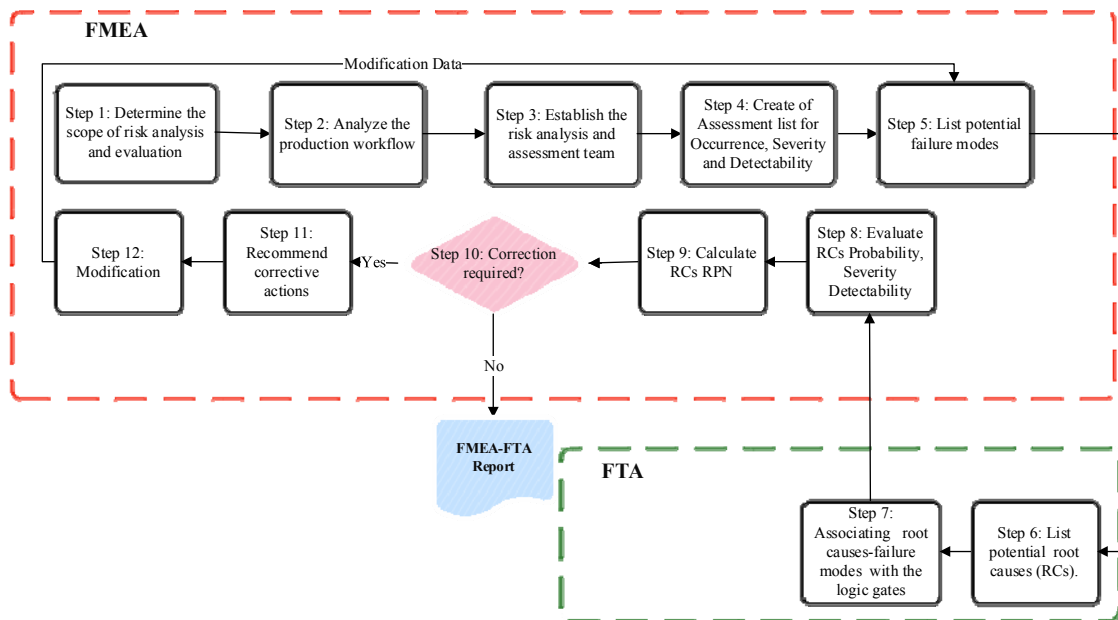


Figure 1. The proposed FTA-FMEA approach.

Table 3. The experts interviewed to obtain the failure information in the ring spinning department

Branch	Department	Experience (year)
<i>Mechanical Engineering</i>	Ring Spinning Manager	20
<i>Mechanical Engineering</i>	Ring Spinning Production Chief	10
<i>Mechanical Engineering</i>	Ring Spinning Maintenance Chief	2
<i>OHS Specialist</i>	Plant Manager	10

7 are related to the FMEA. The steps belong to FMEA calculate the RPN of the potential failures, while the steps belong to FTA identify the potential root causes and find the associations between root causes and failure modes.

The benefit of an integrated analysis are the following [39]:

- FTA is a top-down and FMEA a bottom-up analysis method and use of both deductive and inductive reasoning is regarded as a good argument for providing assurance for the completeness of an analysis;
- Safety standards often demand a single failure and, in some cases, a multiple failure analysis, the first requirement being fulfilled by FMEA. Both single and multiple failure analysis are accomplished by FTA;
- FMEA is also a useful method for a comprehensive identification of basic events or risks, while FTA is a practical method for causal analysis of the undesirable events or hazards.

4. RESULT AND DISCUSSION

A total of 57 failure root causes have been identified in the ring spinning production facility. These faults are classified in three main categories as the failures that decrease the quality of the yarn and increase the cost by adversely affecting the production process, the machine failures that lead to halts in the production, and the hazardous situations

that can cause a fire in the facility. Ring spinning yarn production workflow is given in Figure 2. Figure 3 shows the result of FTA for ring spinning production operation. Ring spinning yarn production workflow is taken into account to identify failure modes in the ring spinning process (See Figure 1). The experts given in Table 3 are interviewed to obtain the failure information in the ring spinning department. Table 4, Table 5 and Table 6 are used for evaluation criteria. The Occurrence (O) value, Severity (S) value and Detection value (D) for the each root causes are given in Table 8. The root causes of failure are ranked based on the experts' evaluations. Twenty-two different RPN values ranging from 16-900 have been obtained for 57 root causes of the failures determined for the ring spinning facility. The possible failure modes and the root causes of the failures of the ring spinning facility are described in Table 7. The rankings of the identified failures are shown in Table 9. It has been determined that 22.80% of the identified failures were intolerable, 15.78% were high, 28.07% were moderate, and 37.35% were tolerable.

5. CONCLUSION

An approach based on FTA and FMEA is proposed to analyze hazard and risk analysis for ring spinning yarn production process. In the first stage of the proposed approach, possible root causes are determined and casual

relations among hazards are found by FTA. There main possible hazards (production process failures, machines failure and fire failure related to occupational health and safety) are defined related to the process under concern. Then, FMEA is utilized to rank risks. The results of the case study show that 60% of failures related to production process and 46.66% of failures related to fire are risky at intolerable level, while failures related to machines are risky at moderate level in ring spinning yarn production process in the textile factory. In addition, the results of this study show that failures are occurred due to at least one root

cause. It is necessary to take action plans to prevent these failures in the production system. Especially, the failures having the highest RPN should be eliminated from root causes in the ring spinning process. If the elimination of the failures are not possible, the RPN of these type failures should be decreased at an acceptable level. In addition, total productive maintenance policies should be applied to ring spinning yarn production process to remove all failures related to machine in practice.

Fuzzy logic can be used for the risk analysis in the future research.

Table 4. The Occurrence related to frequency and probability of occurrence [25]

Rating	Occurrence	Frequency	Probability
10	Very High: Inevitable failure	>100, per thousand operations	$\geq 10^{-1}$
9		50, per thousand operations	5×10^{-2}
8	High: Inevitable failure	20, per thousand operations	2×10^{-2}
7		10, per thousand operations	1×10^{-2}
6		5, per thousand operations	5×10^{-3}
5	Moderate: Occasional failure	2, per thousand operations	2×10^{-3}
4		1, per thousand operations	1×10^{-3}
3	Low: Relatively few failure	0.05, per thousand operations	5×10^{-4}
2		0.1, per thousand operations	1×10^{-4}
1	Remote: Failure is unlikely	<0.001, per thousand operations	$\leq 10^{-5}$

Table 5. The severity evaluation criteria [25]

Severity	Criteria	Ranking
Hazardous without warning	Very high severity ranking when a potential failure mode affects safe vehicle operation and/or involves non-compliance with government regulation without warning.	10
Hazardous with warning	Very high severity ranking when a potential failure mode affects safe vehicle operation and/or involves non-compliance with government regulation with warning.	9
Very high	Vehicle/item inoperable (loss of primary function).	8
High	Vehicle/item operable but at a reduced level of performance.	7
Moderate	Vehicle/item operable but comfort/convenience item(s) inoperable.	6
Low	Vehicle/item operable but comfort/convenience item(s) operable at a reduced level of performance.	5
Very low	Fit and finish/squeak and rattle item does not conform (greater than 75 %).	4
Minor	Fit and finish/squeak and rattle item does not conform (approximately 50 %).	3
Very minor	Fit and finish/squeak and rattle item does not conform (less than 25 %).	2
None	No discernible effect.	1

Table 6. The detection evaluation criteria [25]

Detection	Criteria: Likelihood of detection	Ranking
Absolutely uncertain	Process Control will not and/or cannot detect a potential cause/mechanism and subsequent failure mode; or there is no Process Control.	10
Very remote	Very remote chance the Process Control will detect a potential cause/mechanism and subsequent failure mode.	9
Remote	Remote chance the Process Control will detect a potential cause/mechanism and subsequent failure mode.	8
Very low	Very low chance the Process Control will detect a potential cause/mechanism and subsequent failure mode.	7
Low	Low chance the Process Control will detect a potential cause/mechanism and subsequent failure mode.	6
Moderate	Moderate chance the Process Control will detect a potential cause/mechanism and subsequent failure mode.	5
Moderately High	Moderately high chance the Process Control will detect a potential cause/mechanism and subsequent failure mode.	4
High	High chance the Process Control will detect a potential cause/mechanism and subsequent failure mode.	3
Very high	Very high chance the Process Control will detect a potential cause/mechanism and subsequent failure mode.	2
Almost certain	Process Control will almost certainly detect a potential cause/mechanism and subsequent failure mode.	1

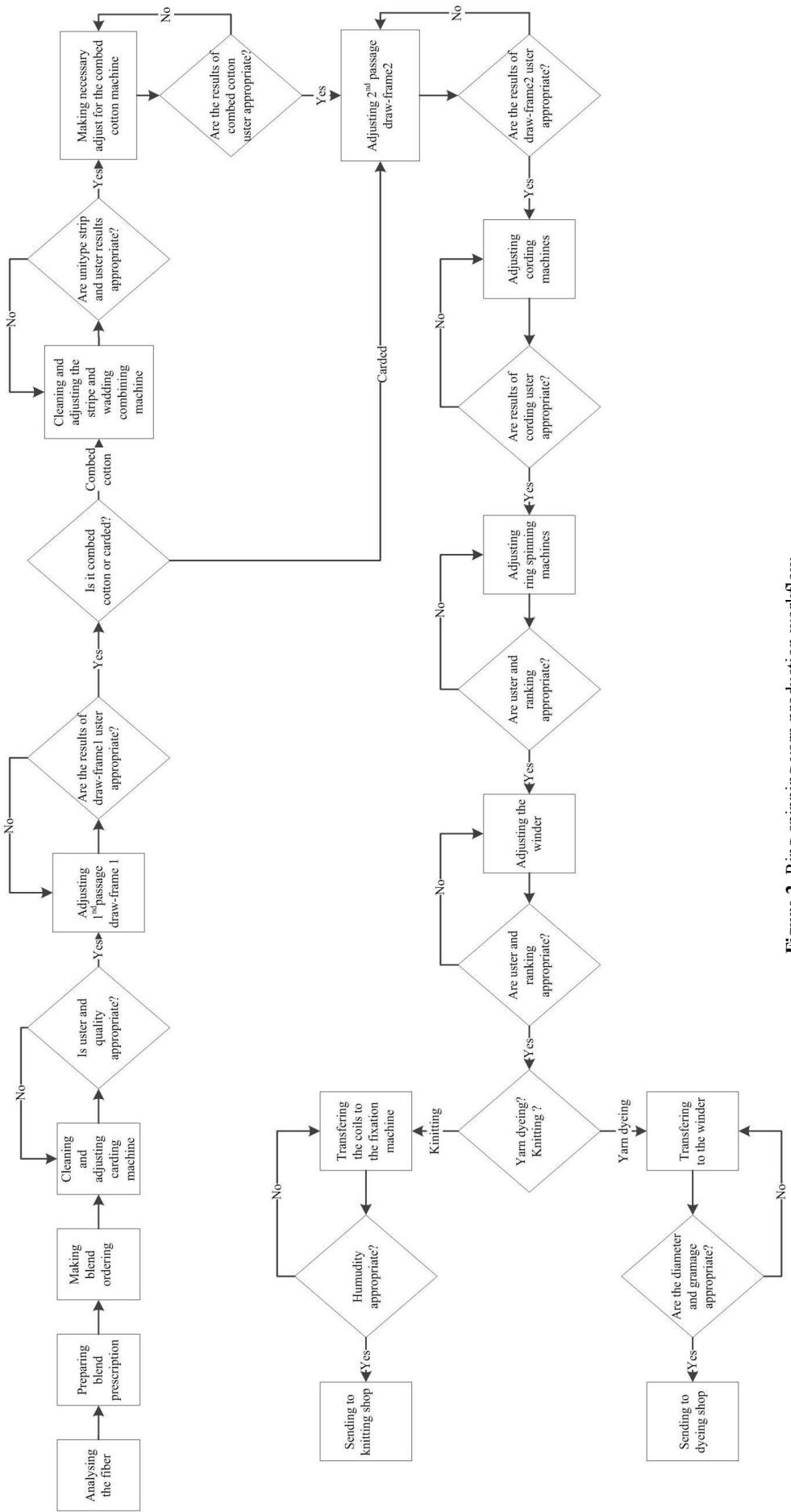


Figure 2. Ring spinning yarn production workflow

Table 7. The possible failure modes and the root causes for the ring spinning yarn production process

Function	Failure Mode	Root Cause of the Failure	FM_i^j
Production Process	Abrage	Blend prescription not prepared correctly	FM ₁ ¹
		The ordering of fiber bundles incompliant with the blend prescription	FM ₁ ²
		Not arranging the carding buckets under the draw-frame in accordance with the desired plan	FM ₁ ³
		Blending differences	FM ₁ ⁴
	Incorrect yarn number	Not setting the yarn number to the machine	FM ₂ ¹
		Failure of the regulation system in the regulated draw-frames	FM ₂ ²
	Quality	Not cleaning the ring spinning machine	FM ₃ ¹
		Formation of neps due to short fibers or immature fibers	FM ₃ ²
		Insufficient cleaning of the flies	FM ₃ ³
	Production	Not procuring cotton with the suitable-quality values for the ring spinning facility	FM ₄ ¹
Machines	Failure of Press Machine	Failure of hydraulic system	FM ₅ ¹
		Failure of automatic bundle opening machine	FM ₆ ¹
	Failure at the blow room line	Failure of the homogenous mixer	FM ₆ ²
		Carding machine failure	FM ₆ ³
		Failure of the fiber cleaning machine	FM ₆ ⁴
		Failure of the draw frame machine	FM ₇ ¹
	Failure of the cord preparation line	Fiber winding around the rotating element of the combed cotton machine	FM ₇ ²
		Breakage of the belt at cording machine	FM ₇ ³
		Bearing failure at cording machine	FM ₇ ⁴
		Engine failure at cording machine	FM ₇ ⁵
	Failure of the Unilap machine	Failure of pneumatic system tube	FM ₈ ¹
		Deformation of the felts of the pneumatic system	FM ₈ ²
		Breaking of the springs in the clutch system	FM ₈ ³
		Distance setting failure	FM ₈ ⁴
		Bearing failure	FM ₈ ⁵
	Failure of ring spinning machine	Servo disk failure	FM ₉ ¹
		Robo-load failure	FM ₉ ²
		Doffer failure	FM ₉ ³
		Motor failure	FM ₉ ⁴
		Failure of spindle system	FM ₉ ⁵
	Carding machine failure	Failure of pulling system	FM ₉ ⁶
		Not replacing the card clothing	FM ₁₀ ¹
	Cot grinding machine failure	Grinding setting failure	FM ₁₁ ¹
	Air conditioning failure	Motor failure	FM ₁₂ ¹
		Front filter failure	FM ₁₂ ²
	Winder failure	Failure of bobbin changer's mechanic element	FM ₁₃ ¹
		Failure of bobbin changer's holder	FM ₁₃ ²
		Bobbin changer setting failure	FM ₁₃ ³
		Suction fan motor bearing failure	FM ₁₃ ⁴
		Suction fan motor winding failure	FM ₁₃ ⁵
		Setting failure of the mechanical element in the spindle	FM ₁₃ ⁶
		Deformation failure in the spindle	FM ₁₃ ⁷

Table 7. The possible failure modes and the root causes for the ring spinning yarn production process (Cont.)

Function	Failure Mode	Root Cause of the Failure	FM _i ¹
Fire	Fire Hazard in the Blowroom line	Getting metal from the condenser	FM ₁₄ ¹
		Getting burning fiber from the condenser	FM ₁₄ ²
		Getting metal from the recycling machine	FM ₁₄ ³
		Getting burning fiber from the recycling machine	FM ₁₄ ⁴
		Electric arc in the press control panel	FM ₁₄ ⁵
	Fire hazard in the carding machine	Uncontrolled spreading of the sparks in the press welding process	FM ₁₄ ⁶
		Fiber winding around the rollers of the carding machine	FM ₁₄ ⁷
		Entry of foreign matter such as metal into the carding machine	FM ₁₄ ⁸
		Fiber winding around the rollers of the combed cotton machine	FM ₁₅ ¹
		Electric arc failure in the ring spinning machine	FM ₁₆ ¹
Fire Hazard in the ring spinning machine	Fire Hazard in the ring spinning machine	Unfunctional switches in the ring spinning machine pulling area	FM ₁₆ ²
		Electric arc failure in the cording machine	FM ₁₇ ¹
	Fire hazard in the cording machine	Fiber winding around the rollers of the cord pulling cylinder	FM ₁₇ ²
		Electric arc failure in the winding machine	FM ₁₈ ¹
Fire hazard in the metal detector	Fire hazard in the metal detector	Putting the cotton coming from the metal detector to recycling without any selection	FM ₁₉ ¹

Table 8. The Occurrence (O) value, Severity (S) value and Detection value (D) for the each root causes

FM _i ¹	O	S	D	FM _i ¹	O	S	D	FM _i ¹	O	S	D
FM ₁ ¹	7	10	10	FM ₈ ¹	2	8	4	FM ₁₃ ⁶	3	4	4
FM ₁ ²	6	10	10	FM ₈ ²	2	8	4	FM ₁₃ ⁷	3	4	4
FM ₁ ³	8	10	5	FM ₈ ³	2	8	4	FM ₁₄ ¹	3	10	7
FM ₁ ⁴	7	10	10	FM ₈ ⁴	2	8	4	FM ₁₄ ²	3	10	7
FM ₂ ¹	8	5	5	FM ₈ ⁵	2	8	4	FM ₁₄ ³	5	10	7
FM ₂ ²	8	5	5	FM ₉ ¹	2	2	4	FM ₁₄ ⁴	5	10	7
FM ₃ ¹	3	8	5	FM ₉ ²	2	2	4	FM ₁₄ ⁵	1	10	7
FM ₃ ²	8	8	5	FM ₉ ³	2	2	4	FM ₁₄ ⁶	1	10	7
FM ₃ ³	8	8	3	FM ₉ ⁴	3	7	4	FM ₁₄ ⁷	2	10	7
FM ₄ ¹	8	10	5	FM ₉ ⁵	2	2	4	FM ₁₄ ⁸	2	10	7
FM ₅ ¹	3	7	2	FM ₉ ⁶	2	2	4	FM ₁₅ ¹	3	10	7
FM ₆ ¹	3	7	2	FM ₁₀ ¹	1	10	4	FM ₁₆ ¹	5	3	7
FM ₆ ²	3	7	2	FM ₁₁ ¹	1	10	4	FM ₁₆ ²	10	7	9
FM ₆ ³	4	3	2	FM ₁₂ ¹	3	7	4	FM ₁₇ ¹	5	3	7
FM ₆ ⁴	3	7	4	FM ₁₂ ²	3	7	4	FM ₁₇ ²	5	3	7
FM ₇ ¹	4	3	4	FM ₁₃ ¹	3	3	4	FM ₁₈ ¹	2	5	7
FM ₇ ²	3	4	4	FM ₁₃ ²	3	3	4	FM ₁₉ ¹	10	10	9
FM ₇ ³	2	8	4	FM ₁₃ ³	3	3	4				
FM ₇ ⁴	2	8	4	FM ₁₃ ⁴	2	6	4				
FM ₇ ⁵	2	8	4	FM ₁₃ ⁵	2	6	4				

Table 9. RPN and ranking for root causes of failure

FM _i ¹	RPN	Ranking	FM _i ¹	RPN	Ranking	FM _i ¹	RPN	Ranking
FM ₁ ¹	700	2	FM ₈ ¹	64	16	FM ₁₃ ⁶	48	17
FM ₁ ²	600	4	FM ₈ ²	64	16	FM ₁₃ ⁷	48	17
FM ₁ ³	400	5	FM ₈ ³	64	16	FM ₁₄ ¹	210	8
FM ₁ ⁴	700	2	FM ₈ ⁴	64	16	FM ₁₄ ²	210	8
FM ₂ ¹	200	9	FM ₈ ⁵	64	16	FM ₁₄ ³	350	6
FM ₂ ²	200	9	FM ₉ ¹	16	22	FM ₁₄ ⁴	350	6
FM ₃ ¹	120	12	FM ₉ ²	16	22	FM ₁₄ ⁵	70	15
FM ₃ ²	320	7	FM ₉ ³	16	22	FM ₁₄ ⁶	70	15
FM ₃ ³	192	10	FM ₉ ⁴	84	14	FM ₁₄ ⁷	140	11
FM ₄ ¹	400	5	FM ₉ ⁵	16	22	FM ₁₄ ⁸	140	11
FM ₅ ¹	42	18	FM ₉ ⁶	16	22	FM ₁₅ ¹	210	8
FM ₆ ¹	42	18	FM ₁₀ ¹	40	19	FM ₁₆ ¹	105	13
FM ₆ ²	42	18	FM ₁₁ ¹	40	19	FM ₁₆ ²	630	3
FM ₆ ³	24	21	FM ₁₂ ¹	84	14	FM ₁₇ ¹	105	13
FM ₆ ⁴	84	14	FM ₁₂ ²	84	14	FM ₁₇ ²	105	13
FM ₇ ¹	48	17	FM ₁₃ ¹	36	20	FM ₁₈ ¹	70	15
FM ₇ ²	48	17	FM ₁₃ ²	36	20	FM ₁₉ ¹	900	1
FM ₇ ³	64	16	FM ₁₃ ³	36	20			
FM ₇ ⁴	64	16	FM ₁₃ ⁴	48	17			
FM ₇ ⁵	64	16	FM ₁₃ ⁵					

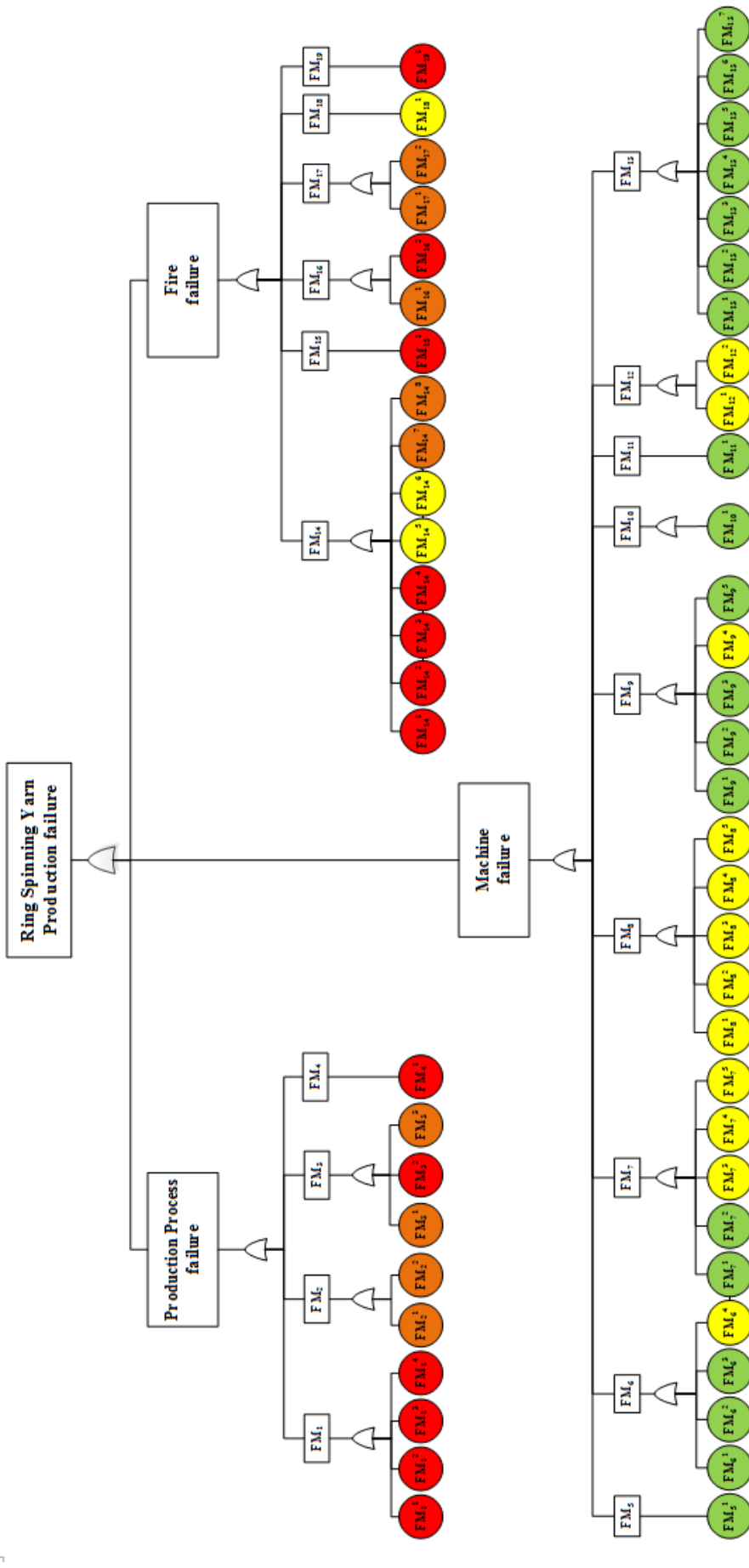


Figure 3. Fault Tree Analysis in the ring spinning yarn production process

REFERENCES

1. Mikulak RJ, McDermott R, Beauregard M. 2008. *The basics of FMEA*. New York:CRC Press.
2. Küçük M, Güner M. 2014. The determination of 2nd quality and export surpluses evaluation efficiency of apparel companies with the methods of performance matrix and fuzzy logic. *Tekstil ve Konfeksiyon* 24(4), 386-392.
3. Küçük M, Güner M. 2015. Bir konfeksiyon işletmesinde süreç analizi yolu ile verimlilik artırma çalışması. *Tekstil ve Mühendislik* 22(98), 33-41.
4. Güner M, İşler M. 2013. The effect of model change processes on the overall equipment effectiveness in clothing production. *Tekstil ve Konfeksiyon* 23(3), 297-302.
5. Burdak A, Krenzczyk D. 2017. June, Risk assessment in a parallel production system with the use of FMEA method and linguistic variables, In IFIP International Conference on Computer Information Systems and Industrial Management, Cham.:Springer, 10244, 379-390.
6. Press D. 2003. *Guidelines for Failure Mode and Effects Analysis (FMEA), for Automotive, Aerospace, and General Manufacturing Industries*. USA:CRC Press.
7. Peddada K. 2014. Risk Assessment and Control, Governance & Control in Finance & Banking: A New Paradigm for Risk & Performance”, pp:95-112.
8. Hiles A. 2010. *The definitive handbook of business continuity management*. UK:John Wiley & Sons.
9. Sette S, Van Langenhove L. 2002. Optimising the fibre-to-yarn production process: finding a blend of fibre qualities to create an optimal price/quality yarn. *Autex Research Journal* 2(2), 257-263.
10. Militký J, Kovačič V, Rubnerová J. 2002. Influence of thermal treatment on tensile failure of basalt fibers. *Engineering Fracture Mechanics* 69(9), 1025-1033.
11. Sette S, Boullart L, Van Langenhove L, Kiekens P. 1997. Optimizing the fiber-to-yarn production process with a combined neural network/genetic algorithm approach. *Textile Research Journal* 67(2), 84-92.
12. Arain FA, Tanwari A, Hafiz-Ur-Rehman S. 2012. Statistical modeling for the effect of rotor speed, yarn twist and linear density on production and quality characteristics of rotor spun yarn. *Mehran University Research Journal of Engineering and Technology* 31(1), 119-128.
13. Özgüney AT, Dönmez Kretzschmar S, Özçelik G, Özerdem A. 2008. The comparison of cotton knitted fabric properties made of compact and conventional ring yarns before and after the printing process. *Textile Research Journal* 78(2), 138-147.
14. Dönmez Kretzschmar S, Özgüney AT, Özçelik G, Özerdem A. 2007. The comparison of cotton knitted fabric properties made of compact and conventional ring yarns before and after the dyeing process. *Textile Research Journal* 77(4), 233-241.
15. van der Werf HM, Turunen L. 2008. The environmental impacts of the production of hemp and flax textile yarn. *Industrial Crops and Products* 27(1), 1-10.
16. Şahin D. 2015. Türkiye ve Çin'in tekstil ve hazır giyim sektöründe rekabet gücünün analizi. *Akademik Bakış* 47, 155-171.
17. Uğurlu AA, Tuncer İ. 2017. Türkiye'de sanayi ve hizmet sektörlerinin büyütme ve istihdama katkıları: girdi çıktı analizi. *Dokuz Eylül Üniversitesi İktisadi ve İdari Bilimler Fakültesi Dergisi* 32(1), 131-165.
18. Wu X, Chen L, Zhou Y, Ding X. 2016. Research in risk assessment for textile and apparel and propose a future research agenda with a conceptual framework. *International Journal of Productivity and Quality Management* 17(3), 273-288.
19. Malik N, Maan AA, Pasha TS, Akhtar S, Ali T. 2010. Role of hazard control measures in occupational health and safety in the textile industry of Pakistan. *Pakistan Journal of Agricultural Sciences* 47(1), 72-76.
20. Khan WA, Mustaq T, Tabassum A. 2014. Occupational health, safety and risk analysis. *International Journal of Science, Environment and Technology*, 3(4), 1336-1346.
21. Guidelines for Chemical Process Quantitative Risk Analysis. 2009. 2nd ed., CCPS, American Institute of Chemical Engineers.
22. Lees FP, Mannan S. 2005. *Lees' loss prevention in the process industries: hazard identification, assessment and control*, vol. 1. UK:Elsevier, 234.
23. Wells G, Wardman M, Whetton C. 1993. Preliminary safety analysis. *Journal of loss prevention in the process industries* 6(1), 47-60.
24. Ericson CA. 2015. *Hazard analysis techniques for system safety*. New Jersey:John Wiley & Sons.
25. IEC 60812:2006: Analysis techniques for system reliability - Procedure for failure mode and effects analysis (FMEA), Retrieved from <https://webstore.iec.ch/publication/3571>, (Date of access: 10 July 2018).
26. Flaus JM. 2013. *Risk analysis: socio-technical and industrial systems*. New Jersey:John Wiley & Sons, 153-309.
27. Beyene TD, Geremew Gebeyehu S, Mengistu AT. 2018. Application of failure mode effect analysis (FMEA) to reduce downtime in a textile share company. *Journal of Engineering, Project & Production Management* 8(1), 40-46.
28. Küçük M, İşler M, Güner M. 2016. An application of the FMEA method to the cutting department of a clothing company. *Tekstil ve Konfeksiyon* 26(2), 205-212.
29. Paired E, Swadeshi AH, Shokohyar S. 2017. Analyzing the enhancement of production efficiency using FMEA through simulation-based optimization technique: A case study in apparel manufacturing. *Cogent Engineering* 4(1), 1284373.
30. Kumar G. 2015. March, Cycle time reduction for T-shirt manufacturing in a textile industry using lean tools. In Innovations in Information, Embedded and Communication Systems (ICIIECS), IEEE, 1-6.
31. Kaewsom P, Rojanarowan N. 2014. The application of FMEA to reduce defective rate from broken filament defects in the direct spin drawing process. *IOSR Journal of Engineering* 4(5), 55-58.
32. Özyazgan V. 2014. FMEA analysis and implementation in a textile factory producing woven fabric. *Tekstil ve Konfeksiyon* 24(3), 303-308.
33. Liu HC, Liu L, Liu N. 2013. Risk evaluation approaches in failure mode and effects analysis: A literature review. *Expert Systems with Applications* 40(2), 828-838.
34. De Queiroz Souza R, Álvares AJ. 2008. FMEA and FTA analysis for application of the reliability centered maintenance methodology: case study on hydraulic turbines. In ABCM Symposium Series in Mechatronics, 803-812.
35. Khaiyum S, Kumaraswamy YS. 2014. An effective method for the identification of potential failure modes of a system by integrating FTA and FMEA. In ICT and Critical Infrastructure: Proceedings of the 48th Annual Convention of Computer Society of India, Springer, Cham., Vol:1, 679-686.

-
-
- 36. Khaiyum S, Kumaraswamy YS. 2014. Integration of FMEA and FTA for effective failure management in real time embedded projects. *Integrated Journal of British* 1(3), 12-25.
 - 37. Zhang YF, Zhou RB, Yang JM, Zhang Z. 2014. Application of FTA-FMEA method in fault diagnosis of tracked vehicle. *Advanced Materials Research* 940, 112-115.
 - 38. Martins LE, Gorscok T. 2017. Requirements engineering for safety-critical systems: overview and challenges. *IEEE Software* 34(4), 49-57.
 - 39. IEC 61025:2006, Fault tree analysis (FTA), Retrieved from <https://webstore.iec.ch/publication/4311>, (Date of access: 10 July 2018).



Physical, Chemical, Morphological and Thermal Characterisation of Natural Fibers for Sound Absorption

J Niresh¹, N Archana², T Karthik³, Tan Wei Hong⁴

¹Department of Automobile Engineering, PSG College of Technology, India

²Department of Electrical & Electronics Engineering, PSG College of Technology, India

³Department of Textile Technology, PSG College of Technology, India

⁴School of Mechatronic Engineering, Universiti Malaysia Perlis, Malaysia

Corresponding Author: J Niresh, nireshcbe@gmail.com

ABSTRACT

The increasing concern over the waste reduction and health hazards associated with the use of synthetic fibers such as glass fibers, carbon fibers, aramides and other fibers have turned the attention towards natural ecofriendly green fibers. In this paper natural fibers namely – milkweed fiber, Agave americana fiber and Sansevieria roxburghiana fibers have been studied experimentally to determine the physical, chemical, morphological and thermal properties by FTIR, SEM, PLM, X-Ray diffraction, DSC and TGA analysis methods. In this study, Sansevieria fiber was observed to have the highest tenacity of 53.58 g/tex and showed maximum degradation temperature of 375 °C. Milkweed fibers were found to have the lowest density of 0.9 g/cc and possessed hollow structure with smooth surface as observed from SEM and PLM techniques.

ARTICLE HISTORY

Received: 06.01.2018

Accepted: 12.06.2019

KEYWORDS

Natural Fibers, FTIR, SEM, PLM, TGA

1. INTRODUCTION

Natural fibers have wide range of applications in the field of textile, automotive and aerospace, particularly in the light of the recent global inclination towards eco-friendly textiles. The emerging green economy is based on energy efficiency, renewable feed stocks in polymer products, industrial processes that reduce carbon emission and recyclable materials. Natural fibers are renewable resources and they have good mechanical strength, low weight and low cost, that has made them particularly attractive to the automotive industry [1]. The utilization of natural fibers as a reinforcement for composite materials is an emerging research area. In recent years, attempts have been observed to reduce the use of synthetics and expensive glass, aramid or carbon fibers and also lighten considerably the car's body by taking advantage of the lower density and cost that natural fibers provide [1].

Milkweed is a type of seed hair fiber which consists of single cell, unlike bast fibres. These fibres, which are

attached to the side wall of the seed, gets dispersed by wind. The typical seed-hair fibres are similar in morphology to cotton, with long lengths and small diameter. Milkweed fibres are hollow with a thin wall and are therefore lightweight. The hollow structure of milkweed fibre has led to its use in items where good insulation or buoyancy properties are needed. Agave and sansevieria fibers are collected from the bast surrounding the stem of their respective plant.

In a literature, pyrolysis of sugar cane bagasse and coconut fiber was studied by thermal analysis by TGA and DSC methods and chemical constituents were determined by FTIR method [2]. Jute/Gelatin composites were characterized for its physical, mechanical and morphological properties and it showed good results [3]. In another study of hemp and kenaf fibers, the effect of alkali and saline treatment on its physical properties and also their FTIR, XPS and ESEM analysis were carried out to study its properties in comparison with glass fiber [4]. Blends of

To cite this article: Niresh J, Archana N, Karthik T, Hong TW. 2019. Physical, chemical, morphological and thermal characterisation of natural fibers for sound absorption. *Tekstil ve Konfeksiyon* 29(3), 219-227.

agave, pineapple leaf fibers, polypropylene fibers, non woven and composites were tested for its mechanical and dynamic mechanical properties and observed that agave-polypropylene fibers possessed superior mechanical properties [5]. A review of agave Americana fibers was performed stating its physical properties, extraction, characterization and its applications [6]. Another review of milkweed fibers concluded about its versatility as an industrial textile material due to its suitable physical and morphological properties exhibited by the fibers [7]. A blended non woven form of milkweed and kapok fibers were studied for their acoustic and thermal properties and found a positive correlation between fabric density and sound reduction and a negative correlation between bulk density and sound reduction, and the effect of kapok fibers with thermal conductivity [8]. Sansevieria cylindrica fiber was studied for its dynamic, mechanical, surface and thermal properties and the effect of alkali treatment on fiber properties and corresponding effects on the mechanical and thermal properties were analyzed [9]. Various other studies were done to characterize the properties of natural fibers, its composites and its nonwovens [1, 10-16].

With respect to the materials considered in this paper, structural properties of milkweed fibers have been studied along with cotton blend [17]. Mechanical characteristics of milkweed and its other properties have also been addressed in the literature [7, 18]. With respect to agave Americana, some studies have been carried out to identify its mechanical and crystalline characteristics [19-21]. A few literature deals with analyzing the properties and physical characteristics of sansevieria roxburghiana fibers [22, 23].

The objective of this paper is to characterize the physical, morphological, chemical and thermal properties of three natural fibers namely – Agave Americana, Sansevieria Roxburghiana, and milkweed fibers. The properties of these three natural fibers were determined experimentally and compared.

2. MATERIAL AND METHOD

2.1. Material

The milkweed fibers were obtained from matured pods of the plant *asclepias syriaca* and the floss was extracted from

the pods by hand and partly dried. Complete drying was done by spreading the floss on hessian sheets in the sun for about three days until the floss becomes lustrous in appearance and a fair amount of dust and dirt separates out from the floss. On drying, the floss loses about 5% of its weight. The agave Americana and sansevieria roxburghiana were extracted by water retting method. Initially the fibers were retted in stagnant water for 7 days and then extracted by mechanical extraction technique. The bast was passed through the rollers of a specially designed machine, which crushed them to separate the fibers and they were washed in running water and dried.

2.2. Physical Properties

The physical properties such as length, fineness, strength, density and moisture were determined as per the ASTM standard test method. Single fiber properties of milkweed fiber were measured and the fiber lengths were also determined by comb sorter diagram as per BS 4044:1989 standard. Linear density of the material was measured by gravimetric method using the ASTM test method D1577 at standard atmosphere conditions. The fibers were placed flat on a cutting device, using the template for standard length (L) the fiber samples were cut and weighed (W). The denier (D) of the fibre sample was calculated using the equation (1).

$$D = \frac{9000W}{LN} \quad (1)$$

The tensile properties of fibres were determined using ASTM D3822-01 standard. After pre-conditioning the samples in a standard atmosphere, the testing was carried out with gauge length of 10 mm. The test was repeated with 50 samples and the values were recorded. The fibre density was determined with a density gradient column having a mixture of xylene and carbon tetrachloride as per ASTM D1505-03 standard, after the fibers were cut into small pieces and made into small balls, otherwise leading to very low density values due to air bubbles inside the canal of the



(a)



(b)



(c)

Figure 1. Extracted fibers (a)Agave Americana (b) Sansevieria Roxburghiana (c) Milkweed

fibers. The moisture regain values were measured as per ASTM D 2654-89a by measuring the weight loss of the sample continuously with an interval of 30 minutes with respect to increasing temperature upto 105 °C until there was no loss in weight.

2.3. Surface Characterisation

The surface morphology of the fibers was studied to understand the behavior of thermal and acoustic properties of the fiber. The surfaces of fibers were observed using scanning electron microscope. Prior to the test, the samples were coated with a thin layer of gold by a plasma sputtering apparatus. The observation was performed in high vacuum mode with secondary electron detector and accelerating voltage between 5 and 10 kV. With an optical microscope (Leica Projection Light Microscope, Model: DM750P), the longitudinal and cross-sectional views of fiber samples were photographed with a magnification of 200x. Average of fifty randomly chosen readings was taken to compute the mean fiber diameter.

2.4. Chemical Characteristics

The crystallinity of raw, alkali treated and dyed milkweed fibers were evaluated by X-ray diffraction. X-ray diffractograms of the samples were obtained with Lab-X, wide angle X-ray diffractometer, having an X-ray tube, producing monochromatic radiation ($\lambda = 1.54 \text{ \AA}$) at 30 kV and 20 mA. To calculate the crystallinity index, software was used to separate the background and the overlapped peaks. The crystallinity index of the fibre was calculated according to the Segal empirical method as given in equations (2) and (3).

$$\text{CrI (\%)} = \frac{I_{002} - I_{am}}{I_{002}} * 100 \quad \text{(II)}$$

$$\text{Cr Ratio} = \frac{I_{002}}{I_{002} + I_{101}} * 100 \quad \text{(III)}$$

where I_{002} is the maximum intensity of the I_{002} lattice reflection and I_{am} is the height of the minimum between the 002 and the 101 peaks. FT-IR spectra of the fibers (raw, alkali treated, dyed) were recorded using Shimadzu FT-IR in KBr matrix with a scan rate of 32 scans per minute with a resolution of 4 cm^{-1} in the wave number region of $400\text{-}4000 \text{ cm}^{-1}$. The fiber samples were chopped into smallest particles and ground well. Then it was mixed with KBr and pelletized by pressurization to record the FT-IR spectra under standard conditions.

2.5. Thermal Characteristics

A Perkin Elmer differential scanning calorimeter and Netzsch thermogravimetric analyzer were used to measure the thermal behavior of the fibers. The sample consisting of 2-3 mg of fibers were cut finely with scissors and placed in aluminum pans for DSC analysis & platinum pan for TGA analysis. Both DSC and TGA were performed in nitrogen gas atmosphere flowing at 50 ml/min. The DSC thermograms of the conditioned (25 °C, RH 75%) raw and treated fiber samples were recorded on Perkin Elmer DSC 7 as well as in Netzsch DSC 204 instruments from room temperature to 400 °C and 200 °C respectively at a heating rate of 10 °C/min in nitrogen atmosphere.

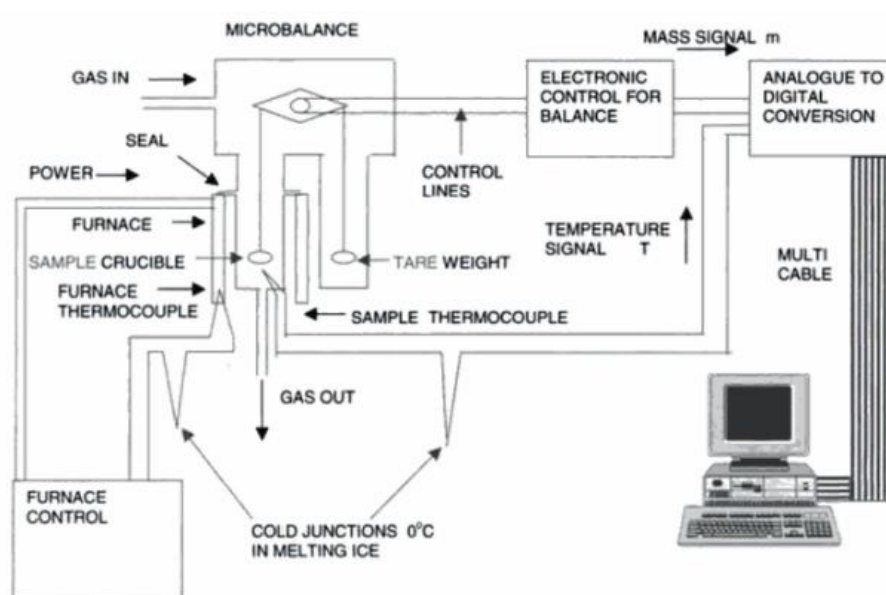


Figure 2. Schematic diagram of thermogravimetric analysis [24]

3. RESULTS AND DISCUSSION

The physical properties of selected fibers such as Milkweed, Sansevieria and Agave are shown in Table 2. The tenacity of the Sansevieria fibers are the highest compared to the three fibers that were selected for the study, which is in the range of the hemp fibers. Agave Americana is a stiff fiber but the tenacity is lower than that of milkweed. Milkweed being a seed hair fiber is finer, whereas Sansevieria has optimum fineness in the range of other bast fibers. Agave Americana fibers are coarser, but if they are fibrillated, the fineness can be improved. The two bast fibers have density comparable to the other bast fibers, while milkweed is lighter than water. The moisture absorption properties of all the three fibers were almost in the same range as that of other bast fibers.

From Figure 3a to Figure 3c it is clear that the surface morphology of the Agave and Sansevieria fibers are similar

to that of the other bast fibers. They have a multi cellular structure and very rough surface morphology with many striations. These rough surfaces are as a result of the frictional contact of the fibers between each other. From Figure 3b it can be seen that the milk weed fibers have a very smooth surface morphology. This smooth and lustrous effect on the fiber surface is observed as a result of the wax content in the fibers.

Like cotton, milkweed fiber is a single cell fiber but without convolutions. It is evident from Figure 4b that the milkweed fibers are hollow in nature, which aids in better capillary action and air permeability, while the other fibers are completely solid structures. In case of agave Americana there are few fibrils floating on the surface of the fiber. Both the bast fibers have uneven surface morphology along the width and diameter of the fiber varying across the length of the fibers.

Table 2. Physical properties of fibers

Property	Milkweed	Sansevieria	Agave Americana	Jute	Hemp
Tenacity (g/tex)	16.575	53.58	13.423	30	55
Fineness (tex)	0.11	5.33	26.22	1.8	20
Density (g/cc)	0.9	1.35	1.38	1.45	1.48
Moisture Content (%)	10.4	10.5	8.85	12.5	8

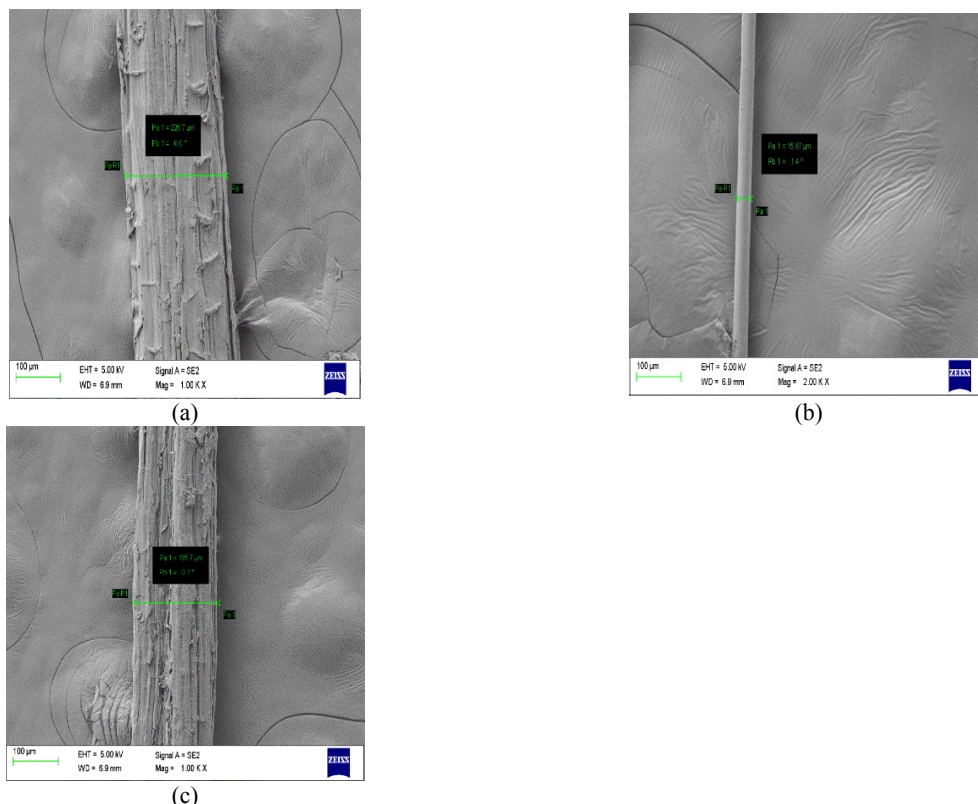


Figure 3. SEM images of fibers (a) Agave Americana (b) Milkweed (c) Sansevieria

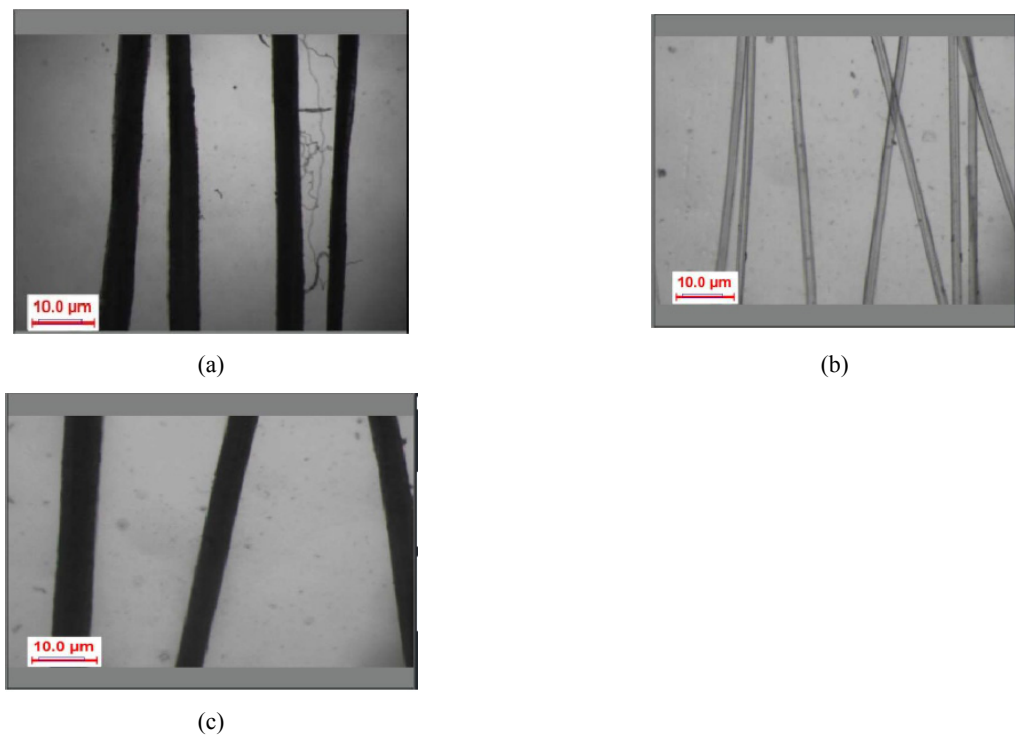


Figure 4. Longitudinal structure of (a) *Agave Americana* (b) Milkweed (c) *Sansevieria*

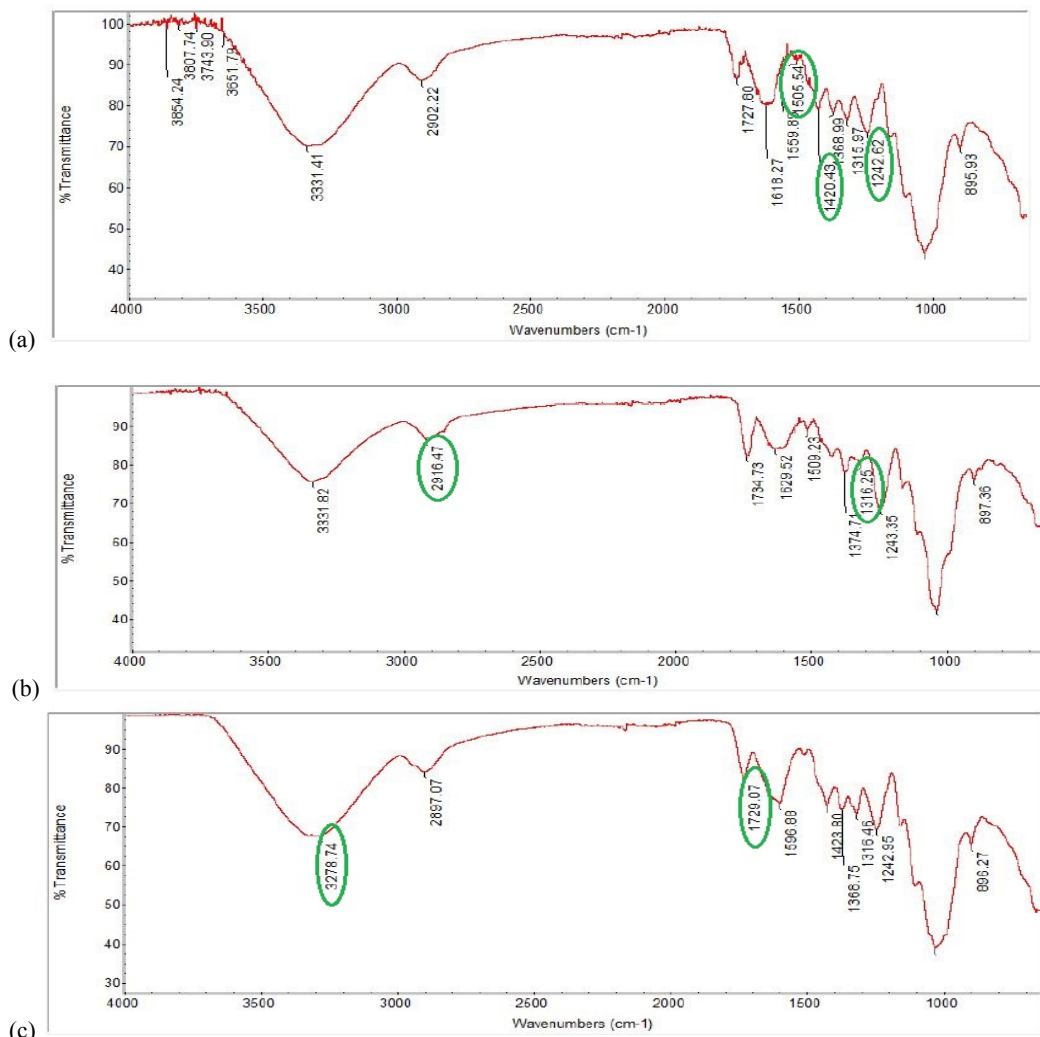


Figure 5. FTIR graphs of (a) *Agave Americana* (b) Milkweed (c) *Sansevieria*

From Figure 5, it can be observed that both the bast fibers have functional groups like lignin, proteins and hemicelluloses (identified by the presence of certain carbon linkages) that are easily soluble. In case of the milkweed fibers polysaccharides form the major portion due to the presence of O-H and C-H linkage.

The crystallinity values of the fibers are calculated by the intensity of light absorption at different wavelengths. The

Sansevieria fibers have the highest crystallinity values which can be observed from Figure 6. This may be due to the relative fineness of the fiber and the chemical groups present in it. In case of the milkweed fibers, the crystallinity values are comparable with the other seed fibers like cotton. From Figure 6a it can be inferred that in case of Agave Americana, the crystalline regions are scattered across the different lattices.

Table 3. Assignment of FT-IR peaks and their relative sources

Wave Number (cm^{-1})	Vibration	Source
1242.62	C-O Aryl Group	Lignin
1420.93	C=C Stretching in Aromatic Groups	Lignin, Hemi cellulose
1505.00	C=C Aromatic symmetrical stretching	Lignin
1727.80	C=O unconjugated	Semi cellulose
3278.74	O-H Stretching	Polysaccharides
2885.00	C-H Symmetrical Stretching	Wax
1335.00	C-O Aromatic Ring	Cellulose

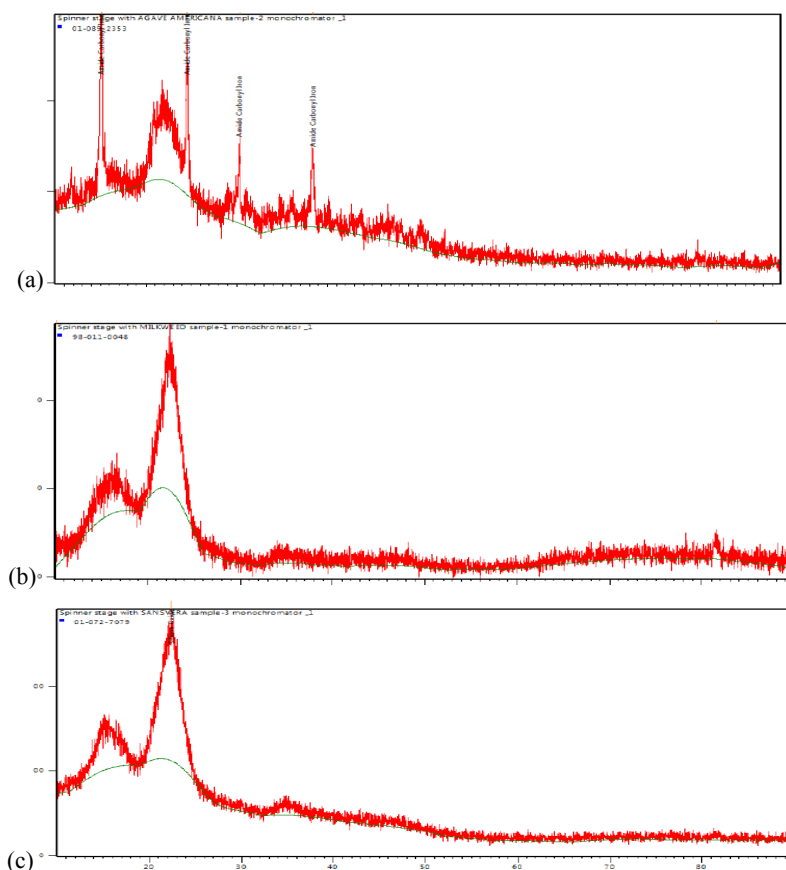


Figure 6. X-Ray diffraction graphs (a) Agave Americana (b) Milkweed (c) Sansevieria

Table 4. Crystallinity of different fibers

Fibers	Crystallinity Index	Crystallinity Ratio (%)
Agave Americana	54.0	68.5
Milkweed	41.3	63.0
Sansevieria	64.8	73.9

From Figure 7, the initial weight loss due to evaporation of water in sample was around 10.5%, 10% and 9% respectively for milkweed, Sansevieria and Agave Americana. From Table 4, it can be observed that the degradation for the Agave Americana starts first at 230 °C which may be due to the reason of low moisture regain values compared to the other fibers. For milkweed and sansviera, the degradation starts at 260 °C and 280 °C respectively after the evaporation of 10% moisture.

The presence of polysaccharides, wax and cellulose in the milkweed fibers results in very low residual content, while for the two bast fibers a residual content of around 25% is

found due to the presence of lignins and proteins. In case of the milkweed fibers, the loss in weight is sudden and continuous where as in case of the bast fibers, degradation starts at a point and then it remains stable over a short period and then continues to degrade.

From Figure 8, it can be observed that the Agave Americana fibers show exothermic peak around 80 °C, milkweed shows around 60 °C and Sansevieria fibers, around 364 °C. In case of Sansevieria, at around 90 °C, there is a small occurrence of a peak, but there is a higher rate of reaction at 364 °C, indicating the presence of a substance that is volatile at higher temperatures.

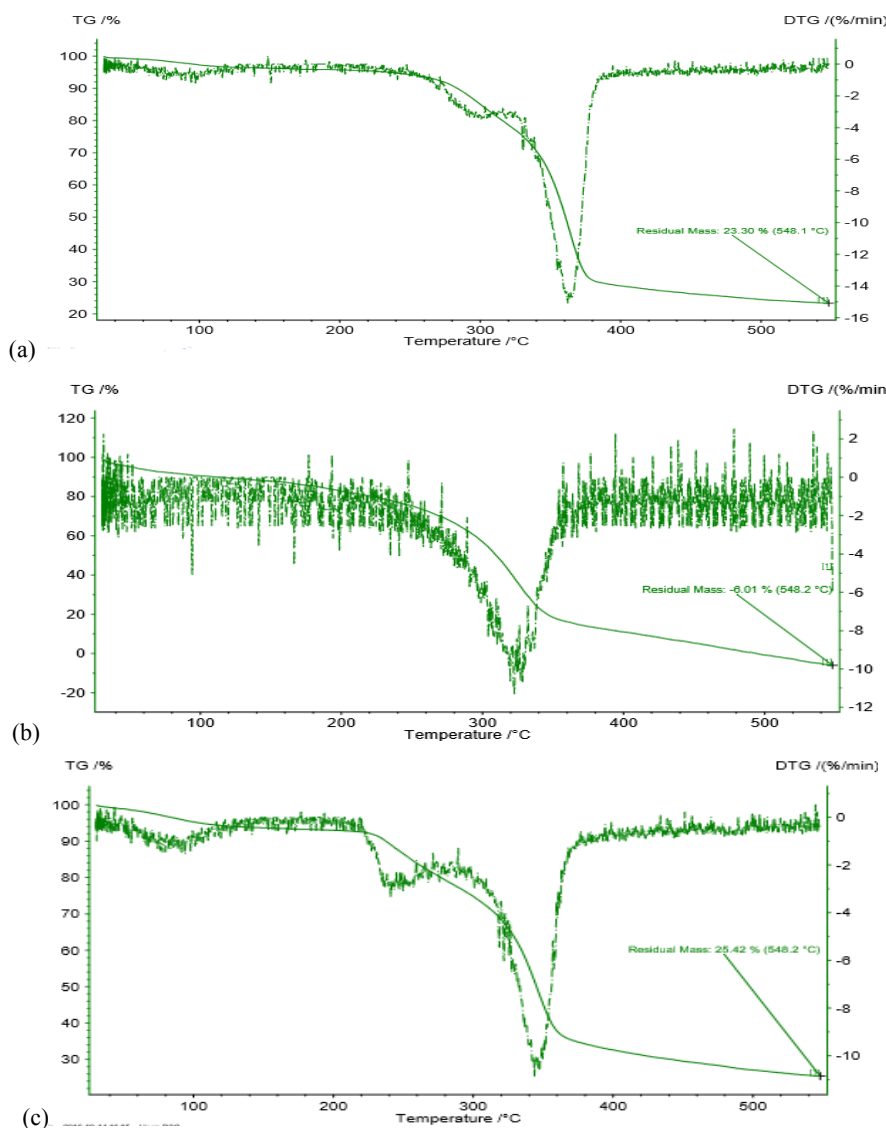


Figure 7. TGA and DTG graphs of fibers (a) Agave (b) Milkweed (c) Sansevieria

Table 5. Thermal degradation values of fibers

Fibers	Degradation Temperature, T_D (°C)	Maximum Degradation Temperature, T_{Dmax} (°C)
Agave Americana	230	360
Milkweed	260	340
Sansevieria	280	375

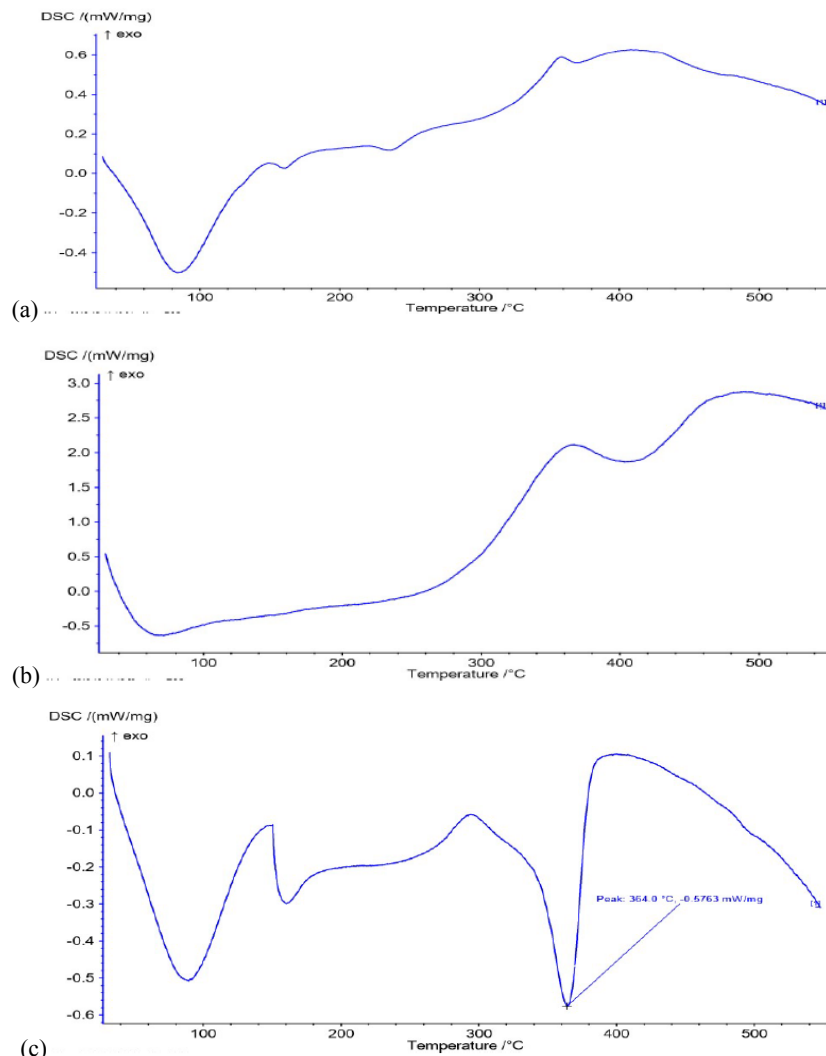


Figure 8. DSC curves of (a) Agave (b) Milkweed (c) Sansevieria

4. CONCLUSION

In this paper natural fibers namely – milkweed fiber, agave Americana fiber and sansevieria roxburghiana fibers have been studied experimentally to determine the physical, chemical, morphological and thermal properties by FTIR, SEM, PLM, X-Ray Diffraction, DSC and TGA analysis methods. Sansevieria fiber was observed to have the highest tenacity of 53.58 g/tex and maximum degradation temperature of 375 °C. Milkweed fibers were found to have the lowest density of 0.9 g/cc and possessed hollow

structure with smooth surface as observed from SEM and PLM techniques. Agave Americana fibers were found to have a crystallinity index of 54% and the highest was recorded for sansevieria fibers having 64.8%. Bast fibers possessed functional groups like lignin, proteins and hemicellulose whereas milkweed fibers possessed polysaccharides as a major constituent. Agave fibers were found to have greater residual mass of 25.42% at 548.2 °C as observed from TGA graphs.

REFERENCES

- Jawaaid M, Salit MS, Alothman OY. 2017. Green biocomposites design and applications. Switzerland: Springer.
- Mothé C, De Miranda L. 2017. Characterization of sugarcane and coconut fibers by thermal analysis and FTIR. *Journal of Thermal Analysis and Calorimetry*, 97(2), 661-665.
- Khan MA, Islam T, Rahman MA, Islam JMM, Khan RA, Gafur MA, Mollah MZI, Alam AKM. 2010. Thermal, mechanical and morphological characterization of jute/gelatin composites. *Polymer-Plastics Technology and Engineering* 49(7), 742-747.
- Sgriccia N, Hawley MC, Misra M. 2008. Characterisation of natural fiber surfaces and natural fiber composites. *Composites Part A: Applied Science and Manufacturing* 39(10), 1632-1637.
- John MJ, Sikampula N, Boguslavsky L. 2015. Agave nonwovens in polypropylene composites-mechanical thermal studies, *Journal of Composite Materials* 49(6), 669-676.

-
- 6. Hulle A, Kadole P, Katkar P. 2015. Agave americana leaf fibers. *Fibers* 3, 64-75.
 - 7. Hassanzaddeh S, Hasani H. 2017. A review on milkweed fiber properties as a high potential raw material in textile applications. *Journal of Industrial Textiles* 46(6), 1412-1436.
 - 8. Ganesan P, Karthik T. 2016. Development of acoustic nonwoven material from kapok and milkweed fibers. *The Journal of the Textile Institute* 107(4), 477-482.
 - 9. Sreenivasan VS, Rajini N, Alavudeen A, Arumugaprabhu V. 2015. Dynamic mechanical and thermo-gravimetric analysis of Sansevieria cylindrica/polyester composite: Effect of fiber length, fiber loading and chemical treatment. *Composites Part B: Engineering* 69, 76-86.
 - 10. Fatima S, Mohanty AR. 2011. Acoustical and fire retardant properties of jute composite materials. *Applied Acoustics* 72, 108-114.
 - 11. Othmani C, Taktak M, Zein A, Hentati T, Elnady T, Fakhfakh T, Haddar M. 2016. Experimental and theoretical investigation of the acoustic performance of sugarcane wastes based material. *Applied Acoustics* 109, 90-96.
 - 12. Jayaraman K. 2003. Manufacturing sisal-polypropylene composites with minimum fibre degradation. *Composites Science and Technology* 63, 367-374.
 - 13. Cerbu C. 2015. Mechanical characterization of flax/epoxy composite material. *Procedia Technology* 19, 268-275.
 - 14. Prabhakaran S, Krishnaraj V, Kumar MS, Zitoune R. 2014. Sound and vibration damping properties of flax fibre reinforced composites. *Procedia Engineering* 97, 573-581.
 - 15. Kant R, Alagh P. 2015. Extraction of fiber from Sansevieria trifasciata plant and its properties. *International Journal of Science and Research* 4(7), 2547-2549.
 - 16. Niresh J, Neelakrishnan S, Subharani S, Shrivastava S. 2016. Analysis of static flow resistivity of a modified impedance tube. *Circuits and Systems* 7, 2253-2261.
 - 17. Karthik T, Murugan R. 2016. Analysis of structural properties of cotton/milkweed blended ring, compact and rotor yarns. *Indian Journal of Fibre & Textile Research* 41, 361-366.
 - 18. Dréan JYF, Patry JJ, Lombard GF, Weltrowski M. 1993. Mechanical characterization and behavior in spinning processing of milkweed fibers. *Textile Research Journal* 63, 443-450.
 - 19. Msahli S, Chaabouni Y, Sakli F, Drean JY. 2007. Mechanical behavior of Agave americana L. fibres: Correlation between fine structure and mechanical properties. *Journal of Applied Sciences* 7(24), 3951-3957.
 - 20. Geethika VN, Rao VDP. 2017. Study of tensile strength of Agave americana fibre reinforced hybrid composites. *Materials Today: Proceedings* 4(8), 7760-7769.
 - 21. El Oudiani A, Chaabouni Y, Msahli S, Sakli F. 2008. Crystalline character of Agave americana L. Fibers. *Textile Research Journal* 78, 631-644.
 - 22. Kanimozhi M, Vasugi N. 2012. Investigations into the physico-chemical, mechanical and structural characterization of Sansevieria roxburghiana L. Fibre. *International Journal of Fiber and Textile Research* 2, 1-4.
 - 23. Teli M, Jadhav A. 2017. Study on the chemical composition, physical properties and structural analysis of raw and alkali treated Sansevieria roxburghiana fibre. *Australian Journal of Basic and Applied Sciences* 11, 35-45.
 - 24. Gaisford S, Kett V, Haines P. 2016. *Principles of thermal analysis and calorimetry*, Second Edition. Royal Society of Chemistry, 10-53.



Cellulose Monoacetate/Nafion (CMA/N) Hybrid Nanofibers as Interface for Electrochemical DNA Biosensors

Ayse Bostancı¹, Nilay Aladag Tanık¹, Yakup Aykut²

¹Textile Engineering, Graduate School of Natural and Applied Sciences, Uludag University, Bursa, Turkey

²Textile Engineering Department, Engineering Faculty, Uludag University, Bursa, Turkey

Corresponding Author: Yakup Aykut, aykut@uludag.edu.tr

ABSTRACT

Cellulose monoacetate/Nafion (CMA/N) hybrid nanofibers were produced via a one-step electrospinning method. Nanofibers morphologies transformed from uniform to bead on a string defect morphology with increasing Nafion ratio in CMA/N hybrid nanofibers. The melting point of CMA was detectable at DSC measurement, but since the addition of Nafion did not allow a proper crystallization of CMA, melting peak disappeared after the Nafion addition. Decomposition temperature decreased dramatically with the addition of Nafion into CMA/N nanofibers and decomposition took place at a broad temperature range. Nanofibers were also electrospun on the cylindrical graphite electrode for DNA electrochemical sensor analysis. Unmodified and NH-modified single strand DNA molecules were immobilized via physical adsorption method on the as-prepared nanofiber sensory system. Electrochemical analysis were performed via differential pulse voltammetry (DPV) to observe the guanine oxidation signal at unmodified and NH-modified DNA. Maximum oxidation signals were detected from pure CMA nanofibers at unmodified DNA. Signal intensity increased with the addition of Nafion into CMA/N nanofibers at NH-modified DNA sample comparing to unmodified DNA. It was concluded that DNA molecules could be properly immobilized on the produced CMA/N hybrid nanofibers via physical adsorption method and used as electrochemical DNA biosensor.

1. INTRODUCTION

Nanofibers are promising structured materials which have very broad application areas including bio-separation, filtration, wound healing, energy production and storage [1–5]. Their high surface area to volume ratio makes nanofibers preferable materials to use in the devices to enhance the device performance. For example, a high surface area of gold nanofiber electrode as fructose base biosensor was prepared by electroless deposition of gold nanoparticles on an electrospun poly(acrylonitrile)-chloroauric acid tetrahydrate [6]. Electrospun poly(vinyl alcohol)/glucose oxidase composite nanofiber membranes were produced as enzymatic electrodes for biosensors by Ren et al. [7]. Titanium dioxide and zinc magnesium oxide ceramic nanofibers were prepared with enhanced optical properties via sol-gel electrospinning method [8, 9].

Cellulose is a biopolymer which can be obtained or extracted from algae, plants and even bacteria [10–12]. Because of its biocompatible and environmentally friendly nature [13], it has been used in a variety of different areas including fibers for textile products [14], in vivo biomedical applications [15], etc. It is inexpensive and readily availability including its environmentally and biocompatible properties makes cellulose a promising candidate to use in biosensor applicaitons. Cellulose and cellulose derivatives are produced in micro and nanostructured fibers forms for different applications [16, 17]. Electrospun cellulose acetate nanofiber by loading vitamins as transdermal and dermal therapeutic agents of vitamin A acid and vitamin E were prepared and studied by Taepaiboon et al. [18]. Ultrafine cellulose nanofiber membranes were produced via electrospinning of cellulose acetate and the following deacetylation process [16]. Electrospinning of cellulose

To cite this article: Bostancı A., Aladag Tanık N, Aykut Y. 2019. Cellulose Monoacetate/Nafion (CMA/N) hybrid nanofibers as interface for electrochemical DNA biosensors. *Tekstil ve Konfeksiyon* 29(3), 228-236.

derivatives including cellulose acetate, hydroxypropyl cellulose, hydroxypropyl methyl cellulose, and ethyl - cyanoethyl cellulose was reviewed by Frey [19].

Nafion nanofibers have been fabricated via electrospinning technology by blending with other polymers. Nafion/polyacrylonitrile blend nanofibers as the precursor of porous carbon nanofibers were prepared by Tran and Kalra [20]. Nafion/poly(ethylene oxide) composite nanofibers with an excellent shape memory properties were prepared via solution electrospinning method [21]. In another study, Dong et al. reported the preparation of Nafion/poly(ethylene oxide) nanofibers (with high Nafion contents) with high proton conductivity that is higher than the bulk Nafion film. They reported that proton conductivity increases by decreasing nanofiber diameter [22]. Polyvinyl alcohol nanofiber reinforced Nafion membranes with good mechanical and thermal properties were produced for fuel cell applications [23]. Nafion/polyvinyl alcohol composite nanofiber structures with high mechanical properties were produced by electrospinning as a functional adsorbent for heavy metals [24].

Electrochemical DNA biosensors have been used as the devices to monitor DNA damage and repair [25, 26] and base oxidation on a DNA molecules [27]. So, there are different applications of DNA biosensors such as clinical diagnosis [28], genetically modified organisms detection in foods [29], forensic analysis, environmental monitoring [30], etc. Nafion has been used with other materials to construct DNA biosensors. DNA damage was detected via electrochemical method by using a hemin/Nafion-graphene/glassy carbon electrode hybrid system [31]. Graphene-ionic liquid-Nafion modified pyrolytic graphite electrode (PGE) was used for the direct detection of DNA damage by electrochemical impedance spectroscopy [32]. Graphene-Nafion composite film was produced and used for a sensitive impedimetric DNA biosensor for the determination of the human immunodeficiency virus gene [33]. A DNA-based biosensor was prepared with Nafion and chitosan membrane to investigate antioxidant properties of beverages (beer, coffee, and black tea) by observing DNA degradation under in vitro conditions [34].

In this study, the preparation of Cellulose monoacetate/Nafion (CMA/N) and their use as electrochemical DNA biosensor have been investigated. Use of the Nafion based nanofibers for electrochemical DNA biosensor applications haven't been reported yet in the literature. In this regards, the polymer blend of CMA and Nafion with the different ratio up to considering a maximum content of Nafion in hybrid nanofibers until obtaining homogeneous solutions were prepared and electrospun into nanofiber structures. Morphologies of as-spun CMA/N hybrid nanofibers were observed by SEM, and chemical analyses of nanofibers were conducted with FTIR spectroscopy. Thermal characterizations of CMA/N hybrid nanofibers were carried out with DSC and TGA methods. In the literature it was pointed out that Guanine in a DNA molecule oxidizes more than other bases in an appropriate condition [27]. So,

electrochemical sensing properties of nanofibers were investigated by focusing on the guanine oxidation signal in adsorbed DNA molecules on CMA/N hybrid nanofiber surfaces."

2. MATERIAL AND METHOD

2.1. Chemicals for CMA/N Electrospinning Solutions

Cellulose monoacetate powder (Mn~30.000, CMA, Sigma Aldrich) and ~5wt. % of Nafion in a mixture of lower aliphatic alcohols and water solution were used for electrospinning. Electrospun polymer solutions were prepared in acetone (99% purity) and all chemicals were used as received without further purifications.

2.2. Electrospinning of Cellulose Monoacetate/Nafion (CMA/N) Hybrid Nanofibers

15 wt. % CMA was appropriately dissolved in acetone. Then, previously received Nafion solution was added into the CMA/acetone solution with the CMA/Nafion volume (solutions) ratio are 4/0, 4/1, 4/2, and 4/3. Mix solutions were magnetically stirred until obtaining a proper homogeneous solution. The prepared solutions were electrospun into the nanofibrous structure by applying 20 kV voltage to the solution. CMA/N solutions were fed with a micropump system via a plastic syringe which has a metal needle set in front of the nanofiber collector system with a distance of ~10 cm. Flow rate was 1 ml/hr. Schematic illustration of the electrospinning process is shown in Figure 1. Because of the applied voltage, the solution droplet just left the needle was ejected from needle to collector. Solvents were evaporated till reaching to the collector and the mixed polymers were collected as the nanofiber forms on the collector. In order to collect nanofibers on the cylindrical graphite electrode, the PGE was attached in front of a rotating apparatus and hold between the tip of the needle and the collector. Consequently, the rotating PGEs were directly coated by these electrospun nanofibers simultaneously during the electrospinning process.

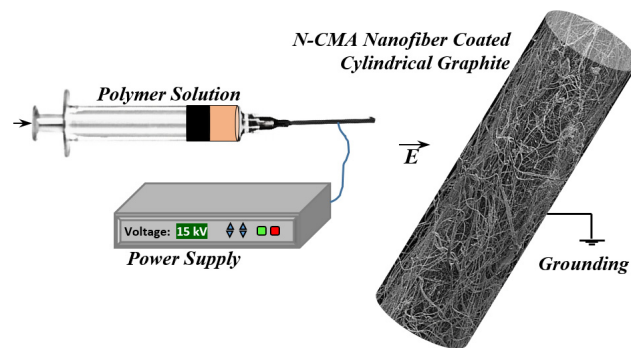


Figure 1. Schematic illustration of CMA/N hybrid nanofibers coating on the cylindrical graphite electrode.

2.3. Characterization of Nanofibers

The morphological characterizations of CMA/N nanofibers both on cylindrical graphite and plain surface were carried

out with a scanning electron microscopy, SEM (ZEISS EVO 40). 15-20 kV acceleration voltages were applied during the measurements. Before SEM analysis, samples were coated with gold-palladium with around 100 nm thickness. Chemical analyses of as-spun CMA/N hybrid nanofibers were performed with an attenuated total reflection Fourier transform infrared spectra (ATR-FTIR, Thermo Nicolet iS50). ATR-FTIR measurements were conducted between the wavenumber ranges of 4000 to 400 cm⁻¹. Thermal analyses of nanofibers were carried out via differential scanning calorimetry (DSC) and Thermogravimetric analysis (TGA) measurements. DSC measurements were conducted from 25 to 250°C with a heating rate of 10 °C/min under the nitrogen atmosphere in a measurement pan and TGA measurements were conducted from 50 to 800°C (heating rate of 10°C min⁻¹) in a nitrogen gas atmosphere.

2.4. Probe Immobilization and Electrochemical Analysis

Two different as unmodified and NH-modified single strand DNA probes were immobilized on CMA/N hybrid nanofibers coated cylindrical graphite electrodes, and electrochemical measurements were conducted via investigating the voltammograms of the guanine oxidation signals of probe immobilized surfaces (Figure 2). Oligonucleotide probe immobilization solutions were prepared at laboratory condition in TBS (pH 7.0) containing 20 μM NaCl and 10 μg/ml prob. Nanofiber coated PGEs were kept 20 min in this solution to properly immobilized ssDNA on the nanofiber surfaces.

Nucleotide sequences of unmodified DNA's are ssDNA: 5'-GAA CAC GTG TAT GTT GAG-3' (ALPHA DNA (Canada)), and NH-modified DNA's are ssDNA: 5'-/ 5

Am/GAA CAC GTG ATA GAA GAG-3' (Sentegen (Ankara, Turkey)). Electrochemical characterizations were carried out in laboratory condition. Probe immobilization solutions of oligonucleotides of samples were prepared as in the published study [35]. Both unmodified and NH-modified ssDNA samples were immobilized on CMA/N coated pencil graphite electrodes (PGEs, (Tombo HB model 0.5 mm)) [36, 37]. All the samples were washed with TBS to remove mobile ssDNA molecules. Electrochemical analyses were performed via Differential Pulse Voltammetry (DPV) measurements by using PGSTAT204 digital potentiostat/galvanostat using NOVA software package (Eco Chemie). Probe immobilized CMA/N hybrid nanofibers were used as the working electrode. The reference electrode was Ag/AgCl and auxiliary electrodes was a platinum wire for the measurements. 1 cm of the probe immobilized part was immersed in ABS solution and electrochemical measurements were performed. During the electrochemical measurement, the oxidation signal of guanine was observed at about +1,0 V.

3. RESULTS AND DISCUSSION

Electrospun CMA/N hybrid nanofibers were produced from different CMA/Nafion solutions volume ratio. Transparent homogeneous solutions were obtained up to 4/3 ratio. Increasing Nafion solution ratio leads to inhomogeneous solution property and solution became blurry after 4/4 CMA/Nafion solution ratio (Figure 3A). Even blurry solutions were obtained at 4/4, the solution was not electrospun into nanofiber structure at this ratio and further increasing Nafion content in the solution. Uniform hybrid CMA/N nanofibers were collected on the cylindrical graphite electrode surfaces on a regular basis (Figure 3B and 3C).

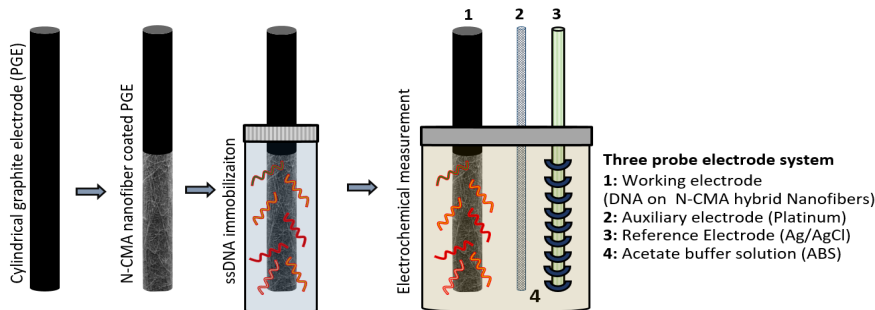


Figure 2. Schematic illustration of CMA/N nanofibers biosensor preparation and the electrochemical procedure for detecting guanine oxidation on the ssDNA.

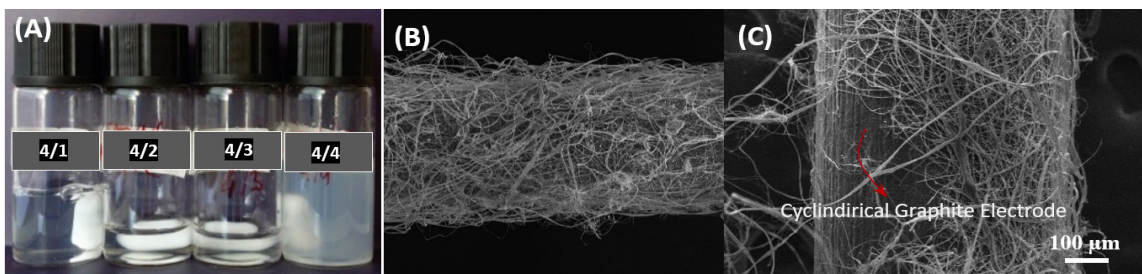


Figure 3. (A) Photograph images of prepared CMA/Nafion solutions in acetone, and (B, C) SEM images of CMA/N hybrid nanofiber coated PGEs.

3.1. Morphology

Nanofibers were also collected on a plain aluminum surface to better investigate the effect of CMA/ratio on the nanofiber morphologies. Low magnification SEM images of pure CMA and different ratio of CMA/N hybrid nanofibers are shown in Figure 4. Pure CMA nanofibers are more uniform (Figure 4A), and increasing Nafion ratio in CMA/N hybrid nanofibers, nanofibers uniformity transforms to bead on a string morphological structures and the number of beads increases dramatically with increasing Nafion ratio in CMA/N nanofibers (Figure 4D). This might be the effect of inhomogeneous properties of the solution with increasing Nafion solution ratio.

Low and high magnification SEM images of pure CMA and CMA/N hybrid nanofibers in 3D network structures are shown together in Figure 5 to better investigate the effect of polymer ratio on nanofiber uniformities. Irregularity increases tremendously with increasing Nafion ratio, nanoparticulate formations are observed on and among the nanofibers, and ultrafine nanofibers are also seen in the mat. Both ultrafine and bigger nanofibers are observed

comparing pure CMA nanofibers. More flattened nanofibers structure at pure CMA, and nanofibers turned to more rounded nanofiber morphologies with the addition of Nafion.

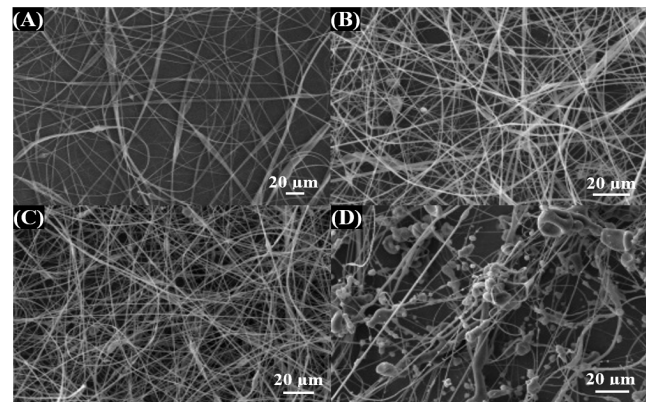


Figure 4. Low magnification SEM images of CMA/Nafion nanofibers depending on CMA/N ratio in electrospinning solution: (A) 4/0, (B) 4/1, (C) 4/2, and (D) 4/3

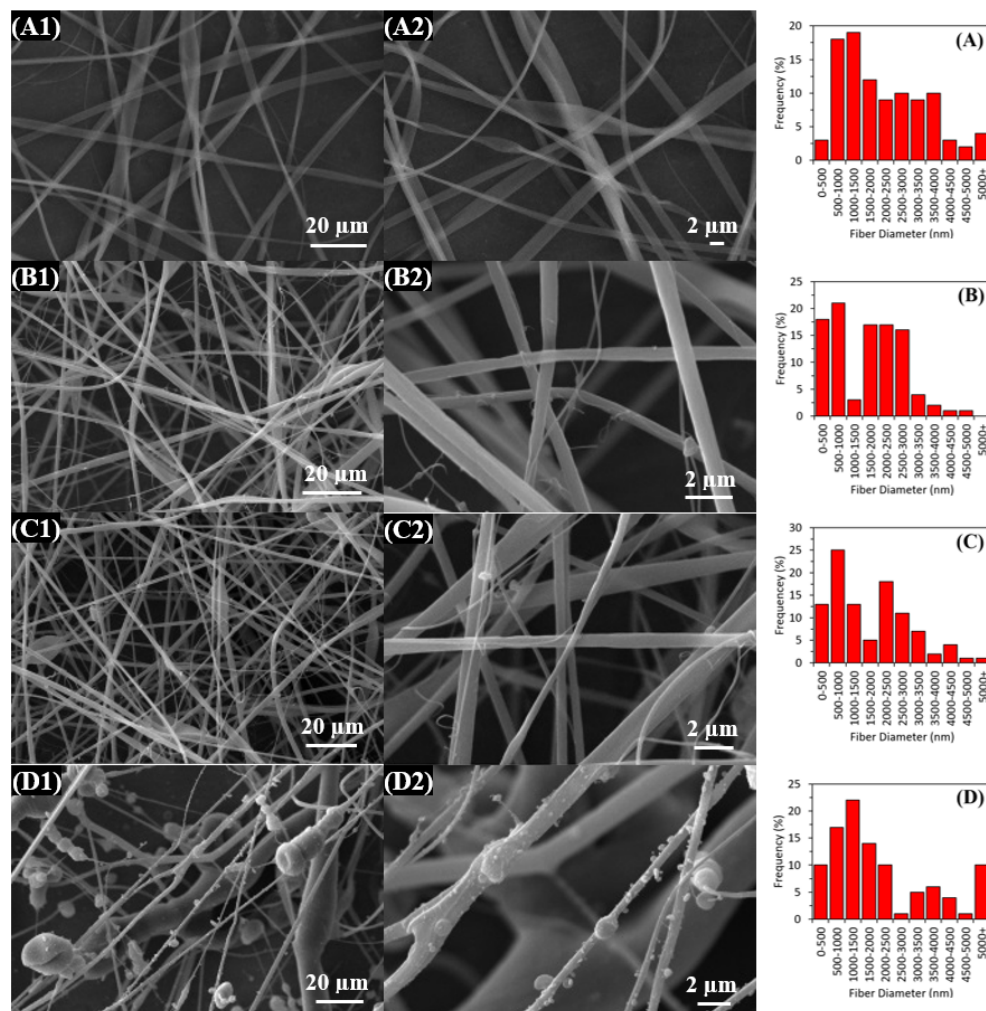


Figure 5. SEM images of CMA/Nafion nanofibers depending on CMA/N ratio in electrospinning solution: (A1, A2) 4/0, (B1, B2) 4/1, (C1, C2) 4/2, and (D1, D2) 4/3

Electrospun fiber diameter distribution charts were given in Figure 5. Majority of fiber diameters are set between 500 nm and 1,5 μ m in pure CMA nanofibers. Addition of Nafion into CMA nanofibers causes nonhomogeneous fiber diameter distribution and two different fiber diameter phases and both nano- and micro-fibers are exist in the fibrous mat structure. Increasing the Nafion content in CMA/N hybrid nanofibers the average diameters of both nano- and micro-fibers increased in the nanofibrous mat structure.

As seen from Table 1, viscosity decreased with nafion addition into CMA/acetone solution. But, increasing nafion ration in the solution leaded to increase of viscosity again. This related to inhomogenous solution property of the solution. As seen from Figure 3, solutions were transparent at low nafion content and transformed into blurry look with increasing nafion ration. In Figure 5D, existence of thick fibers in the nanofiber mat could be related with this viscosity increase. Occurance of beaded structure in the mat could be related to increase of solution viscosity with the addition and increase of nafion content. Formations of the beaded morphologies in the nanofibrous mat structure could also be related to increase of electrical conductivity of the solution by increasing Nafion ratio. Since there is no dramatic change at the surface tension, it was concidered that there is no significant effect of surface tension on the nanofiber diameter change in this study.

3.2. Chemical Analysis via ATR-FTIR

ATR-FTIR investigation of pure CMA dried Nafion, and CMA/N hybrid nanofibers were demonstrated in Figure 6. In the pure CMA nanofibers, predominant peaks are located at 1047 and 1234 cm^{-1} related to (C-O-C), peak at 1379 cm^{-1} corresponds to (C-CH₃), and the peak at 1743 cm^{-1} can be attributed to (C=O from acetyl groups) [38, 39]. OH stretching band was observed as a broad peak around 3450 cm^{-1} [40], and this peak intensity increases and shifted to lower wavenumber by increasing Nafion ratio in CMA/N hybrid nanofibers. Since the amount of HSO₃ group increase with increasing Nafion ratio, and HSO₃ groups hold water molecules, OH stretching also increased with increasing Nafion ratio as a result of absorbed water molecules [41]. Characteristic Nafion peaks were seen at CMA/N hybrid nanofibers. Peaks at 1141 and 1205 cm^{-1}

correspond to the symmetric and asymmetric stretching vibrations modes of -CF₂ [21, 42]. Bending vibration of CF₂ was detected at 632 cm^{-1} [21]. The peak at 1057 cm^{-1} is related to the SO₃H groups and it can be attributed to the stretching vibration of SO₃ [21,43]. The peaks are seen at 966 and 986 cm^{-1} may arise from the stretching vibration of C-O-C, respectively [42, 43]. Characteristic peaks come from Nafion were not seen clearly at CMA/N hybrid nanofibers that may be due to mostly CMA molecules exist at the surface of the nanofibers.

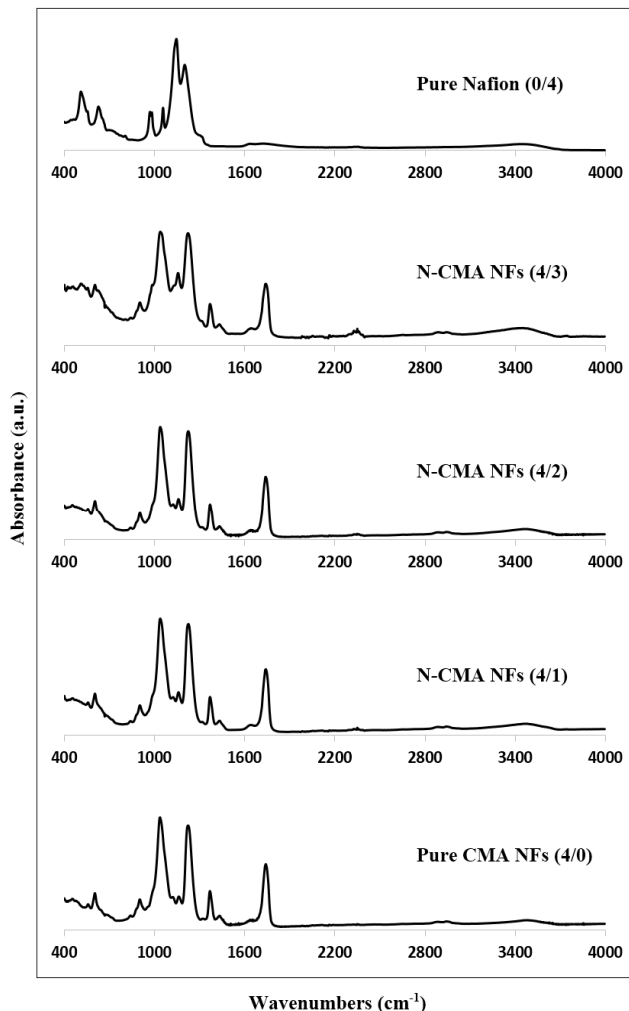


Figure 6. ATR-FTIR spectra of CMA/Nafion hybrid nanofibers with differing mixing ratio.

Table 1. Characteristics of measured electrospinning solution parameters

CMA/N Ratio	Shear viscosity (cP)	Surface tension (mN m^{-1})	Conductivity ($\mu\text{S cm}^{-1}$)
4/0	700	31.52	6
4/1	500	33.05	65
4/2	400	34.98	127
4/3	600	34.30	237

^aCMA/N = Cellulose monoacetate/Nafion hybrid nanofiber

3.3. Thermal Analysis of As-spun NFs with DSC and TGA

Pure CMA nanofibers (Figure 7a) present a broad peaks around 226 °C, which is associated with the melting temperature of CMA nanofibers [2]. Glass transition of CMA is detected around 197 °C [44]. Even though melting temperature is clearly seen at CMA nanofibers, since it may be Nafion addition does not allow an appropriate crystallization of CMA, melting points for CMA are not detectable at CMA/N hybrid nanofibers. These peaks disappeared with the addition of Nafion to CMA as a result of a proper blend of Nafion and CMA in the electrospinning solution (This can be seen at the transparent solution phase in Figure 3A). The broad peaks observed around 150, 157 and 161°C for 4/3, 4/2 and 4/1 CMA/N hybrid nanofiber samples may be associated to thermal energy absorbed to loosen the strong association of the pendant sulfonic acid groups [45]. This peak shifts to higher temperature with increasing CMA content in CMA/N hybrid nanofibers (Figure 7d).

Thermal stability and weight loss with the temperature of pure CMA and CMA/N hybrid nanofibers in a nitrogen atmosphere are observed by TGA and DTG plots and demonstrated in Figure 8. Weight loss between 50-100°C corresponds to the removal of water from the nanofibers. As it is seen from the TGA plot, comparing pure CMA nanofibers weight loss originated from water removal is higher at CMA/N nanofibers and increase with increasing Nafion ratio since more water molecules are held by CMA/N hybrid nanofibers. Single major weight loss is observed around between 272-398°C for pure CMA

nanofibers that related to removal of volatiles produced from the decomposition of the polymer [46]. Major weight loss is divided into different parts and weight loss temperature fluctuated at CMA/N hybrid nanofibers. Thermal degradation temperature decreases dramatically with the addition of Nafion into CMA nanofibers and decomposition occurs at a broad temperature range. Residual of the materials after TGA measurements are about 18.05, 20.02 and 20.01 wt. % respectively for 4/0, 4/1 and 4/3 CMA/N hybrid nanofibers.

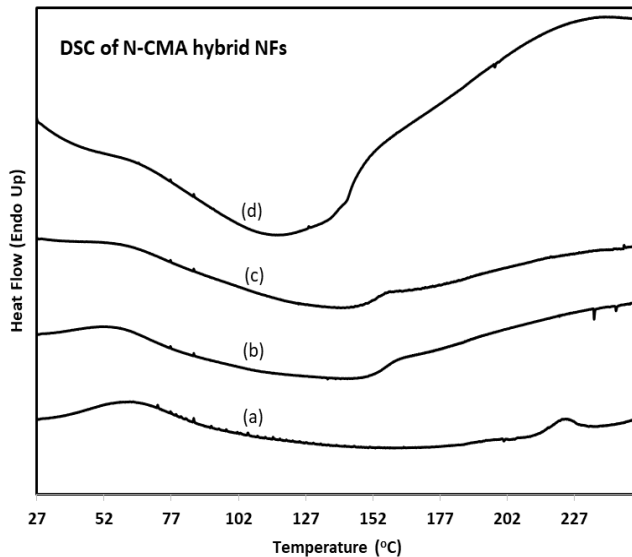


Figure 7. DSC thermograms of CMA/N hybrid nanofibers depending on CMA/N ratio in electrospinning solution: (a) 4/0, (b) 4/1, (c) 4/2, and (d) 4/3.

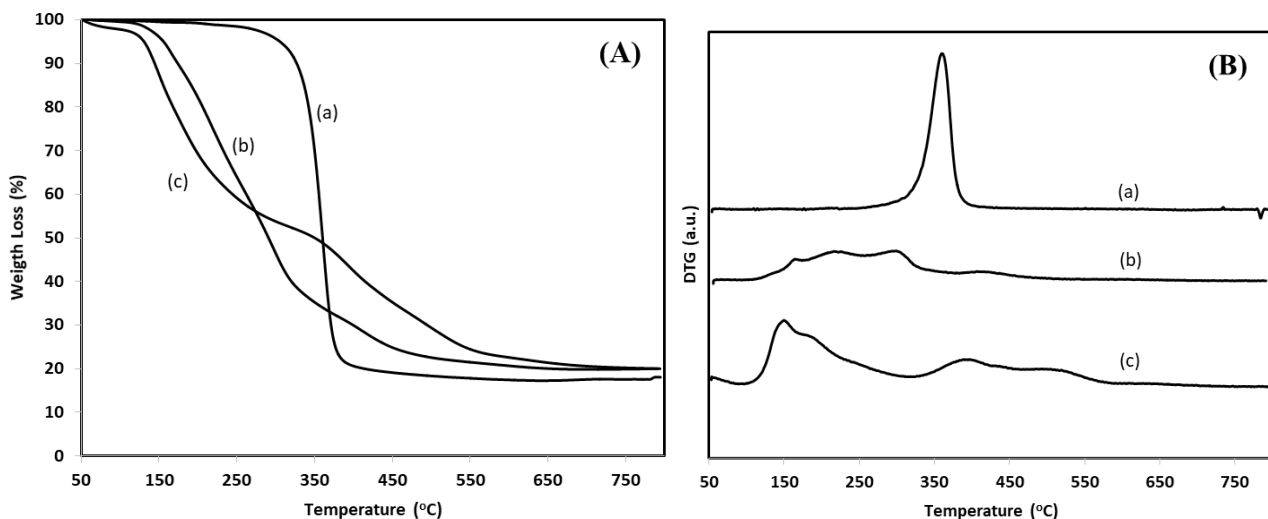


Figure 8. (A) TGA and (B) DTG thermograms of CMA/N hybrid nanofibers in nitrogen gas atmosphere (depending on CMA/Nafion ratio in electrospinning solution): (a) 4/0, (b) 4/1, (c) 4/3.

a. Electrochemical Biosensor Analysis of As-spun Hybrid NFs

As mentioned that electrochemically guanine oxidation is most detectable than other bases, so guanine oxidation signal is focused in this study [47]. During the electrochemical measurement, oxidation signal of guanine was observed at about +1,0 V by using CMA/N nanofiber electrodes for both neat ssDNA (Figure 9A) and NH-modified (Figure 9B) ssDNA samples. As it is seen from Figure 9A, signal intensity is maximum (1.69 μ A) for pure CMA nanofibers at neat ssDNA sample. Intensities are 1.69, 1.16, 0.89, 1.27 μ A for 4/0, 4/1, 4/2 and 4/3 for neat ssDNA on CMA/N nanofiber samples tested sequentially. Initial addition of Nafion into CMA nanofibers decreased the signal intensity comparing to pure CMA nanofibers. Increasing the Nafion ratio in CMA/N nanofibers first decreased the intensity of the signal and increased it again if the Nafion ratio continuously increased, but the signal intensity did not pass the intensity of pure CMA. Intensities are 0.09, 0.38, 1.06, 0.79 μ A for 4/0, 4/1, 4/2 and 4/3 for NH-modified ssDNA on CMA/N nanofiber samples tested sequentially. Comparing neat DNA, signal intensity increases with the addition of Nafion into CMA/N nanofibers at NH-modified ssDNA sample since it may be an interaction between NH groups on ssDNA and SO₃ groups on Nafion. Negatively charged Nafion molecules in CMA/N hybrid nanofibers could be interacted more positively charged guanine bases between biosensor surface and ssDNA molecule leads to signal enhancement [48]. Hu et al. reported that DNA molecules could be bonded to sulfonic groups from the amine groups of DNA [49]. So, NH modified DNA molecules could be strongly attached to the nafion containing CMA nanofibers comparing to unmodified DNA samples and the electrochemical signal intensity could be enhanced. Guanine oxidation enhancement was also reported by Cam et al, by addition of polyaniline into polyacrylonitrile nanofibers [35]. DNA molecules were physically adsorbed on the polyacrylonitrile/polyaniline

nanofibers and the signal enhancement was related to the conductive nature of polyaniline comparing. So, it was concluded that if there is a strong interaction between the surface of nanofibers and the DNA molecules, the electrochemical signal intensity increases properly.

4. CONCLUSION

In this study, cellulose monoacetate/Nafion hybrid nanofibers have been fabricated via electrospinning technique on the cylindrical graphite substrates. Increasing the Nafion ratio leads to inhomogeneous solution property and solution transform from transparent to blurry phase. At the same time, nanofibers morphologies transform from uniform structure to bead on a string defect morphology with increasing Nafion ratio in CMA/N hybrid nanofibers. Neat and NH-modified single strand DNA molecules were immobilized on as-prepared nanofiber-PGE systems. Guanine oxidation signal intensity changes were observed regarding CMA and addition of Nafion into CMA/N nanofibers at NH-modified ssDNA. The strong interaction between biosensor surface and ssDNA molecule leads to signal enhancement. The examined CMA/N hybrid nanofibers could be a promising interface for DNA biosensor devices.

ACKNOWLEDGEMENT

This study was supported by Scientific Research Project Unit (BAP) of Bursa Uludağ University, under project number: KUAP (MH) 2018/11. The authors thank Bursa Uludag University. The study is Ayşe Bostancı's Master thesis at the Graduate School of Natural and Applied Sciences, Bursa Uludağ University. Ayse Bostancı thanks to Karima Sahtani for her help on nanofiber preparation.

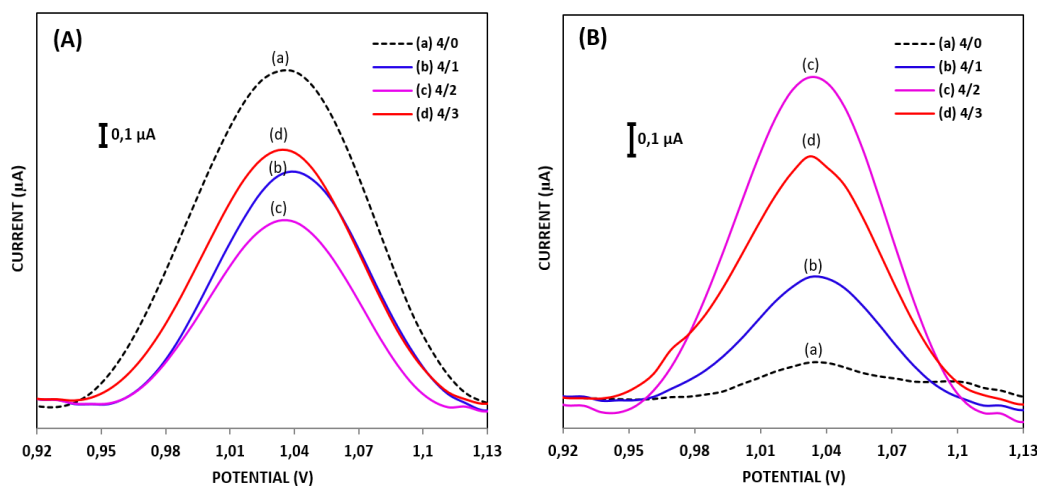


Figure 9. Electrochemical measurements: Voltammograms of the guanine oxidation signals of probe coated surfaces. (A) ssDNA, (B) NH-modified ssDNA

REFERENCES

1. Zhang L, Menkhaus TJ, Fong H. 2008. Fabrication and bioseparation studies of adsorptive membranes/felts made from electrospun cellulose acetate nanofibers, *Journal of Membrane Science* 319, 176-184.
2. Ma Z, Kotaki M, Ramakrishna S. 2005. Electrospun cellulose nanofiber as affinity membrane, *Journal of Membrane Science* 265, 115-123.
3. Croisier F, Jerome C. 2013. Chitosan-based biomaterials for tissue engineering, *European Polymer Journal* 49, 780-792.
4. Kim ID, Hong JM, Lee BH, Kim DY, Jeon EK, Choi DK, Yang DJ. 2007. Dye-sensitized solar cells using network structure of electrospun ZnO nanofiber mats, *Applied Physics Letter* 91, 163109.
5. Bai Y, Wang Z, Wu C, Xu R, Wu F, Liu Y, Li H, Li Y, Lu J, Amine K. 2015. Hard carbon originated from polyvinyl chloride nanofibers as high-performance anode material for Na-ion battery, *ACS Applied Materials Interfaces* 7(9), 5598-5604.
6. Marx S, Jose MV, Andersen JD, Russell AJ. 2011. Electrospun gold nanofiber electrodes for biosensors, *Biosensors and Bioelectronics* 26, 2981-2986.
7. Ren G, Xu X, Liu Q, Cheng J, Yuan X, Wu L, Wan Y. 2006. Electrospun poly(vinyl alcohol)/glucose oxidase biocomposite membranes for biosensor applications, *Reactive Functional Polymers* 66, 1559-1564.
8. Aykut Y, Saquing CD, Pourdeyhimi B, Parsons GN, Khan S.A. 2012. Templating quantum dot to phase-transformed electrospun TiO₂ nanofibers for enhanced photo-excited electron injection, *ACS Applied Materials Interfaces* 4(8), 3837-3845.
9. Aykut Y, Parsons GN, Pourdeyhimi B, Khan SA. 2013. Synthesis of mixed ceramic Mg_xZn_{1-x}O nanofibers via Mg²⁺ doping using Sol-Gel electrospinning *Langmuir* 29 (12), 4159-4166.
10. Liu Y, Chen JY. 2016. Enzyme immobilization on cellulose matrixes, *Journal of Bioactive and Compatible Polymers* 31, 553-567.
11. Esa F, Tasirin SM, Rahman NA. 2014. Overview of Bacterial Cellulose Production and Application, *Agriculture and Agricultural Science Procedia* 2, 113-119.
12. Ek R, Gustafsson C, Nutt A, Iversen T, Nyström C. 1998. Cellulose powder from Cladophora sp. algae, *Journal of Molecular Recognition* 11, 263-265.
13. Credou J, Berthelot T. 2014. Cellulose: From biocompatible to bioactive material, *Journal of Materials Chemistry B* 2, 4767-4788.
14. Majumdar A, Mukhopadhyay S, Yadav R. 2010. Thermal properties of knitted fabrics made from cotton and regenerated bamboo cellulosic fibres, *International Journal of Thermal Sciences* 49, 2042-2048.
15. Helenius G, Bäckdahl H, Bodin A, Nannmark U, Gatenholm P, Risberg B. 2006. In vivo biocompatibility of bacterial cellulose, *Journal of Biomedical Materials Research* 76A, 431-438.
16. Liu H, Hsieh YL. 2002. Ultrafine fibrous cellulose membranes from electrospinning of cellulose acetate, *Journal of Polymer Science Part B Polymer Physics* 40, 2119-2129.
17. Fan X, Zhang T, Zhao Z, Ren H, Zhang Q, Yan Y, Lv G. 2013. Preparation and characterization of bacterial cellulose microfiber/goat bone apatite composites for bone repair, *Journal of Applied Polymer Science* 129, 595-603.
18. Taepaiboon P, Rungsardthong U, Supaphol P. 2007. Vitamin-loaded electrospun cellulose acetate nanofiber mats as transdermal and dermal therapeutic agents of vitamin A acid and vitamin E, *European Journal of Pharmaceutics Biopharmaceutics* 67, 387-397.
19. Frey M.W. 2008. Electrospinning cellulose and cellulose derivatives, *Polymer Reviews* 48, 378-391.
20. Tran C, Kalra V. 2013. Co-continuous nanoscale assembly of Nafion-polyacrylonitrile blends within nanofibers: A facile route to fabrication of porous nanofibers, *Soft Matter* 9, 846-852.
21. Zhang F, Zhang Z, Liu Y, Leng J. 2014. Shape memory properties of electrospun nafion nanofibers, *Fibers and Polymers* 15, 534-539.
22. Dong B, Gwee L, Salas-De La Cruz D, Winey KI, Elabd YA. 2010. Super proton conductive high-purity nafion nanofibers, *Nano Letters* 10(9), 3785-3790.
23. Molla S, Compan V. 2011. Polyvinyl alcohol nanofiber reinforced Nafion membranes for fuel cell applications, *Journal of Membrane Science* 372, 191-200.
24. Sharma DK, Li F, Wu YN. 2014. Electrospinning of Nafion and polyvinyl alcohol into nanofiber membranes: A facile approach to fabricate functional adsorbent for heavy metals, *Colloids Surfaces A Physicochemical Engineering Aspects* 457, 236-243.
25. Fojta M, Daňhel A, Havran L, Vyskočil V. 2016. Recent progress in electrochemical sensors and assays for DNA damage and repair, *TrAC - Trends in Analytical Chemistry* 79, 160-167.
26. Palecek E, Fojta M, Tomschik M, Wang J. 1998. Electrochemical biosensors for DNA hybridization and DNA damage, *Biosensors and Bioelectronics* 13, 621-628.
27. Halliwell B. 2000. Why and how should we measure oxidative DNA damage in nutritional studies? How far have we come?, *The American Journal of Clinical Nutrition* 72, 1082-1087.
28. Lee HE, Kang YO, Choi SH. 2014. Electrochemical-DNA biosensor development based on a modified carbon electrode with gold nanoparticles for influenza a (H1N1) detection: Effect of spacer, *International Journal of Electrochemical Science* 9, 6793-6808.
29. Jamaluddin RZAR, Heng LY, Tan LL, Chong KF. 2018. A Biosensor for Genetic Modified Soybean DNA Determination via Adsorption of Anthraquinone-2-sulphonic Acid in Reduced Graphene Oxide, *Electroanalysis* 30, 250-258.
30. Wang J, Rivas G, Cai X, Palecek E, Nielsen P, Shiraishi H, Dontha N, Luo D, Parrado C, Chicharro M, Farias P.A.M, Valera FS, Grant DH, Ozsoz M, Flair MN. 1997. DNA electrochemical biosensors for environmental monitoring, *Analytica Chimica Acta* 347, 1-8.
31. Ni Y, Wang P, Song H, Lin X, Kokot S. 2014. Electrochemical detection of benzo(a)pyrene and related DNA damage using DNA/hemin/nafion-graphene biosensor, *Analytica Chimica Acta* 821, 34-40.
32. Qiu Y, Qu X, Dong J, Ai S, Han R. 2011. Electrochemical detection of DNA damage induced by acrylamide and its metabolite at the graphene-ionic liquid-Nafion modified pyrolytic graphite electrode, *Journal of Hazardous Materials* 190, 480-485.
33. Gong Q, Wang Y, Yang H. 2017. A sensitive impedimetric DNA biosensor for the determination of the HIV gene based on graphene-Nafion composite film, *Biosensors and Bioelectronics* 89, 565-569.
34. Hlavatá L, Vyskočil V, Beníková K, Borbélyová M, Labuda J. 2014. DNA-based biosensors with external Nafion and chitosan membranes for the evaluation of the antioxidant activity of beer, coffee, and tea, *Central European Journal of Chemistry* 12(5), 604-611.
35. Cam E, Aladag Tanik N, Cerkez I, Demirkhan E, Aykut Y. 2018. Guanine oxidation signal enhancement in single strand DNA with polyacrylonitrile/polyaniline (PAN/PAni) hybrid nanofibers, *Journal of Applied Polymer Science* 135(3), 45567.
36. Aladag N, Trnkova L, Kourilova A, Ozsoz M, Jelen F. 2010. Voltammetric Study of Aminopurines on Pencil Graphite Electrode in the Presence of Copper Ions, *Electroanalysis* 22, 1675-1681.
37. Topkaya SN, Aydinlik S, Aladag N, Ozsoz M, Ozkan-Ariksoysal D. 2010. Different DNA immobilization strategies for the interaction of anticancer drug irinotecan with DNA based on electrochemical DNA biosensors, *Combinatorial Chemistry & High Throughput Screening* 13, 582-589.

-
38. Joshi MK, Tiwari AP, Pant HR, Shrestha BK, Kim HJ, Park CH, Kim CS. 2015. In Situ Generation of Cellulose Nanocrystals in Polycaprolactone Nanofibers: Effects on Crystallinity, Mechanical Strength, Biocompatibility, and Biomimetic Mineralization, *ACS Applied Materials & Interfaces* 7 (35), 19672–19683.
39. Zhao Y, Zhu X, Liu H, Luo Y, Wang S, Shen M, Zhu M, Shi X. 2014. Dendrimer-functionalized electrospun cellulose acetate nanofibers for targeted cancer cell capture applications, *Journal of Materials Chemistry B* 2, 7384–7393.
40. Liu R, Peng Y, Cao J, Chen Y. 2014. Comparison on properties of lignocellulosic flour/polymer composites by using wood, cellulose, and lignin flours as fillers, *Composite Science Technology* 103, 1-7.
41. Jiang G, Zhang J, Qiao J, Jiang Y, Zarrin H, Chen Z, Hong F. 2015. Bacterial nanocellulose/Nafion composite membranes for low temperature polymer electrolyte fuel cells, *Journal of Power Sources* 273, 697-706.
42. Yao Y, Li J, Lu H, Gou J, Hui D. 2015. Investigation into hybrid configuration in electrospun nafion/silica nanofiber, *Composites Part B Engineering* 69, 478-483.
43. Shao ZG, Wang X, Hsing IM. 2002. Composite Nafion/polyvinyl alcohol membranes for the direct methanol fuel cell, *Journal of Membrane Science* 210, 147-153.
44. Ali S, Khatri Z, Oh KW, Kim IS, Kim SH. 2014. Zein/cellulose acetate hybrid nanofibers: Electrospinning and characterization, *Macromolecular Research* 22, 971-977.
45. Guo B, Liu Z, Hong L. 2011. Doping Nafion® matrix by paramid flakes for a proton transport less reliant on moisture, *Journal of Materials Chemistry* 21, 12414-12421.
46. Li R, Dou J, Jiang Q, Li J, Xie Z, Liang J, Ren X. 2014. Preparation and antimicrobial activity of β -cyclodextrin derivative copolymers/cellulose acetate nanofibers, *Chemical Engineering Journal* 248, 264-272.
47. Halliwell B. 2000. Why and how should we measure oxidative DNA damage in nutritional studies? How far have we come?, *The American Journal of Clinical Nutrition* 72, 1082–1087.
48. Yin H, Zhou Y, Ma Q, Ai S, Ju P, Zhu L, Lu L. 2010. Electrochemical oxidation behavior of guanine and adenine on graphene-Nafion composite film modified glassy carbon electrode and the simultaneous determination, *Process Biochemistry* 45, 1707-1712.
49. Hu YW, Yang T, Wang XX, Jiao K. 2010. Highly Sensitive Indicator-Free Impedance Sensing of DNA Hybridization Based on Poly(m-aminobenzenesulfonic acid)/TiO₂ Nanosheet Membranes with Pulse Potentiostatic Method Preparation, *Chemistry - A European Journal* 16, 1992–1999.



The Performance Analysis of Geotextile Materials Used for Irrigation Water and Weed Control in Stone Garden Landscape Design

Handan Çakar¹, Özlem Akat Saraçoğlu¹, Cenk Ceyhun Kılıç¹, Hülya Akat², Önder Yücel¹

¹Ege University, Bayındır Vocational Training School, Bayındır-İzmir, Turkey

²Muğla Sitki Koçman University, Ortaca Vocational Training School, Ortaca-Muğla, Turkey

Corresponding Author: Handan Çakar, handan.cakar@ege.edu.tr

ABSTRACT

In recent years, the droughts which have been occurring as a result of global warming, indicate that we need to take serious measures regarding water saving. Contributing to the preservation of the ecological equilibrium by creating environmentally conscious projects in landscape design confronts us as a requirement of professional discipline. In this regard, the necessity to gravitate towards uses which can save water instead of wide grass fields becomes obvious. Stone garden designs, which we encounter in this very moment, present an environmentally friendly alternative to aquatic gardens.

It is thought that, alongside saving water with stone garden designs, the geotextile materials used in these designs would prevent the stones sinking into soil as well as preventing the occurrence of weed, hence lessening the usage of chemicals thus generating gains with regards to decreasing soil pollution. Based on this, the performances of the texturally and structurally different geotextile materials chosen as samples were tested at the testing grounds at the Ege University Bayındır Vocational Training School Campus. Recommendations with regards to ecologically conscious stone garden landscape designing have been made in accordance with the gathered findings.

ARTICLE HISTORY

Received: 17.12.2018

Accepted: 16.07.2019

KEYWORDS

Geotextile, technical textiles, stone garden, water use efficiency, weed control

1. INTRODUCTION

In the agricultural sector, the climatological conditions which take place from planting to harvest have great consequences on the economic value and the quality of the produce. During the production of agricultural produce, agricultural technical textiles have been begun to be used in order to minimise the effects of adverse natural conditions and protecting, harvesting and the preservation of the products.

Technical textiles, by definition, are based on the uniting quality of bringing together the performance and decorative attributes and the functions of a quickly increasing number of textile products, thus expressed as "Textile material and

products made for their technical performances and functional attributes instead of their aesthetic or decorative attributes" [1].

In many applications such as fishing, the packaging of agricultural produce, in the acceleration of the growing processes of plants, the protection of products from UV-rays, protecting animals from adverse weather conditions in husbandry, the disinfestation of agricultural areas, in preventing weed growth, erosion and many other applications such as drainage, agricultural technical textiles are used [1, 2].

The protection of natural resources such as soil, air and water, which are essential elements of life itself, is a very

To cite this article: Çakar H, Akat Saraçoğlu Ö, Kılıç C.C. Akat H, Yücel Ö. 2019. The performance analysis of geotextile materials used for irrigation water and weed control in stone garden landscape design. *Tekstil ve Konfeksiyon* 29(3), 237-245.

important ecological topic. The recent population growth, technological advances, quickly increasing consumption alongside growing industrialism and climate change caused by global warming, cause the quick deterioration and destruction of natural resources [3]. In this vein, the emphasis put on “natural resources not being completely consumed short term and consumed in a manner which would create a balance between humankind and the nature and allowing the future generations to subsist” in the 1987 report by the World Commission On Environment And Development, has caused the subject of environmental sustainability to gain increasing importance [4]. At this juncture, the choice of water-efficient landscape designs over traditional landscape designs which require great water consumption confronts us as an obligation [5-7].

Water, which is amongst natural resources; is a massively important element which affects life directly, causes maximum efficiency between natural resources, which cannot be produced artificially by humankind and has no alternative. In this day, due to the increased water demand connected to technological advancements and climate change connected to global warming continuously lessen the number of clean water sources [8, 9].

Corresponding to the increasing population on soil, the fastest consumed resource on soil is water. In order to at least preserve the status quo of this crucial resource, it needs to be used efficiently. The efficient usage of irrigation water may be achieved by using it in the amount the plant being grown requires. With this objective, irrigation can be carried out in a controlled and regulated manner by supplying irrigation water consistent with the requirements of the plant to be irrigated.

The water consumption reaching great heights in large outdoor areas such as parks or gardens require the development of new landscape designs which use the least amount of water possible in these areas. Due to this reason, under the larger concept of Water-Efficient Landscaping using water in an efficient manner has come up under different names [Water-Wise, Water-smart, Low Water] and gave birth to a new concept against traditional landscape design [10].

In present day when the water resources are quickly being diminished, trailing plants need to be chosen instead of large grass facets which require a great amount of water. Moreover, as an alternative to the aesthetic uses of grass, “stone garden” landscaping designs are being talked about. The concept of “stone gardens” which gives ease of maintenance and minimises water consumption plays a great role in creating environmentally conscious projects [11-13].

For the stone gardens which present themselves as an aesthetically valuable and environmentally conscious water

saving alternative to be long-lasting, the necessary attention must be paid during the preparation stage of the application.

Failing that, the aesthetic effect produced during the erroneous executions during the application of the stone garden landscape designs will not last long, the stones laid on the ground will sink and the stone gardens will leave their places to a sight completely taken over by weeds.

Aim of this research is to find out the most suitable geotextile materials used in garden designs would prevent the stones sinking into soil as well as preventing the occurrence of weed, hence lessening the usage of chemicals thus generating gains with regards to decreasing soil pollution. Additionally, recommendations have been made to be able to create long lasting and environmentally conscious projects by establishing weed control in stone garden landscape designs and ascertaining the requirements to desired outcome long lasting without maintenance.

2. MATERIAL AND METHOD

The research was carried out at the Ege University Bayındır Vocational Training School during the 3-month long summer period of 2018. In the research which is an open field experiment, different geotextile materials were used to prevent the detrimental effects of the practical materials used in landscape designs. Alongside this, stone materials which are popular in the stone garden landscape designs were used. With this objective, 4 different geotextile materials and 4 different stone materials were taken under trial during the examination application. The materials used for this purpose are summarized below.

2.1 Research Subjects

Uncovered group (G0): It has formed the examination application subjects in the research. No geotextile material has been used. In this research topic only the topics regarding the soil surfaces on which the stones were laid have been examined.

Covered group (GT): They are research subjects which consist of geotextile materials which have different attributes. All the geotextile materials and stone materials which have been included in the research are shown on Table 1.

The research was carried out with 3 replications according to the experimental design on randomized blocks. The research, which was conducted as an open field pot experiment, used square cut plastic pots sized 25x25x25 cm with a drainage exit at the bottom. 60 pots were filled with gravels and then local soil silt in texture which has national attributes to establish 15.625 litre root volume.

Table 1. Some physical properties of geotextile and stone materials used in the research

Code	Geotextile Materials	Abbreviation	g/m ²
G1	Polyethylene layer (0.30 mm)	PE	160
G2	Polypropylene	PP	78
G3	%100 Polyester un-textured surface	PES	175
G4	Jute sack	JU	280
Code	Stone Materials	Colour	Grain Size (cm)
S1	Sand (washed creek sand)	Natural colour	0,1-0,2
S2	Creek Pebble	Grey	2*3
S3	Dolomite	White	1*3
S4	Volcanic Tuff	Dark shade	1,2-1,8

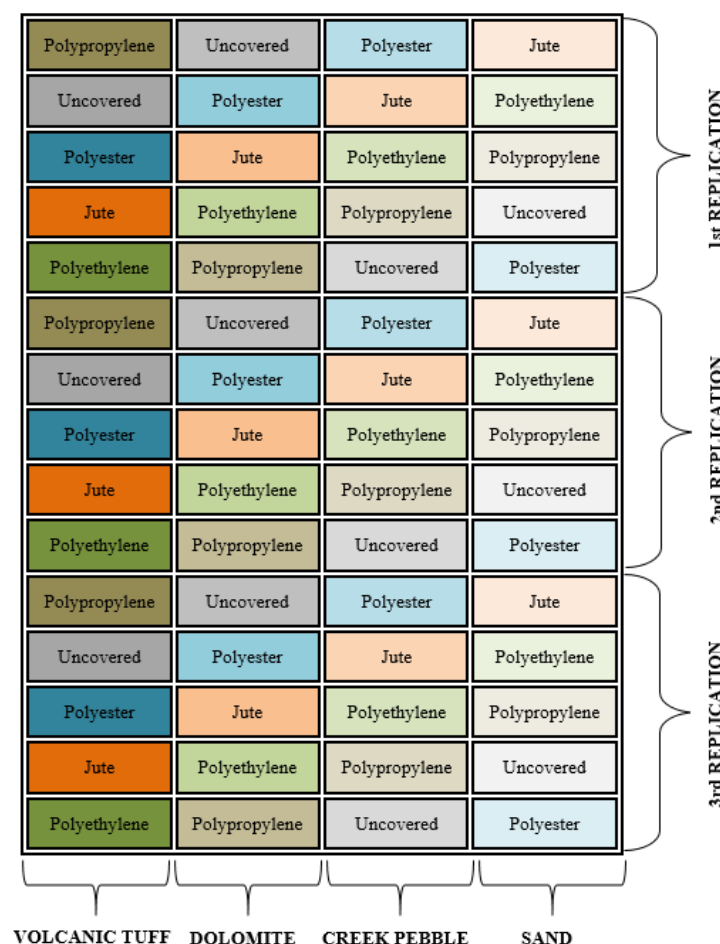


Figure 1. Distribution of applications in the study area and experimental design.

As botanical material; small leafed the sedge plant (*Cyperus roduntus*) which can develop much more than the wide leafed cultivated plants in the Aegean Region, which is hard to combat the adversary effects of, and commonly seen in the region and the common purslane (*Portulaca oleracea*) which is wide leafed so that the differences may be observed in leaf forms, which stays in vegetation throughout the summer season, were used.

The culture of the examined *Cyperus roduntus* herbs was obtained by the plantation of the *Cyperus roduntus* tubers gathered from the land which makes up the experiment area of 5 each in every pot. Also, in order to observe the reaction of seed germination under geotextile material, 43 seeds each from the *Portulaca oleracea* plant was planted into each pot. Because the seed germination ratio for the *Portulaca oleracea* is 94% according to Tulukcu [14], the

germinated number of *Portulaca oleracea* is estimated to be 40 for every 43 seed.

Later on, by laying the stone materials on top of the geotextile materials, with for different geotextile materials and 1 control group, the pots were made ready in order to form combinations of the 4 different stone groups.

Drip irrigation system was used during the dispersal of irrigation water to the pot environments and the application of it. With this objective, drip irrigation laterals made of PE pipes with an outside diameter of 16 mm have been placed on the pots and a dripper with a flow rate of 2.3 litre/hour for each plant was placed on the lateral line. The automation was established by using a pressure regulator on the pump exit, valve, filter and an electro-valve.

The amount of water used for the irrigation of the materials in the experiment field pots was ascertained by the usage of the aforementioned meter. The drained irrigation water which couldn't be held by the geotextile material and the soil was discharged using 1 drainage hole in the middle of the pot, with a diameter of 16mm. Before the drained water was discharged from the system, it was tested for volume and the electrical conductivity (EC) and pH measurements were made. The amount of the irrigation water applied to the pot environment was regulated based on the amount of yearly rainfall the Aegean Region receives.

In order to ascertain how much the used geotextile material hampers light, one of the most important competitive factors between plants, the volume of light beneath and above the geotextile was measured using a luxmeter on a regular basis. The temperature of the soil in the pots was also measured on a regular basis using a pot type digital thermometer. External temperature measurements were also made during the research in order to gather meteorological data for the duration of the research.

The findings gathered at the end of the experiment were entered to the digital environment using the Microsoft Office 2010 Excel programme. Later on using this data, the necessary statistical analyses such as the Kruskal Wallis Test and Mann-Whitney U Test were carried out on the SPSS programme and the data gathered after the analyses were interpreted.

3. RESULTS AND DISCUSSION

The research findings were given out in 3 different groups, labelled as "Per the type of geotextile material", "Per the type of stone material" and "Per the condition of having geotextile material".

- The evaluation carried out per the type of the geotextile material was carried out by having the same common stones on the geotextile material for every group.

- The evaluation carried out per the type of stone material was carried out by having the same common geotextile materials underneath for every group.

- The evaluation carried out per the condition of having geotextile material was carried out by comparing the pots which contain geotextile material (the geotextile material is the same for all the groups) to the ones which do not.

Per the type of geotextile material;

Per the type of the geotextile materials used in the research, when they were viewed in terms of permeability, while polyethylene shows no drainage at all, the highest amount of drainage has been detected with polypropylene. The group which contained no geotextile material demonstrated less drainage than the drainage in polypropylene (Table 2).

When the EC and pH values obtained from the drainage water were observed, no significant statistical difference has been found between the groups.

While the soil temperature was found to be the highest in the group which contains no geotextile material, it has been found out to be the least in the group which contains polyethylene. Polypropylene group was found out to have the highest soil temperature in the groups which contain geotextile materials (Table 3).

While light transmittance was found to be at its highest level in the group which contains no geotextile material, it was recorded to be the least in the Jute group. Polyethylene was recorded to be the highest light transmitting geotextile containing group (Table 4).

In the evaluation made to ascertain the weed prevention performance; while the weed growth has the largest ratio in the group which has no geotextile material, polyethylene and polyester were observed to give the same result for both *Cyperus roduntus* and *Portulaca oleracea* and both materials did not allow any weed to grow. Polypropylene showed similar results to polyethylene and polyester when it comes to *Cyperus roduntus*. Jute, on the other hand, was more successful in terms of curtailing *Portulaca oleracea* while showing very low levels of performance against *Cyperus roduntus* (Table 5).

Per type of stone materials;

When the permeability, pH and weed prevention performance of the stone materials used in the research were compared, the groups showed no statistical difference.

While the highest levels of EC were observed in sand, the lowest were observed in volcanic tuff (Table 6).

The highest levels of soil temperature were observed with sand while the lowest were observed with dolomite (Table 7).

The highest values pertaining to light transmittance were observed with dolomite while the lowest were observed with sand (Table 8).

Table 2. The level of drainage per the type of geotextile materials

Variable	Cover type	Qty.	Mean	Minimum	Maximum	Mean Rank	Km. Sq.	Degree of Freedom	P value
Drainage (ml)	G0	12	578.17	170	930	29.75			
	G1	12	0.00	0	0	7.5			
	G2	12	967.70	617	1225	50	36.67***	4	0
	G3	12	723.76	507.5	966.67	33.46			
	G4	12	607.86	0	1040	31.79			

*** significance level $\alpha < 0.01$; ** significance level $\alpha < 0.05$; * significance level $\alpha < 0.1$

Table 3. The soil temperatures per the type of geotextile materials

Variable	Cover type	Qty.	Mean	Minimum	Maximum	Mean Rank	Km. Sq.	Degree of Freedom	P Value
Temperature (°C)	G0	12	27.75	25.37	29.78	39.46			
	G1	12	26.64	25.6	28.32	20.96			
	G2	12	27.68	26.43	29.78	36.96	9.427*	4	0,051
	G3	12	27.21	25.32	29.78	29.71			
	G4	12	26.87	25.65	29.83	25.42			

*** significance level $\alpha < 0.01$; ** significance level $\alpha < 0.05$; * significance level $\alpha < 0.1$

Table 4. The light transmittance levels of the geotextile materials per type

Variable	Cover type	Qty.	Mean	Minimum	Maximum	Mean Rank	Km. Sq.	Degree of Freedom	P Value
Light (lux)	G0	12	13.68	1	34	42.33			
	G1	12	6.43	1	16.5	35.46			
	G2	12	3.26	1	10.17	30.54	12.415**	4	0,015
	G3	12	1.93	1	5.33	22.58			
	G4	12	1.71	1	4	21.58			

*** significance level $\alpha < 0.01$; ** significance level $\alpha < 0.05$; * significance level $\alpha < 0.1$

Table 5. The amount of weed growth per type of geotextile material

Variable	Cover type	Qty.	Mean	Minimum	Maximum	Mean Rank	Km. Sq.	Degree of Freedom	P value
Cyperus roduntus (number)	G0	12	11.17	5	20	54.04			
	G1	12	0.00	0	0	21			
	G2	12	0.17	0	2	22.83	46.417***	4	0
	G3	12	0.00	0	0	21			
	G4	12	2.17	0	8	33.63			
Portulaca oleracea (number)	G0	12	10.92	0	23	52.33			
	G1	12	0.00	0	0	23			
	G2	12	0.25	0	1	29.13	42.276***	4	0
	G3	12	0.00	0	0	23			
	G4	12	0.08	0	1	25.04			

*** significance level $\alpha < 0.01$; ** significance level $\alpha < 0.05$; * significance level $\alpha < 0.1$

Table 6. EC values per type of stone material

Variable	Stone group	Qty.	Mean	Minimum	Maximum	Mean Rank	Km. Sq.	Degree of Freedom	P value
EC ($\mu\text{S}/\text{cm}$)	S1	11	791.65	613	997.67	36.82	19.201***	3	0
	S2	11	667.53	577.83	765.25	26.05			
	S3	12	636.97	577.83	828.25	18.88			
	S4	12	602.93	538.33	701.25	13.58			

*** significance level $\alpha < 0.01$; * significance level $\alpha < 0.1$

Table 7. Soil temperatures per stone material type

Variable	Stone Group	Qty.	Mean	Minimum	Maximum	Mean Rank	Km. Sq.	Degree of Freedom	P value
Temperature ($^{\circ}\text{C}$)	S1	15	27.80	25.72	29.83	38.8	18.938***	3	0
	S2	15	27.21	26.08	29.2	32.03			
	S3	15	26.21	25.32	27.63	14.07			
	S4	15	27.70	26.23	29.78	37.1			

*** significance level $\alpha < 0.01$; * significance level $\alpha < 0.1$

Table 8. The light transmittance levels of stone materials per type

Variable	Stone group	Qty.	Mean	Minimum	Maximum	Mean Rank	Ki. Sq.	Degree of Freedom	P Value
Light (lux)	S1	15	1.01	1	1.17	10.17	36.058***	3	0
	S2	15	5.80	1.17	16.5	40.17			
	S3	15	11.00	1.33	34	44.47			
	S4	15	3.80	1	24.5	27.2			

*** significance level $\alpha < 0.01$; * significance level $\alpha < 0.1$

Per the condition of having geotextile material;

During the research when the permeability, EC and pH were compared per the condition of having geotextile material, no difference was found between the groups.

It was ascertained that the soil temperatures were higher in the group which had no geotextile material (Table 9).

It was observed that light transmittance is greater in the group which has no geotextile material (Table 10).

When the evaluation was made under the context of curtailing weed growth, the amount was ascertained to be higher in the group which had no geotextile material compared to the group which did (Table 11).

Table 9. Soil temperatures per the condition of having geotextile material

Variable	Cover	Qty.	Mean	Mean Rank	Mean Sum	Mann-Whitney U	Z value	P value
Temperature ($^{\circ}\text{C}$)	G0	12	27.75	39.46	473.5	180.5**	-1.987	0,047
	GT	48	27.10	28.26	1356.5			

*** significance level $\alpha < 0.01$; ** significance level $\alpha < 0.05$;

Table 10. Light transmittance levels per the condition of having geotextile material

Variable	Cover	Qty.	Mean	Mean Rank	Mean Sum	Mann-Whitney U	Z value	P value
Light (lux)	G0	12	13.68	42.33	508	146***	-2.661	0,008
	GT	48	3.33	27.54	1322			

*** significance level $\alpha < 0.01$; ** significance level $\alpha < 0.05$;

Table 11. The amount of weed growth per the condition of having geotextile material at the end of the evaluation

Variable	Cover	Qty.	Mean	Mean Rank	Mean Sum	Mann-Whitney U	Z value	P value
<i>Cyperus roduntus</i> (number)	G0	12	11.17	54.04	648.5	5,5***	-6.327	0
	GT	48	0.58	24.61	1181.5			
<i>Portulaca oleracea</i> (number)	G0	12	10.92	52.33	628	26***	-6.37	0
	GT	48	0.08	25.04	1202			

*** significance level $\alpha < 0.01$; ** significance level $\alpha < 0.05$;

The level of weed prevention per the type of stone materials in the group without geotextile materials;

The results stemming from the evaluation which was made per the type of the stone materials placed on geotextile materials is not listed due to the lack of meaningful statistical difference between the groups. This is thought to have been caused by geotextiles underneath which display the character of curbing weed growth. Therefore, a different evaluation was made with means of pots containing merely stone materials and no geotextiles beneath them with 6 evaluations made of 3 loops. The initial weed amount and the amount at the end of the measurement were compared and the ratio of the difference in between was taken into account as the weed growth percentage (Table 12). As a result of the calculations, the increase ratio was spotted to be a positive one with the *Cyperus roduntus*. With the *Portulaca oleracea*, it showed no increase and it has shown

an actual decrease in the overall amount which has reflected upon the increase value in a negative manner. The total sum which was reflected upon the result has shown that there was a decrease in total weed growth.

As a result of this, when the stone materials were evaluated in terms of their weed growth prevention performances, while the greatest increase for the *Cyperus roduntus* was spotted with dolomite, the smallest increase was detected with Volcanic tuffs. With the *Portulaca oleracea*, the greatest increase was seen with dolomite with volcanic tuffs being a close second, while the smallest increase was seen with creek pebble. When the weed types *Cyperus roduntus* and *Portulaca oleracea* are collectively taken into account, while the greatest weed prevention performance was seen to be had with Volcanic tuff, the least was seen to be had with the creek pebble in an environment.

Table 12. Wild weed growth ratios in pots containing no geotextile material but merely stone material

ENVIRONMENT	WEED		
	<i>Cyperus roduntus</i> increase ratio (%)	<i>Portulaca oleracea</i> increase ratio (%)	Collective increase ratio (%)
S1	93.40	(-)74.18	(-)55.56
S2	133.40	(-)54.18	(-)33.33
S3	213.40	(-)82.50	(-)49.62
S4	53.40	(-)80.00	(-)65.18

* (-) shows the amount of decrease.

4. RESULTS AND DISCUSSION

When the geotextile materials per type were evaluated with regards to their permeability, polyethylene showed no drainage. With its lack of permeability, this material presents a great obstacle with letting rainfall through to the soil. Until water left the environment through vaporisation, the water accumulated on the stone laid on polyethylene and caused moss growth.

With polypropylene showing as a geotextile material even greater permeability than groups which had no geotextile materials, it showed a great degree of success in terms of draining water. The reason for the groups containing no geotextile material showing less permeability is thought to be the weed growth and the usage of the said water by the weeds.

The lowest soil temperature with the geotextile material containing group was spotted to be the polyethylene group. Polypropylene group on the other hand was spotted to be the group with the highest soil temperature. Based on this, it is seen important to choose polypropylene rather than polyethylene with regards to keeping soil temperatures high.

Soil temperature affects all the physical, chemical and biological processes taking place in soil directly [15]. The existence of water in the soil, its movement, vaporization and air capacity, dissolution processes, microbiological activity, root respiration and plant activity all being influenced by the soil temperature was stated by Tonkaz et al., [16] and Ekberli and Sarilar [17]. In general, in most climatic environments, biochemical activity increases when temperatures rise. [17-19]. The temperatures at seed depth level were understood to be especially important for germination periods and shoot growth [20].

Temperature first affects the seed germination during the development of plants. In general, it is slower for germination to take place in cold soil. Cold soil also is not suitable for plant roots to develop and for plants to grow [20]. The processes which take place during plant development such as assimilation, respiration, perspiration and photosynthesis are also closely related to temperature. Most of the chemical reactions which take place within a plant and soil are quicker to happen in higher temperature than cold [17, 21]. In general, with temperatures rising the activities also become quicker. Therefore high temperatures hasten development in most plants. Also, temperatures also exert strong influence over the root development of plants and the dissolvability of the sustenance elements in soil and their digestability by the plants [20].

Jute was seen to be the geotextile material with the lowest light transmittance. Due to this low level of light transmittance, even if weeds grow above the surface, they are expected to die off due to the lack of light. However, even though Jute has a low level of light transmittance, due

to its big pored characteristics it allowed a small amount of weeds to grow. Polyester which displayed a similar level of light transmittance showed no weed growth due to its complete lack of pores.

No meaningful difference was detected between the *Cyperus roduntus* and *Portulaca oleracea* growth rates. In general, all of the geotextile materials showed high degrees of success in preventing weed growth. In this group, polyester and polyethylene came forward due to their complete lack of weed growth.

Sand particles have a size of 2-0.05mm. It is formed through the rocks being disintegrated due to various climatic events and its structure is connected to its source rock with little capacity to hold water. Under conditions where organic materials are not plentiful and due to a lack of clay clusters, grains of sand can't bond with each other. While their good permeability prevents accumulation of water in rainy climates, it also causes the loss of plant sustenance materials [22]. As it could be inferred, the washed salts accumulated in the drainage and the highest EC values were gathered from sand.

Dark surfaces absorb a great amount of radiation while bright surfaces reflect it. Therefore due to its dark shade sand was able to increase soil temperatures more compared to the white coloured dolomite and dolomite had the least measured amount of soil temperature.

The light transmittance factor which is directly related with the germination of weed seeds was observed to be at the highest level in the group which contains dolomite while it was observed to be at the smallest levels in sand. This is thought to be due to the smaller grain sized nature of sand compared to stones. Based on this, the results were similar between dolomite and creek pebble due to their similar particular sizes. Therefore, it could be said that light transmittance grows in parallel with grain size of the rocks.

In the research, per the condition of having geotextile material, it was gathered that soil temperatures and light transmittance were greater in the group which had no geotextile material. This could be explained with the geotextile material obstructing the rays of sun from reaching the soil. Also, when evaluated in the context of weed growth prevention performance, the weed growth was gathered to be far less in the group with geotextile material. As a result of this, it is thought that the geotextile materials are successful at curtailing weed growth. It was in particular observed that the *Portulaca oleracea* due to its wide leaves had a smaller growth rate compared to the narrow leaved *Cyperus rodantus* and it was concluded that geotextile materials are more effective at curtailing the growth of the wide leaved plants.

When geotextile materials were not used, while the greatest weed growth was observed with creek pebble the least was observed with volcanic tuff. Amongst the stone materials

used in this research, it could be said that volcanic tuff are the most successful at curtailing weed growth.

5. CONCLUSION

The usage of the geotextile materials occur as an important factor which should be paid attention to in the installation of the stone garden landscape designs which present an environmentally friendly alternative to the aquatic gardens. For the desired effect to be continuously had without maintenance with the stone garden landscape designs, the usage of geotextile materials presents itself as a necessity.

Polyethylene which is the most popular geotextile in the applications in the market, while showing great success in terms of curtailing weed growth, allows no permeability or light transmittance due to its pore-less nature. In landscape designs where landscaping plants are used, its nature which allows no transmission of water and light causes problems

while the accumulation of water on the textile causes growth of moss on the rocks which creates a bad look. In addition, it is possible to rip the covering material in the part pressed on it and it will be possible to weed out. Polypropylene presented itself as a geotextile material which can by-pass all of these drainage disadvantages, is successful weed-curting wise and can maintain soil temperatures at a higher level. Due to its permeability, it can discharge excess water away from the environment thus preventing negative factors and diseases from fostering. Therefore, by extension, it would also lessen usage of chemicals and have a positive effect on the environment. Due to these attributes, in stone garden landscaping designs it is recommended to use polyethylene as the geotextile material of choice. Also, depending on the results of the research, a combination of Polypropylene and Volcanic tuff is recommended for maximum performance in weed control.

REFERENCES

1. Özdzidar A. 2004. T İstanbul Ticaret Odası, Teknik Tekstiller Sektör Araştırması s.32.
2. Fung W. 2004. Handbook of Technical Textiles 490-522, TheTextile Institute. England.
3. Saltürk M., 2006, Problem of water in the Middle East and analysis of the problem within the perspective of Turkey, Journal of Security Strategies, Vol:3, 21-38
4. Kaypak Ş. 2011. Küreselleşme sürecinde sürdürülebilir bir kalkınma için sürdürülebilir bir çevre. KMÜ Sosyal ve Ekonomik Araştırmalar Dergisi 13(20), 19-33.
5. Knox GW. 2005. Landscape design for water conservation, University of Florida, IFAS Extension, p:3.
6. Aklanoğlu F. 2007, 18-20 October. Climate change impacts on landscape designand practices, international conference on climate change and environmental effects (UKİDEK), Konya, Turkey.
7. Ertop G. 2009. Global warming and xeriscape planning, Ankara University, Thesis of Master, p 164, Ankara.
8. Evsahibioğlu NA, Akhüzüm T, Çakmak B. 2010. Su yönetimi, su kullanımları stratejileri ve sınırlı aşan sular, Türkiye Ziraat Mühendisliği VII. Teknik Kongresi.
9. Bayramoğlu E, Ertek A, Demirel Ö. 2013. Su tasarrufu amacıyla peyzaj mimarlığı uygulamalarında kısıtlı sulama yaklaşımı, İnönü Üniversitesi Sanat ve Tasarım Dergisi 3(7), 45-53.
10. Önder S, Polat AT. 2009, 16-18 Haziran. Yeşil alan uygulamalarında su tasarrufuna yönelik olarak sukkulent yerortüçü bitki türlerinden yararlanma. 1. Ulusal kuraklık ve çölleşme sempozumu, 480-485. Konya, Turkey.
11. Lightfoot DR. 1993. The cultural ecology of puebloan pebble-mulch gardens, human ecology 21, 115–143
12. Anonymous, 2014. Pebble Garden. Web: <http://uniquegarden.in/pebblegarden.html>, erişim 11.06.2018.
13. Anonymous, 2016. Garden Design Ideas With gravels. Architecture and Design. Web: <https://www.architecturendesign.net/garden-design-ideas-with-pebbles/> erişim 11.06.2018
14. Tulukcu E. 2012. Bazı tıbbi bitki tohumlarının çimlenme özelliklerinin tespiti. Tarım bilimleri araştırma dergisi 5(1), 101-103.
15. Öztekin T, Öztekin S, Oğuz İ. 2008. Tokat-Kazova koşullarında saatlik torak sıcaklıklarının periyodik sinüs dalga eşitliği ile tahmini, Tarım Bilimleri Araştırma Dergisi 1(1), 55-60.
16. Tonkaz T, Doğan E, Aydemir S. 2007. GAP bölgesi toprak sıcaklıklarının alansal değişimleri ve hava sıcaklığı ile ilişkileri, HR.Ü.Z.F.Dergisi 11(1/2), 55-61.
17. Ekberli İ, Sarilar Y. 2015. Toprak sıcaklığı ve ısisal yayınının belirlenmesi. Anadolu Journal Agriculture Science 30, 74-85.
18. Zibilske LM, Makus DJ. 2009. Black oat cover crop management effects on soil temperature and biological properties on a mollisol in Texas, USA. Geoderma, 149: 379385.
19. Terrence HB, Hugh ALH. 2011. Fine scale variability in soil extracellular enzyme activity is insensitive to rain events and temperature in a mesic system. Pedobiologia 54, 141–146
20. Aksak et al., 1995. Toprak Sicaklığı. Çukurova Üniversitesi Ziraat Fakültesi Toprak Bölümü Mezuniyet Çalışması. Adana
21. Flerchinger GN, Pierson FB. 1997. Modelling plant canopy effects on variability of soil temperature and water: model calibration and validation. Journal of Arid Environments 35, 641-653
22. Altınbaş Ü, Çengel M, Uysal H, Okur B, Okur N, Kurucu Y, Delibacak S. 2004. Toprak Bilimi. Ege Üniversitesi Ziraat Fakültesi Yayınları No:557, 355.



Structural Investigation of UV Aged Tent Fabrics

Emrah Temel¹, Faruk Bozdoğan¹, Deniz Mizmizoğlu²

¹ Ege University, Engineering Faculty, Textile Engineering Department, İzmir, Turkey

² Ege University, Institute of Science, Textile Engineering Department, İzmir, Turkey

Corresponding Author: Emrah Temel, textile.temel@gmail.com

ABSTRACT

Emergency tent is a basic human need and a critical determinant for survival and coping in the majority of crises. There are many reasons people might need temporary shelters. Natural disasters like hurricanes, earthquakes, floods, fires, and tornados are some of them. Millions of people around the globe have had their lives disrupted by these disasters. The environmental health conditions faced by people are largely affected by the conditions where they are obliged to live in the days, weeks or months after a disaster. The quality of emergency tent has a great impact on human health and well-being. Therefore, mechanical properties of a tent fabric will be vital for sufferers. Since these tents are used under natural environment, tent fabrics have to face with natural exposures that force the mechanical strength of the fabric. One of the most important of these effects is UV exposure. It is known that fabrics lose their strength under UV light. In this study ammonium dihydrogen phosphate (ADP) coated 100% cotton tent fabrics were aged under UV exposure (35 W/m^2) for 0, 250, 500 and 750 hours. Due to cellulose UV degradation mechanism exhibits oxidation of hydroxyl side groups and rupture of glycosidic bonds between cellulose units, tent fabric lost 40% of its tensile strength and 70% of its tearing strength compared to unaged fabric after 500 hours of UV aging process. FTIR (Fourier Transform Infrared Spectroscopy) analysis and SEM analysis were also held to investigate the degradation mechanism.

ARTICLE HISTORY

Received: 09.11.2018

Accepted: 14.04.2019

KEYWORDS

Tent fabrics, mechanical properties, tensile strength, fiber deterioration, UV aging

1. INTRODUCTION

Millions of people around the globe have had their lives disrupted by disasters. The provision of emergency shelter is a last resort when no other solution can be found for homeless people. Therefore, emergency tents must exhibit high strength against environmental conditions and exposures. Physical properties of emergency tents are directly related to the living standards of the users [1, 2].

One of the most important problems faced by emergency tents is UV exposure. Tents are constantly exposed to UV exposure as they remain under the sun light during the day. Since UV radiation degrades the molecular chains of the fabric material, tent fabric loses its strength over time [3].

The phenomenon of 'weathering' of polymeric materials is usually caused by a complex series of chemical reactions initiated by the absorption of ultra-violet light which ultimately result in the deterioration of the physical properties of the polymer [4].

The deterioration of polymers in outdoor weathering is caused primarily by sunlight, especially ultraviolet radiation. Sunlight reaching the earth is filtered through the atmosphere, removing shorter wave-lengths up to 280-310 nm before it reaches the surface of the earth. Beyond 380-400 nm, the light becomes visible to the human eye. Thus, ultraviolet effects on polymers result primarily from wave-lengths of approximately 300-400 nm, which is ~5% of the total solar radiation reaching the earth. The sun has an

To cite this article: Temel E, Bozdoğan F, Mizmizoğlu D. 2019. Structural investigation of UV aged tent fabrics. *Tekstil ve Konfeksiyon* 29(3), 246-252.

approximate Boltzmann distribution of energy with a peak maximum at a wavelength of approximately 400-500 nm. However, the shorter wavelengths are not available at the earth's surface because they are absorbed by the ozone layer in the upper atmosphere. As a general rule, only light having a wavelength exceeding 300 nm reaches the earth's surface. This restricts the number of reactions which may occur [5].

Polymers such as plastics and rubbers consist of long molecular chains. These can vary in length, complexity and orientation, and these factors all contribute to the overall material behavior. Specific polymers possess specific chemical groups and bonds in their structure. These different chemical groups absorb differing amounts of energy. Unfortunately, most of these chemical groups have big absorbance within the UV spectrum. Furthermore, ultraviolet can cause breakdown of many polymer [6]. Figure 1, demonstrates some of the typical chemical groups and their absorption energies. Table 1, demonstrates ultraviolet wave lengths for typical commercial polymers.

Pure native cellulose absorbs UV radiation strongly between 200 and 300 nm, but only very weakly up to 400 nm. Two pathways are important in cellulose degradation: oxidation of the hydroxyl side groups (changes in the color, polarity, solubility and water absorption-desorption properties) and rupture of the glycosidic bonds between cellulose units [7].

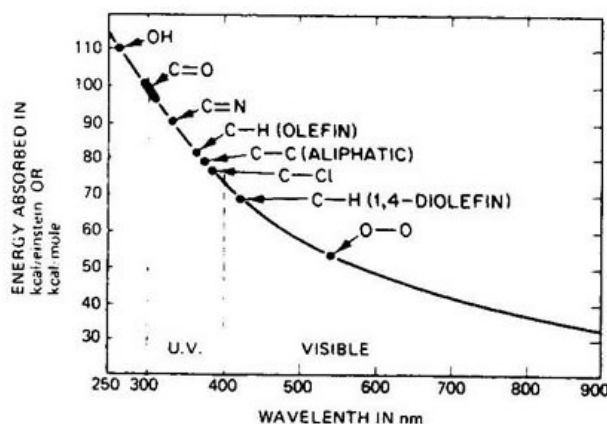


Figure 1. UV absorption energies and wavelengths of chemical groups [6].

Table 1. Ultraviolet wavelengths for typical polymers [5].

Polymer	Ultraviolet wavelength of maximum sensitivity (nm)
Polyester	325
Polystyrene	318
Polyethylene	300
Polypropylene	310
Polymethyl Methacrylate	290-315
Polyformaldehyde	300-320

Hence the addition of energy via UV photons can produce significant absorptions of energy by the material and if the energy is sufficient can lead to breaking of the molecular bonds, effectively cutting the molecular chains. This situation leads to a reduction in molecular weight and subsequent loss in elastic behavior, cracking and general reduction in the mechanical properties [6].

The chemical changes caused by short-term UV irradiation are confined to fibers at the fabric surface and UV is unable to penetrate beyond the surface to weaken the bulk fibers responsible for the mechanical strength. This has enabled the potential application of UV technology as a surface-specific treatment in several areas [8].

UV degradation impact of a fabric may be affected by many textile properties. These parameters include mass per unit area, fiber type, yarn construction, finishing process and coloration process etc. [9]. Nevertheless, the most important factor affecting the fabric strength is UV exposure duration.

The physical specifications required for emergency tent fabrics are provided in official standards. However, the values in these standards indicate performances of fabrics not aged in ambient conditions. It should be noted that these fabrics are used in harsh environmental conditions and must exhibit the same/sufficient physical performance throughout the duration of use.

Therefore, in this study tent fabrics were aged under UV exposure for different periods and investigated their mechanical properties. Further to that, the degradation mechanism due to UV exposure is explained by internal structure analysis.

2. MATERIAL AND METHOD

In this study the aim is to investigate the time dependent strength change of emergency tent fabric after UV exposure. For this purpose, ammonium dihydrogen phosphate (ADP) coated 100% cotton tent fabrics were aged in a UV aging cabin for 250, 500 and 750 hours. After aging process, aged fabrics and unaged tent fabric were conducted to tensile strength tests, tearing strength tests and air permeability tests. Tensile strength and tearing strength tests were performed on Zwick Universal Tensile Testing Machine by using TS EN ISO 13934-1 and TS EN ISO 13937-2 test standards respectively. Tearing strength test was also conducted to test samples on Elmendorf Ballistic Pendulum Tear Tester by using TS EN ISO 13937-1 test standard. Air permeability test were applied on TEXTTEST FX 3300 Air Permeability Tester under 200 Pa air pressure. Furthermore, aging and degradation mechanisms of tent fabrics were also investigated by inner structure analyses. For this purpose, FTIR (Fourier Transform Infrared Spectroscopy) analyses were performed on aged and unaged tent fabrics to determine the structural changes

between chemical bonds and groups. FTIR analyses were applied on Perkin Elmer FTIR Spectrometer. In order to observe fiber structural decomposition, SEM (Scanning Electron Microscope) analyses were applied by Thermo Scientific Apreo S SEM equipment. After UV exposure, color changes were occurred on fabrics. Fabric color alteration and yellowing degrees were also investigated by HunterLab UltraScan Pro Spectrophotometer according to ASTM E 313 standard.

The detailed description of the test material is given below in Table 2.

Aging process was applied to test materials on Prowhite UV Test Box under 35 watt/m² light intensity for 250, 500 and 750 hours.

Table 2. Description of test material

Property	Description
Material	100% cotton
Weaving pattern	1x1 plain weave
Warp density	20 ends/cm
Weft density	11 ends/cm
Mass per unit area	580 g/m ²
Coating material	Ammonium dihydrogen phosphate (ADP)

3. RESULTS AND DISCUSSION

0, 250, 500 and 750 hours aged 100% cotton tent fabrics were conducted to tensile strength, tear strength and air permeability tests. Test results are given below in Table 3 and Table 4.

When the effect of the UV exposure duration on tensile strength is examined, it can be denoted that increase in exposure time results in loss in tensile strength both in warp

and weft direction. It is thought that, the result mainly depends on deterioration of hydroxyl side groups and rupture of the glycosidic bonds between cellulose units as Wypych mentioned in his study. He also stated that deterioration of hydroxyl side groups cause change in material color [7]. In Figure 3, it can be clearly seen that, the sample that was exposed to the maximum UV light was the sample that was most yellowish and darkest. Nevertheless, according to color analysis results (Table 5), no significant color changes between 500 and 750 hours was observed. Furthermore, when the color measurement results are examined in Table 6, it is seen that the fabric treated for 500 hours has the same yellowing rate as the fabric treated with 750 hours. Again, according to the color measurements in Table 6; 750 hours of processed fabric became darker than 500 hours. It's thought that this situation emphasizes, the effect of UV exposure after 500 hours is significantly reduced. Although yellowing mechanism has stopped, the degradation mechanism has continued slightly. Similarly, when the strength loss values in Figure 2 are examined, no significant loss of strength is observed in the samples after 500 hours.

As all specimens were considered, no significant difference is observed between the elongation values of the samples, except warp direction for unaged sample. Since the unaged sample was not degraded and the test was performed in warp direction, unaged sample showed very high tensile strength values. For that reason, the elongation value is thought to be high. As work of rupture values were evaluated, it can be clearly seen that, work of rupture values highly depend on tensile strength and breaking elongation values. Therefore, it can be pointed out that the shorter the sample exposed to UV degradation, the higher work of rupture value has.

Table 3. Tensile strength test results of samples

Samples	Tensile strength (N)		Elongation (%)		Work of rupture (N.mm)	
	Warp direction	Weft direction	Warp direction	Weft direction	Warp direction	Weft direction
Unaged	2297.16	1263.70	22.19	9.63	21477.00	5008.00
250 hours treated	1551.31	934.40	17.94	8.62	12037.75	3172.00
500 hours treated	1330.84	777.54	17.01	7.99	10167.75	2510.75
750 hours treated	1150.75	682.62	15.95	7.65	9765.00	1916.75

Table 4. Tear strength and air permeability test results of samples

Samples	Tear strength (Trouser tear) (N)		Tear strength (Ballistic pendulum) (N)		Air permeability (l/m ² /s)
	Warp direction	Weft direction	Warp direction	Weft direction	
Unaged	34.18	42.62	38.58	57.63	12.49
250 hours treated	23.53	26.73	29.70	39.02	12.88
500 hours treated	10.93	14.92	25.27	32.13	13.28
750 hours treated	9.88	13.55	21.39	29.91	12.67

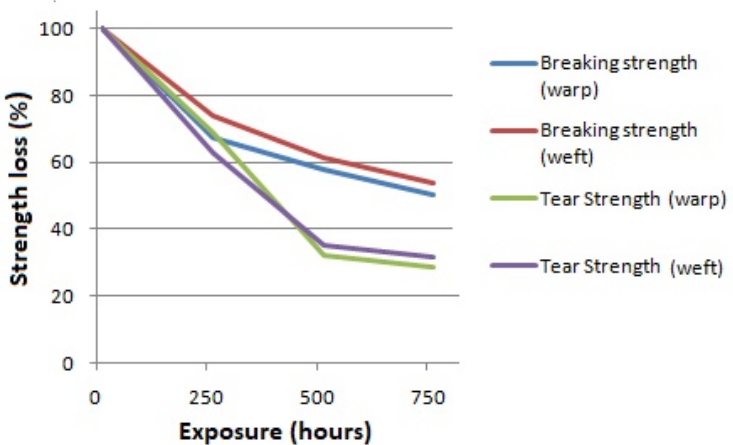


Figure 2. Time dependent strength loss (%) of samples

Table 5. Color changes between UV treated fabrics

	Color change (ΔE)	
	According to unaged sample	According to 250 hours treated sample
250 hours treated	37.63	0.00
500 hours treated	41.41	5.77
750 hours treated	39.97	5.57

Table 6. Results of color measurements

	L*	a*	b*	Yellowness Index
Unaged	86.25	1.89	9.18	19.88
250 hours treated	64.67	11.86	37.90	85.92
500 hours treated	59.10	13.57	38.01	96.05
750 hours treated	58.92	12.69	36.21	94.49

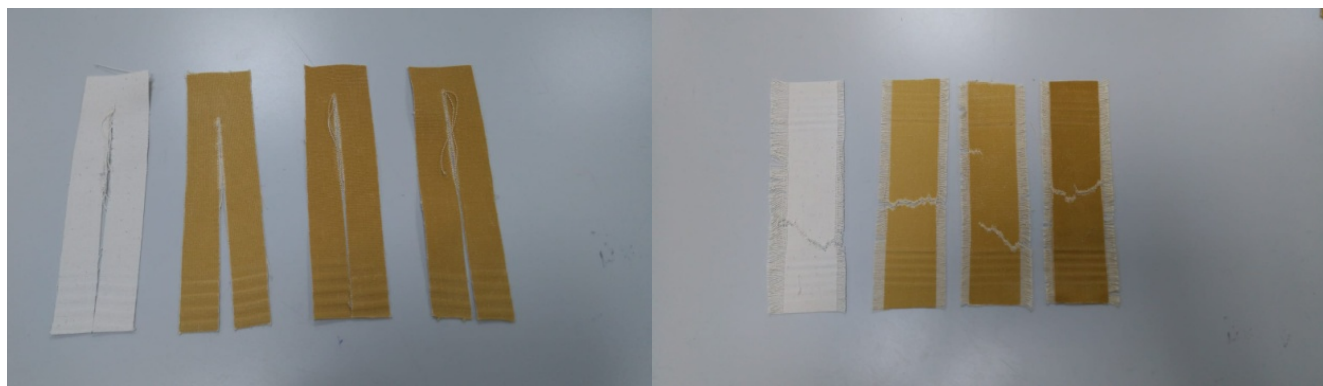


Figure 3. Samples that were conducted to tearing (a) and breaking (b) strength tests after UV exposure for 0, 250, 500 and 750 hours respectively.

When the ballistic pendulum and trousers tearing strength test results are examined, it can be stated that, the fabric the most exposed to UV degradation has the most loss of tearing strength, as expected. This situation is also associated with deterioration of hydroxyl side groups and rupture of the glycosidic bonds between cellulose units as mentioned above.

When air permeability test results are examined, it was determined that samples demonstrated nearly same air

permeability test values with 12-13 (l/m²/s). The ADP coating material on the fabric provides the fabric flame retardancy and waterproof properties. For that reason, fabric coating also limits and affects the air permeability properties. As the air permeability test results were evaluated, it was revealed that, UV exposure did not cause a remarkable degradation on fabric coating. Therefore, no significant change was observed on air permeability properties. FTIR analysis also support that the coating material is not damaged.

In order to investigate degradation mechanism, FTIR analyses were conducted to UV treated samples. And the FTIR spectra of these samples are given in Figure 4.

FTIR spectrum given in Figure 4 shows the characteristic peaks of both cellulose and ammonium dihydrogen phosphate. Some peaks of ammonium dihydrogen phosphate and cellulose create overlaps, while some peaks exhibit characteristic vibrations. Vibration peaks appear around 3200-3300 cm⁻¹ pointed out O-H stretching of both cellulose and ADP [10-12]. The peaks at region around 1430 cm⁻¹ indicate the N-H bonding stretching of ADP and CH₂ vibrations of cellulose [13, 14]. Another group of overlapping peaks could be seen around 1000-1100 cm⁻¹. These multiple peaks are stated as both P-O vibrations of ADP and C-O vibrations of cellulose [12, 15]. The vibration peaks appeared around 1640 cm⁻¹ and 2400 cm⁻¹ indicated existence of N-H and P=O bending vibrations of ADP respectively [16, 17].

It is stated above that, two pathways are important in cellulose degradation: oxidation of the hydroxyl side groups and rupture of the glycosidic bonds between cellulose units [7]. As seen in Table 6, deterioration of hydroxyl side groups caused color change from white to yellow in the

samples. This situation can also be observed in FTIR diagrams. The peaks responsible for the hydroxyl groups in the cellulose structure are displayed at around 3200 cm⁻¹. In Figure 4, it was determined that the decomposition of the hydroxyl structure appeared as a vibration increase in FTIR spectra.

Glycosidic bonds are linkages that hold together cellulose units. In the FTIR spectra the band at 1130-1160 cm⁻¹ assigned to glycosidic bond stretching vibrations [18]. When the UV exposed samples were examined, it was observed that the vibration peak was stated in the spectrum of 1155 cm⁻¹. However, when the exposure duration of the samples increased, this peak was gradually disappeared (Figure 4).

The effects of UV exposure on the appearance of the cotton tent fabrics was observed by SEM. And the images show distinctive stages of degradation (Figure 5). The micrograph of the unaged fiber reveals a uniform and smooth surface, but as the exposure time increases, a coarser and cracked texture begins to emerge, and 750 hours of UV exposure can produce dramatic erosion on the fiber surface.

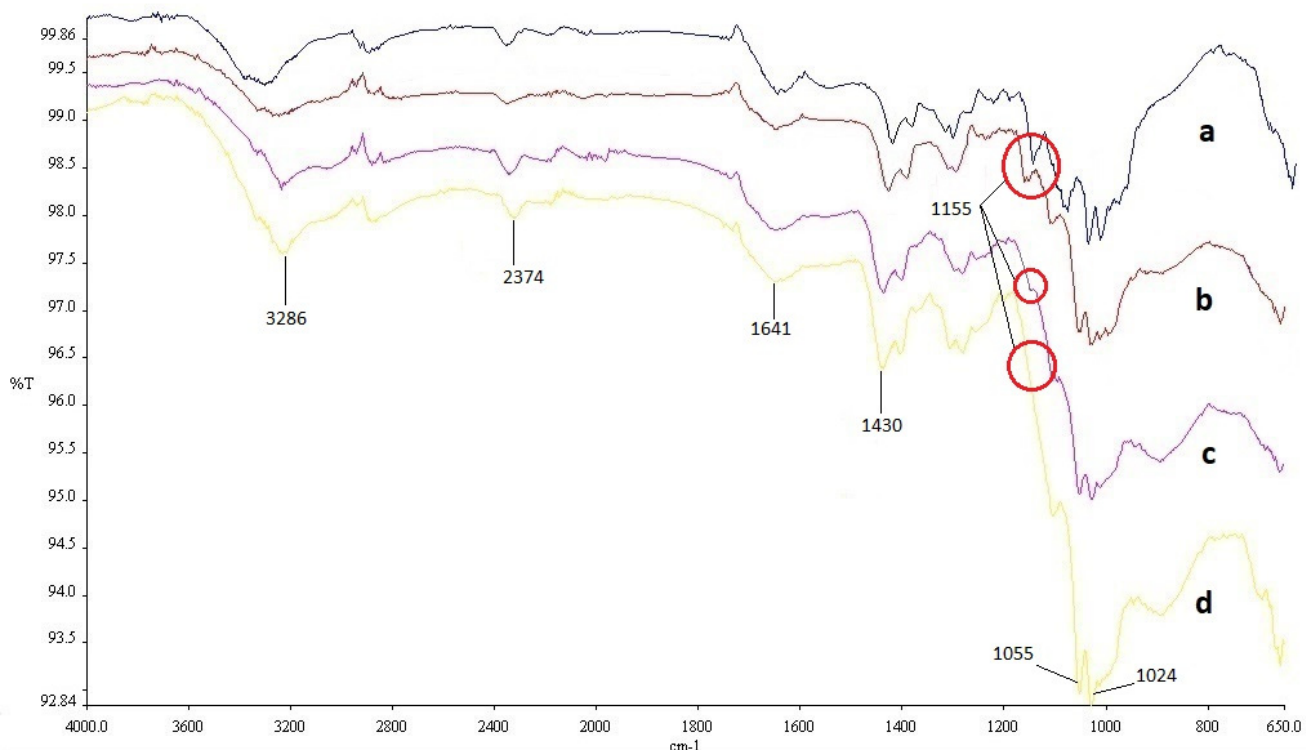


Figure 4. FTIR analyses of fabric samples: (a) unaged, (b) 250 hours treated, (c) 500 hours treated, (d) 750 hours treated

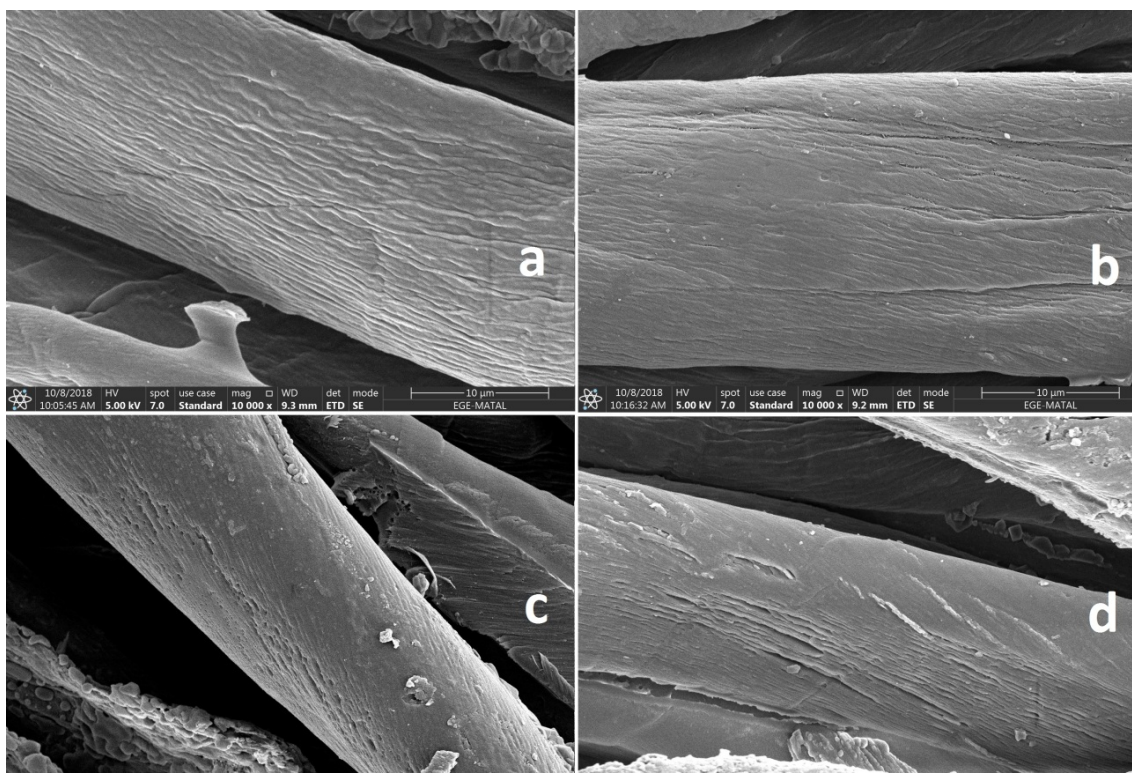


Figure 5. 10.000 X magnified SEM images of samples. (a) Unaged, (b) 250 hours treated, (c) 500 hours treated, (d) 750 hours treated.

4. CONCLUSION

Sunlight, especially ultraviolet radiation can cause massive degradation on polymers. Therefore, fabrics which are exposed to sunlight for a long time are under the risk of mechanical disruption. Since tents are equipments that are used under sunlight, tent fabrics are also among those at risk.

Cellulose absorbs UV radiation strongly between 200-300 nm, and this gap is involved by the ultraviolet region that reaches the world from atmosphere. In this study, ADP coated 100% cotton tent fabrics were aged under UV exposure in a UV cabin with 35 W/m^2 light intensity for 250, 500 and 750 hours. After aging process, mechanical strength changes were compared upon unaged tent fabric. In addition, internal structure changes and degradation mechanisms were investigated by FTIR and SEM analyses.

Due to cellulose UV degradation mechanism exhibits oxidation of hydroxyl side groups and rupture of glycosidic bonds between cellulose units, tent fabric lost 40% of its tensile strength and 70% of its tearing strength compared to

unaged fabric after 500 hours of UV aging process (Figure 2). This situation also corresponds to the loss of 1155 cm^{-1} peak in the FTIR spectra depending on the UV exposure time. Although there was no significant change in “strength loss” was observed after 500 hours. Tensile strength loss reached 50% and tear strength reached 75% at the end of 750 hours (Figure 2).

Degradation of hydroxyl side groups also cause color change from white to yellow as stated in Table 6. However, after 500 hours, the yellowing of the fabric has ended and the color has become darker (Table 6). It's thought that, this situation mainly depends on the end of yellowing mechanism, but the continuation of the degradation mechanism after 500 hours. The time-dependent changes in the FTIR spectra of the OH groups that cause color change can also be observed as an increment in 3286 cm^{-1} peak.

The fact that there is no change in the air permeability properties of the fabric after 750 hours of UV exposure indicates that, there is no remarkable damage existed on the coating structure of treated fabrics.

REFERENCES

1. Manfield P. 1999. *A comparative study of temporary shelters used in cold climates*. Martin Centre for Architectural and Urban Studies Department of Architecture, Cambridge University.
2. Crawford C, Manfield P, McRobie A. 2005. Assessing the thermal performance of an emergency shelter system. *Energy and Buildings* 37, 471 – 783.
3. De P, Sankhe M D, Chaudhar SS, Mathur MR. 2005. UV-resist, water-repellent breathable fabric as protective textile. *Journal of Industrial Textiles* 34(4), 209 – 222.
4. Guillet JE. 1972. Fundamental Processes In The UV Degradation and Stabilization Of Polymers. In Rado R, *Chemical transformation of polymers*. Elsevier, 135-144.

-
5. Deanin RD, Orroth SA, Eliasen RW, Greer TN. 1970. Mechanism of ultraviolet degradation and stabilization in plastics. *Polymer Engineering & Science* 10(4), 228-234.
 6. <http://www.drb-mattech.co.uk/uv%20degradation.html>
 7. Wypych G. 2015. *Handbook of UV degradation and stabilization*. ChemTec Publishing
 8. Millington KR. 2000. Comparison of the effects of gamma and ultraviolet radiation on wool keratin. *Coloration Technology* 116(9), 266-272.
 9. Kursun S, Ozcan G. 2010. An investigation of UV protection of swimwear fabrics. *Textile Research Journal* 80(17), 1811-1818.
 10. Takacs E, Wojnárovits L, Bors J, Földvár C, Hargittai P, Zöld O. 1999 Effect of γ -irradiation on cotton-cellulose. *Radiation Physics and Chemistry* 55(5-6), 663-666.
 11. Ciolacu D, Kovac J, Kokol V. 2010. The effect of the cellulose-binding domain from clostridium cellulovorans on the supramolecular structure of cellulose fibers. *Carbohydrate Research* 345(5), 621-630.
 12. Jegatheesan A, Murugan J, Neelagantaprasad B, Rajarajan G. 2012. FTIR, XRD, SEM, TGA investigations of ammonium dihydrogen phosphate (ADP) single crystal. *International Journal of Computer Applications* 53(4), 15-18.
 13. Colom X, Carrillo F, Nogués F, Garriga, P. 2003. Structural analysis of photodegraded wood by means of FTIR spectroscopy. *Polymer Degradation and Stability* 80(3), 543-549.
 14. Rajesh P, Ramasamy P. 2009. Growth of dl-malic acid-doped ammonium dihydrogen phosphate crystal and its characterization. *Journal of Crystal Growth* 311(13), 3491-3497.
 15. Wattanakornsiri A, Tongnunui S. 2014. Sustainable green composites of thermoplastic starch and cellulose fibers. *Songklanakarin Journal of Science & Technology*, 36(2), 149-161.
 16. Shingade BA, Sawadh PS, Rewatkar KG. 2016. Synthesis of different parameters and NLO properties of a new mixed L-Leucine doped in ammonium dihydrogen phosphate crystals. *International Journal of Engineering Research & Technology* 4(30).
 17. Renganayaki V, Syamala D, Sathyamoorthy R. 2012. Growth, Structural and spectral studies on pure and doped ammonium dihydrogen phosphate (ADP) single crystals. *Archives of Applied Science Research* 4(3), 1453-1461.
 18. Nikonenko NA, Buslov DK, Sushko NI, Zhbankov RG. 2000. Investigation of stretching vibrations of glycosidic linkages in disaccharides and polysaccharides with use of IR spectra deconvolution. *Biopolymers: Original Research on Biomolecules* 57(4), 257-262.



Increasing the Process Cycle Efficiency of Men's Trousers Assembly Line

Duygu Selen Kansul, Gülsen Karabay

Dokuz Eylül University, Textile Engineering Department, İzmir, Turkey

ABSTRACT

Value is known as the price, which the customer is ready to pay for and the ultimate customer defines the value. Eliminating the waste is important for reduction of costs and meeting the demands of customers in short delivery times. Process Cycle Efficiency (PCE) is defined as the measurement of the amount of value-added time in a process. In this study, the PCE of men's trousers assembly line was tried to be increased. To achieve this aim, the value stream map of the line was examined. Overall equipment efficiency (OEE) values of the operations were calculated, the operations with OEE values under 85% were selected, and improvement activities were defined. At the end of these activities, total process lead time and work in process (WIP) stocks decreased and PCE increased from 0.9% to 1.5%.

ARTICLE HISTORY

Received: 18.12.2018

Accepted: 28.08.2019

KEYWORDS

Value stream mapping, lean, process cycle efficiency, overall equipment efficiency, process lead time, work in process, assembly line

1. INTRODUCTION

The apparel industry has a volatile structure with a high variation in product mix, small order quantities and short delivery times. In order to be competitive and to fulfil the orders on time, the companies have to be flexible to produce a high variety of models [1]. To be competitive, many apparel companies have to improve their manufacturing processes, constantly revise themselves according to the needs and expectations of their customers. Manufacturing processes have to be analyzed accurately to minimize the costs. Waste consumes resources but does not add any value to the product [2]. Toyota production system accepted the waste types as overproduction, waiting, transport, inappropriate processing, unnecessary inventory, unnecessary motion, defects [3].

Lean thinking is doing more with less and it starts with value [4]. Value is known as the price which is the customer is

ready to pay for and the ultimate customer defines the value. A value stream can be described as any value-adding and non-value-adding activities, which are done to make a product. Value stream mapping (VSM) is one of the most important tools for lean strategy with its visualization the non-value adding activities in the material and information flow of product. Wastes should be visualized and VSM is a very useful tool as it underlines kaizen activities for waste reduction. The first step in VSM is to choose a product family as the target for improvement [5]. The second step is to identify the wastes by drawing current value stream map. Unlike most process mapping techniques that often only document the basic product flow, VSM also documents the flow of information within the system. Where the materials are stored (raw materials and WIP) and what triggers the movement of material from one process to the next are key pieces of information [1]. The final stage in VSM is to create the future state map. The future state map highlights the lean

To cite this article: Kansul DS, Karabay G. 2019. Increasing the process cycle efficiency of men's trousers assembly line. *Tekstil ve Konfeksiyon* 29(3), 253-262.

Corresponding Author: Gülsen Karabay, gulseren.karabay@deu.edu.tr.

tools, which are needed to eliminate the waste in the product value stream [6].

OEE is one of basic tools in lean manufacturing and it is an indicator, which defines the waste points in VSM. OEE is the measure of efficient usage of time for producing quality product. While the OEE is calculated, the time, which the machine is producing, is taking into account, not the amount of the output [7]. The waste hinders the capacity and performance. Machine breakdowns, setup and adjustments, reduced speed, minor stoppages, quality losses are the causes of low OEE. By removing waste in the manufacturing processes, the companies can manage to meet the demands with shorter lead time, high quality and they can get a competitive advantage over the other companies in recent volatile conditions by having flexibility to change schedules and giving priorities more quickly [8]. The studies in the literature, some of which are given below, show that lean principles can be applied to apparel companies.

Kumar and Thavaraj identified the target areas of improvement to eliminate the process wastages in current state. They fixed the problem of low flexibility by cellular layout, kaizen and 5s tools [6].

Kumari *et al.* applied lean tools in an apparel company in order to reduce the WIP and the number of workers by removing checking operations [9].

Akcagun *et al.* outlined a case study in an outerwear company. They decreased the total process of outwear from 27-33 weeks to 9-14 weeks by using value stream mapping [10].

Yildiz and Guner analyzed the manufacturing processes from incoming quality control to shipping to eliminate the wastes in a jeans producing company [11].

Silva revealed that VSM can be applied to mass production in apparel industries in order to derive positive results such as reducing wastes in inventory and defects. Current and future state VSM was drawn for analyzing the raw material, cutting, sewing and finish goods departments' processes [12].

Kumar used VSM as a key lean tool to analyze machine cycle time, inventory, setup time and information flow on men's trouser production layout. Sewing room was revised by VSM analysis. [13].

Most of these studies try to decrease the total process lead time of a product from supplying process to shipment by using lean production principles and methods. In these studies, value stream mapping, kaizen, 5S and SMED applications were explained in detail with case studies. However, OEE and PCE were not the main topic of these studies. In this research, it was tried to determine and decrease the non-value-added time and eventually, to improve the rate of process cycle efficiency in the men's trousers production line by the help of lean principles. As

defined before, OEE is an indicator, which defines the waste points in VSM. This research was conducted with the aim of emphasizing the importance of OEE and showing its application in an apparel company in detail as an example for other apparel companies.

Value Stream Mapping, Process Cycle Efficiency and Overall Equipment Efficiency

When creating a flowchart of a garment, the cycle times of all the operations in a line are summed and the line with the longest duration is determined as the mainline. Lines which have shorter durations are segment lines and they are located outside of the mainline and they join the mainline at the related matching points. The difference between the duration of the segment and mainline is also important in the management of work in processes (WIP). The sewing process starts in the segments and the mainline at the same time and the segments create overstock at the points where they join the mainline. In order to determine the optimum WIP in a segment, the duration of the segment and the duration in the mainline from the first operation to the last operation, where the segment joined the mainline, should be compared. The difference between these two durations causes WIP inventory. WIP stock is very important for making improvements and reducing waste time.

Cycle time (CT) is the time, which takes to complete the production of one unit from start to finish. Cycle time is consisting of value-added and non-value-added times. Value-added time is the process time part of cycle time, which elapses during making the activities, which are defined as value by the customer. Cycle time equals the process time of the task in the garment assembly line. The cycle time of the operation is the ideal time for finishing that operation, however, in real life, the production conditions, which are measured by OEE, can deviate this balance.

Overall Equipment Effectiveness (OEE) is a simple metric, which shows how much right-first-time product is produced at a single equipment in the given time. In other words, it measures how effectively the time is used to produce a quality product at that equipment. OEE can be calculated with equation (1) and the following sub-equations (2), (3), (4).

$$\text{OEE} = \text{Performance} \times \text{Availability} \times \text{Quality} \quad (1)$$

$$\text{Performance} = \frac{\text{Actual output} \times \text{Cycle time}}{\text{Daily working time} \times \text{Workload}} \times 100 \quad (2)$$

$$\text{Availability} = \frac{(\text{Daily working hours} - \text{Breakdown and adjustment times})}{\text{Daily working time} \times \text{Workload}} \times 100 \quad (3)$$

$$\text{Quality} = \left(1 - \frac{\text{Daily repairing time}}{\text{Daily working time} \times \text{Workload}} \right) \times 100 \quad (4)$$

OEE value of 100% is the sign of perfect production, which means manufacturing right-first-quality product without time loss. Adversely, OEE value of under 100% is accepted

as loss factor and OEE percentages should be used to define the actual cycle time (ACT) as in equation (5).

$$ACT = \frac{CT}{OEE} \quad (5)$$

The actual cycle time will cause longer process lead time (PLT). Process lead time is the total time for a unit product to go its way through the operation from starting with the raw material's arrival to receiving money and can be calculated with equation (6). Process lead time is consisting of waiting time before the process, setup time, process time, waiting time after the process and transfer time between processes. The lead time of an operation should not be much higher than the cycle time of that operation, otherwise, there will be an overstock of WIP and this will decrease the process cycle efficiency of the line. Total process lead time is the sum of process lead times of all operations in the line.

$$PLT = ACT \times WIP \quad (6)$$

Process cycle efficiency (PCE) means that the duration of one job from the beginning of production to the arrival of the warehouse is completed in the shortest time.

PCE is improved by reducing non-value adding activities, and minimizing the necessary but non-value adding activities. In reality, the PCE is typically in the 5% to 10% range. While the PCE is the efficiency of the whole assembly line, OEE is valid only for one operation. PCE can be calculated with equation (7).

$$PCE = \frac{\text{Total cycle time (total value-added time)}}{\text{Total Process lead time}} \quad (7)$$

VSM shows the current situation in the line and it is easy to detect OEE values less than 85% and high WIP inventories. These are the key places, which have to be improved.

2. MATERIAL AND METHOD

In this study, the OEE values of the operations were used in order to make improvements and increase the process cycle efficiency in the apparel company. Daily work time is 540 minutes and daily customer demand is 450 pieces. Men's trousers line was chosen as the product family. Men's trousers are made of belt and pocket preparation, front and back pants mounting sections. The cycle time of each operation is measured with the help of a stopwatch. WIP stock of each operation was counted three times a day for both current and future states. The average value of these three WIP stocks were used as WIP quantities in each operation. OEE values of each operation were calculated by using collected performance, machine availability and quality data. After WIP stock and cycle time of each operation are determined, actual cycle times of operations were calculated by using OEE values. Process lead times of operations were found by using the actual cycle times and WIP levels of operations. VSM of the men's trousers assembly line was generated, by sequencing the unit cell of each operation. Figure 1 shows a unit cell of this VSM. After defining the current cycle time (process time), WIP, OEE, process lead time data, current process cycle efficiency of men's trousers production line was calculated.

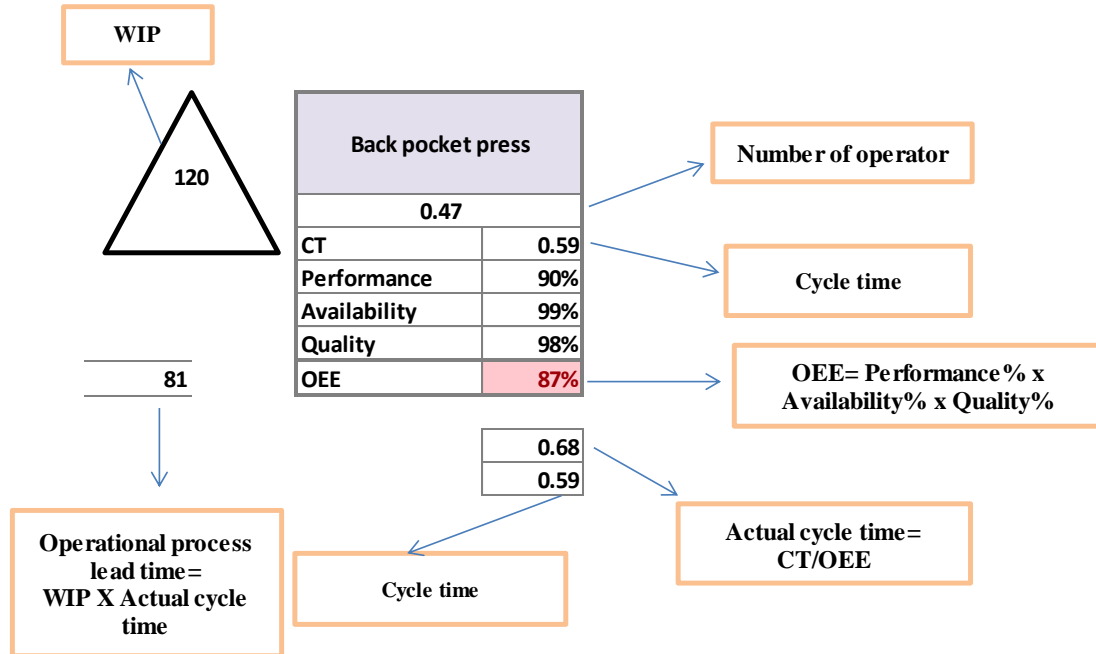


Figure 1. A unit cell of a value stream

Calculations of above operation were given in the following lines as an example. The daily target was 450 pieces and the daily working time is 540 minutes. Cycle time (CT) is 0,59 minutes. The operator produced 404 piece/day. The counted average WIP stock for this operation is 120 pieces. Machine breakdown is 278 minutes and repairing time is 5 minutes.

The related calculations were made for all operations in the line. All of these values were written on the VSM in Figure 2.

$$\text{Workload} = \left(\frac{\text{Daily target} \times \text{Cycle time}}{\text{Daily working time}} \right) = \frac{450 \times 0,59}{540} = 0,49$$

$$\text{Performance} = \frac{\text{Actual output} \times \text{Cycle time}}{\text{Daily working time} \times \text{Workload}} \times 100 = \frac{404 \times 0,59}{540 \times 0,49} \times 100 = 90\%$$

$$\text{Availability} = \frac{(\text{Daily working hours} - \text{Breakdown and adjustment times})}{\text{Daily working time} \times \text{Workload}} \times 100 = \frac{540 - 278}{540 \times 0,49} \times 100 = 99\%$$

$$\text{Quality} = \left(1 - \frac{\text{Daily repairing time}}{\text{Daily working time} \times \text{Workload}} \right) * 100 = \left(1 - \frac{5}{540 \times 0,49} \right) \times 100 = 98\%$$

$$\text{OEE} = \text{Performance} \times \text{Availability} \times \text{Quality} = 90\% \times 99\% \times 98\% = 87\%$$

OEE values were examined in VSM and the operations, which have OEE values under 85% were determined for improvement. After doing the planned activities, before and after values of PCE were compared.

3. RESULTS AND DISCUSSION

The value stream of material and information flow of the current situation in the men's trousers line is as in Figure 2.

Segment 1(Belt preparation line)

Belt fusing		Belt lining		Loop attaching		Waistband press	
467	0,32	250	0,45	100	0,3	160	0,96
CT	0,26	CT	0,47	CT	0,35	CT	0,9
Performance	100%	Performance	99%	Performance	102%	Performance	100%
Availability	100%	Availability	98%	Availability	95%	Availability	99%
Quality	99%	Quality	100%	Quality	89%	Quality	95%
123	OEE	121	OEE	41	OEE	153	OEE
	99%		97%		86%		94%
	0,26		0,48		0,41		0,96
	0,26		0,47		0,35		0,9

Segment 2 (Pocket preparation line)

Pocket facing seam		Fusing fly		Pressing fly lining		Zipper attaching to fly		Front pocket facing overlock	
660	1,04	436	0,16	120	0,21	130	0,21	230	0,25
CT	0,98	CT	0,17	CT	0,15	CT	0,17	CT	0,32
Performance	98%	Performance	99%	Performance	77%	Performance	100%	Performance	90%
Availability	80%	Availability	100%	Availability	100%	Availability	98%	Availability	80%
Quality	91%	Quality	100%	Quality	100%	Quality	97%	Quality	80%
907	OEE	75	OEE	23	OEE	23	OEE	128	OEE
	71%		99%		77%		95%		58%
	1,37		0,17		0,19		0,18		0,56
	0,98		0,17		0,15		0,17		0,32

Mainline (Front piece)

500	Color separation and opening	230	Color separation and dispatching	475	Front cuff overlock	120	Frontcrotch overlock	79	Sewing right fly	105	Sewing left fly	150	Facing seam
	0,95		0,1		0,96		0,65		0,38		0,32		0,67
CT	0,64	CT	0,04	CT	0,92	CT	0,75	CT	0,27	CT	0,45	CT	0,67
Performance	100%	Performance	100%	Performance	102%	Performance	99%	Performance	99%	Performance	86%	Performance	88%
Availability	100%	Availability	100%	Availability	95%	Availability	97%	Availability	98%	Availability	98%	Availability	92%
Quality	100%	Quality	100%	Quality	95%	Quality	96%	Quality	99%	Quality	99%	Quality	93%
320 OEE	100%	9 OEE	100%	475 OEE	92%	98 OEE	92%	22 OEE	96%	57 OEE	83%	133 OEE	75%
	0,64 0,64		0,04 0,04		1,00 0,92		0,81 0,75		0,28 0,27		0,54 0,45		0,89 0,67
150	Facing seam	40	Front pocket press	67	Side pocket tacking	66	Front pocket bagging	90	Sewing sides	78	Top stitch inseam	130	Press side in seams
	0,67		0,3		1,96		0,64		1,67		0,76		0,82
CT	0,67	CT	0,21	CT	1,78	CT	0,52	CT	1,4	CT	0,6	CT	0,7
Performance	88%	Performance	82%	Performance	100%	Performance	94%	Performance	99%	Performance	96%	Performance	107%
Availability	92%	Availability	100%	Availability	100%	Availability	100%	Availability	99%	Availability	94%	Availability	98%
Quality	93%	Quality	99%	Quality	100%	Quality	99%	Quality	98%	Quality	93%	Quality	93%
133 OEE	75%	10 OEE	81%	119 OEE	100%	37 OEE	93%	131 OEE	96%	56 OEE	84%	93 OEE	98%
	0,89 0,67		0,26 0,21		1,78 1,78		0,56 0,52		1,46 1,4		0,71 0,6		0,72 0,7
78	Attaching waistband	40	Right fly lining bagging and label attaching	27	Left belt end finishing	35	Right and left belt end ironing	21	Left fly foot stitch	25	Sewing right fly	14	Hook tacking
	1,81		0,83		0,32		0,65		0,34		0,32		0,5
CT	1,72	CT	0,75	CT	0,25	CT	0,59	CT	0,45	CT	0,38	CT	0,35
Performance	105%	Performance	90%	Performance	100%	Performance	104%	Performance	89%	Performance	86%	Performance	86%
Availability	98%	Availability	90%	Availability	99%	Availability	95%	Availability	95%	Availability	100%	Availability	86%
Quality	90%	Quality	91%	Quality	98%	Quality	100%	Quality	92%	Quality	95%	Quality	98%
145 OEE	93%	41 OEE	74%	7 OEE	97%	21 OEE	99%	12 OEE	78%	12 OEE	82%	7 OEE	72%
	1,86 1,72		1,02 0,75		0,26 0,25		0,60 0,59		0,58 0,45		0,47 0,38		0,48 0,35
22	Stop	35	Point check	100	Back rise closure	20	Back rise sewing and pressing	34	Waistband blindstitch	55	Crotch Bartacking	12	Crotch point bartacking
	0,4		0,51		1,66		0,51		0,71		0,35		0,65
CT	0,3	CT	0,65	CT	1,71	CT	0,56	CT	0,62	CT	0,2	CT	0,7
Performance	100%	Performance	42%	Performance	108%	Performance	104%	Performance	98%	Performance	42%	Performance	74%
Availability	95%	Availability	100%	Availability	98%	Availability	98%	Availability	91%	Availability	92%	Availability	93%
Quality	95%	Quality	98%	Quality	89%	Quality	95%	Quality	90%	Quality	92%	Quality	98%
7 OEE	90%	55 OEE	41%	182 OEE	94%	12 OEE	97%	26 OEE	80%	29 OEE	38%	12 OEE	67%
	0,33 0,3		1,58 0,65		1,82 1,71		0,58 0,56		0,77 0,62		0,53 0,2		1,04 0,7
35	Pocket and loop bartacking	45	Bartacking	50	Check before pressing	65	Trimming blindstitch	19	Cuff press	3	Sewing trimming band	15	Leg Press
	1,87		0,72		1,66		0,33		0,45		0,45		0,97
CT	1,8	CT	0,53	CT	1,7	CT	0,29	CT	0,47	CT	0,46	CT	1,05
Performance	107%	Performance	102%	Performance	100%	Performance	56%	Performance	38%	Performance	52%	Performance	100%
Availability	95%	Availability	98%	Availability	100%	Availability	95%	Availability	95%	Availability	97%	Availability	84%
Quality	90%	Quality	98%	Quality	98%	Quality	94%	Quality	95%	Quality	96%	Quality	96%
69 OEE	91%	24 OEE	98%	87 OEE	98%	38 OEE	50%	26 OEE	34%	3 OEE	48%	20 OEE	81%
	1,97 1,8		0,54 0,53		1,73 1,7		0,58 0,29		1,37 0,47		0,95 0,46		1,30 1,05
5	Pressing	10	Ceasing press	17	Final inspection								
	3,21		0,95		3,02								
CT	3,4	CT	0,8	CT	2,98								
Performance	95%	Performance	90%	Performance	100%								
Availability	100%	Availability	85%	Availability	100%								
Quality	100%	Quality	85%	Quality	98%								
18 OEE	95%	12 OEE	65%	52 OEE	98%								
	3,58 3,4		1,23 0,8		3,04 2,98								

Segment 3 (Back Piece)

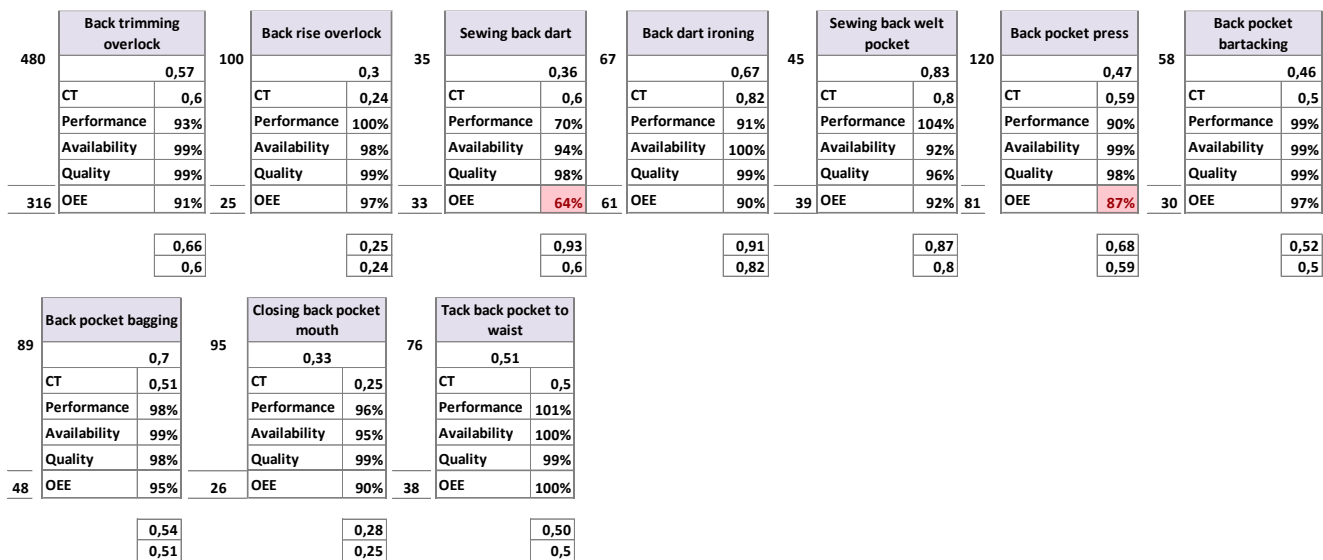


Figure 2. Value stream of men's trousers assembly line

Total cycle time is 40.84 min, total WIP stock in the line is 6630 and total process lead time is 4762 minutes for current state as seen in Table 2. The process cycle efficiency of the current situation is 0.9%. Nakajima indicated that under ideal conditions, the companies should have availability>90%, performance>95%, quality>99% values which result in OEE>84% and this OEE value is a good benchmark for a typical manufacturing capability [14]. When the current situation map is examined, the sources of inefficiency for each operation can be seen by checking the OEE values, which are under 85%. The reasons of losses at performance, availability and the quality values should be examined in order to increase low OEE values. The improvement points and the activities to be done were determined as in Table 1.

After these improvements, OEE values of 21 operations changed as given in the future state part of Table 2. As a result of the improvement studies, no changes have been observed in the information flow, material flow and raw material supply processes. Only control checking operation has been removed. Therefore, future state map was not shown again. After the elimination of this operation, the future cycle time is 40.19 min. Improvements in availability, performance and quality ratios increased most of the OEE values over 85% and accordingly, WIP levels dropped as seen in Table 2.

In the future state, the WIP stock level has been reduced from 6630 to 4460. The time losses because of WIP stocks have been eliminated and the total process lead time decreased from 4762 to 2702 minutes. This has led to the implementation of lean flow in production. Thus, the PCE value of the line increased from 0.9% to 1.5% and the production pace raised.

4. CONCLUSION

The apparel companies try to cater for the customer demands, which have high variety of models with low quantities in recent volatile market. This situation forces the companies work flexible with low costs. Therefore, the companies have to revise themselves according to the needs and expectations of their customers continuously. Lean manufacturing provides being highly responsive to customer demand while producing quality products economically and efficiently by reducing various waste in workforce, inventory, time to market. Shorter process lead time provides increasing customer satisfaction and gives flexibility to change schedules. OEE infers how much the equipment is doing compared to it is expected to do. Losses are activities that absorb resources without creating value and OEE reveals the losses that hinders equipment from performing its maximum effectiveness.

The present study aimed to find the hidden waste present in the men's trousers assembly line with the help of VSM and OEE values of operations and eventually to increase the PCE value in this line. After the calculation of OEE values of operations, the OEE values under 85% were determined. In these operations, main reason of the losses was rhythm problem, which stem from the minor stoppages and these stoppages affect the performance of the worker. Some precautions were taken to minimize the stoppages. Machine breakdowns and the setup times were the reasons of low machine availability in some operations. Machine changes and the maintenance program were planned for these wastes. In order to accelerate the speed and to overcome some quality problems, some machine changes were made. As a result of these activities, the WIP stock level in the assembly line was reduced from 6630 to 4460 pieces and the total

process lead time decreased from 4762 to 2702 minutes. Finally, the process cycle efficiency of the line increased from 0.9% to 1.5%.

OEE is one of the most important performance measurements in manufacturing companies. The companies

can increase capacity, decrease costs, improve quality in production lines by optimizing OEE. It is expected that this research will be a good example of OEE application for other apparel companies.

Table 1. Problems and improvements in current situations

No	OPERATION	PROBLEM	ARRANGEMENTS
Segment 2 (Pocket preparation)			
1	Pocket facing seam	Sewing adjustment	Machine to be exchanged
2	Pressing fly lining	Rhythm problem	Apparatus to be made for fly pressing
3	Front pocket facing overlock	Sewing adjustment problem	Machine to be exchanged
Segment 3 (Back Piece)			
5	Sewing back dart	Long SMED time in one and double dart models	The machine will be modified in order to put apparatus on the machine for both models at the same time.
MAINLINE (Front Piece)			
6	Sewing left fly	Fly- lining notch alignment problem	A nest will be made on the machine in order to align the notch.
7	Facing seam	Rhythm problem	Pieces to be sewn will be on the operator's lap and the facing pieces will be stacked on the machine. The operator will take a piece from his lap and place it on the machine with his two hands. After placing the facing on the piece and sewing it, he will leave the finished piece to the table on the left.
8	Front pocket press	Rhythm problem	The pieces will be stacked in the direction of the press and there will be no need for the worker to turn the piece for placing on the press.
9	Topstitch inseam	Rhythm problem	Machine speed and type will be changed.
10	Right fly lining bagging and label attaching	Fly cutting problem	Blade machine will be used to eliminate cutting time.
11	Left fly foot stitch	Rhythm problem	A line will be drawn 1 cm away from the presser foot in order to make the pursuance of the sewing line easy.
12	Right fly edge stitch	Rhythm problem	An auxiliary piece will be put near to presser foot to lean the fabric for making the tracking of the sewing line easy.
13	Hook tacking	Frequent machine breakdown	Machine engine will be changed
14	Inspection	Hand-to-hand flow deceleration between operations	The steps of control operations that affect the finished product quality will be eliminated by integrating it into other operations.
15	Waistband blind stitch	Failure to set the depth of needle penetration of blind stitch machine	Needle and yarn number will be changed.
16	Bartacking crotch	Loss of time during transport of crotch components	Stock space will be made on the machine for the pieces.
17	Crotch point bartacking	Rhythm problem	In the current situation, the work piece standing at the table on the left was taken, the bartacking process was done, and the work piece was moved to the table on the right side. In the new case, the piece is shifted to the table, which is placed in front of the sewing machine. Thus, the transport was reduced.
18	Trimming blind stitch	Rhythm problem	The worker stops more than expected in order to arrange the piece because of the round and narrow shape of the hem. A guide piece will be attached around the cylinder arm of the blind stitching machine. The worker will stop less with the guidance of this piece.
19	Sewing tape to hem	Rhythm problem	To make the worker less stop for checking the distance from edge of hem, laser light will be used to keep the distance
20	Trousers cuffs pressing	Rhythm problem	For decreasing the bundle transporting time, another bundle holding apparatus will be put oppose the current one.
21	Leg Press	Failure to set machine according to fabric type.	All machine maintenance will be done and upper buck material will be changed with 10 mm thick silicone foam. This material will prevent shine and pressure problem and reduce the time for setting machine.
22	Creasing press	Failure of size fixing during ceasing press and chronic machine failure	The machine will be maintained every week and the laser will be installed at the starting and end points to prevent the measurement problem for ceasing.

Table 2. Comparison of current and future state

	CURRENT STATE								FUTURE STATE						
	Cycle time	Actual cycle time	Performance	Availability	Quality	OEE	WIP	PLT	Performance	Availability	Quality	OEE	Actual cycle time	WIP	PLT
Segment 1(Belt preparation)															
Belt fusing	0,26	0,26	100%	100%	99%	99%	467	121	100%	100%	99%	99%	0,26	230	59
Belt lining	0,47	0,48	99%	98%	100%	97%	250	121	99%	98%	100%	97%	0,48	45	22
Loop attaching	0,35	0,41	102%	95%	89%	86%	100	41	102%	95%	89%	86%	0,41	90	37
Waistband press	0,9	0,96	100%	99%	95%	94%	160	153	100%	99%	95%	94%	0,96	70	67
Segment 2 (Pocket preparation)	Cycle time	Actual cycle time	Performance	Availability	Quality	OEE	WIP	PLT	Performance	Availability	Quality	OEE	Actual cycle time	WIP	PLT
Pocket facing seam	0,98	1,37	98%	80%	91%	71%	660	907	100%	95%	96%	91%	1,07	450	484
Fusing fly	0,17	0,17	99%	100%	100%	99%	436	75	99%	100%	100%	99%	0,17	375	64
Pressing fly lining	0,15	0,19	77%	100%	100%	77%	120	23	92%	100%	100%	92%	0,16	70	11
Zipper attaching to fly	0,17	0,18	100%	98%	97%	95%	130	23	100%	98%	97%	95%	0,18	95	17
Front pocket facing overlock	0,32	0,56	90%	80%	80%	58%	230	128	95%	99%	98%	92%	0,35	375	130
Mainline (Front piece)	Cycle time	Actual cycle time	Performance	Availability	Quality	OEE	WIP	PLT	Performance	Availability	Quality	OEE	Actual cycle time	WIP	PLT
Color separation and opening	0,64	0,64	100%	100%	100%	100%	500	320	100%	100%	100%	100%	0,64	475	304
Color separation and dispatching	0,04	0,04	100%	100%	100%	100%	230	9	100%	100%	100%	100%	0,04	200	8
Front cuff overlock	0,92	1,00	102%	95%	95%	92%	475	474	102%	95%	95%	92%	1,00	90	90
Frontcrotch overlock	0,75	0,81	99%	97%	96%	92%	120	98	95%	100%	96%	91%	0,82	0	0
Sewing right fly	0,27	0,28	99%	98%	99%	96%	79	22	100%	98%	99%	97%	0,28	45	13
Sewing left fly	0,45	0,54	86%	98%	99%	83%	105	57	95%	98%	99%	92%	0,49	45	22
Facing seam	0,67	0,89	88%	92%	93%	75%	150	133	98%	92%	93%	84%	0,80	45	36
Front pocket press	0,21	0,26	82%	100%	99%	81%	40	10	95%	100%	99%	94%	0,22	40	9
Side pocket tacking	1,78	1,78	100%	100%	100%	100%	67	119	100%	100%	100%	100%	1,78	45	80
Front pocket bagging	0,52	0,56	94%	100%	99%	93%	66	37	100%	100%	99%	99%	0,53	45	24
Sewing sides	1,4	1,46	99%	99%	98%	96%	90	131	100%	99%	98%	97%	1,44	50	72
Top stitch inseam	0,6	0,71	96%	94%	93%	84%	78	56	97%	100%	95%	92%	0,65	20	13
Press side in seams	0,7	0,72	107%	98%	93%	98%	130	93	105%	98%	93%	96%	0,73	45	33
Attaching waistband	1,72	1,86	105%	98%	90%	93%	78	145	105%	98%	90%	93%	1,86	45	84
Right fly lining bagging and label attaching	0,75	1,02	90%	90%	91%	74%	40	41	93%	98%	99%	90%	0,83	0	0
Left belt end finishing	0,25	0,26	100%	99%	98%	97%	27	7	100%	99%	98%	97%	0,26	35	9
Right and left belt end ironing	0,59	0,60	104%	95%	100%	99%	35	21	104%	95%	100%	99%	0,60	35	21
Left fly foot stitch	0,45	0,58	89%	95%	92%	78%	21	12	99%	96%	95%	90%	0,50	21	10
Sewing right fly	0,38	0,47	86%	100%	95%	82%	25	12	100%	100%	95%	95%	0,40	25	10
Hook tacking	0,35	0,48	86%	86%	98%	72%	14	7	93%	100%	98%	91%	0,38	14	5
Stop	0,3	0,33	100%	95%	95%	90%	22	7	100%	95%	95%	90%	0,33	22	7
Point check	0,65	1,58	42%	100%	98%	41%	35	55					ELIMINATED		
Back rise closure	1,71	1,82	108%	98%	89%	94%	100	182	108%	98%	89%	94%	1,82	45	82
Back rise sewing and pressing	0,56	0,58	104%	98%	95%	96%	20	12	104%	98%	95%	97%	0,58	20	12
Waistband blindstitch	0,62	0,77	98%	91%	90%	80%	34	26	100%	95%	94%	89%	0,69	34	24
Crotch Bartacking	0,2	0,53	42%	98%	92%	38%	55	29	98%	98%	94%	90%	0,22	20	4
Crotch point bartacking	0,7	1,04	74%	93%	98%	67%	12	12	98%	95%	98%	91%	0,77	12	9
Pocket and loop bartacking	1,8	1,97	107%	95%	90%	91%	35	69	107%	95%	90%	91%	1,97	35	69
Bartacking	0,53	0,54	102%	98%	98%	98%	45	24	102%	98%	98%	98%	0,54	45	24
Check before pressing	1,7	1,73	100%	100%	98%	98%	50	87	100%	100%	98%	98%	1,73	50	87
Trimming blindstitch	0,29	0,58	56%	95%	94%	50%	65	38	86%	100%	94%	81%	0,36	35	13
Cuff press	0,47	1,37	38%	95%	95%	34%	19	26	83%	95%	95%	75%	0,63	0	0
Sewing trimming band	0,46	0,95	52%	97%	96%	48%	3	3	90%	97%	96%	84%	0,55	5	3
Leg Press	1,05	1,30	100%	84%	96%	81%	15	20	100%	94%	96%	90%	1,16	15	17
Pressing	3,4	3,58	95%	100%	100%	95%	5	18	97%	100%	100%	97%	3,51	5	18
Ceasing press	0,8	1,23	90%	85%	85%	65%	10	12	100%	95%	85%	81%	0,99	10	10
Final inspection	2,98	3,03	100%	100%	98%	98%	17	52	100%	100%	98%	98%	3,04	17	52
Segment 3 (Back Piece)	Cycle time	Actual cycle time	Performance	Availability	Quality	OEE	WIP	PLT	Performance	Availability	Quality	OEE	Actual cycle time	WIP	PLT
Back trimming overlock	0,6	0,66	93%	99%	99%	91%	480	316	100%	95%	95%	90%	0,66	475	316
Back rise overlock	0,24	0,25	100%	98%	99%	97%	100	25	100%	98%	99%	97%	0,25	200	49
Sewing back dart	0,6	0,93	70%	94%	98%	64%	35	33	97%	96%	98%	91%	0,66	90	59
Back dart ironing	0,82	0,91	91%	100%	99%	90%	67	61	91%	100%	99%	90%	0,91	0	0
Sewing back welt pocket	0,8	0,87	104%	92%	96%	92%	45	39	104%	92%	96%	92%	0,87	45	39
Back pocket press	0,59	0,68	90%	99%	98%	87%	120	81	98%	99%	98%	95%	0,62	25	16
Back pocket bartacking	0,5	0,52	99%	99%	99%	97%	58	30	99%	99%	99%	97%	0,52	45	23
Back pocket bagging	0,51	0,54	98%	99%	98%	95%	89	48	100%	99%	98%	97%	0,53	45	24
Closing back pocket mouth	0,25	0,28	96%	95%	99%	90%	95	26	100%	92%	99%	91%	0,27	45	12
Tack back pocket to waist	0,5	0,50	101%	100%	99%	100%	76	38	101%	100%	99%	100%	0,50	0	0
Total	40,84						6630	4762					4460	2702	

REFERENCES

1. Singh B, Sharma SK. 2009. Value stream mapping as a versatile tool for lean implementation: An Indian case study of a manufacturing firm. *Measuring Business Excellence* 13(3), 58-68, <https://doi.org/10.1108/13683040910984338>.
2. Russell RS, Taylor BW. 1999. *Operations Management*, 2nd ed. Prentice-Hall, Upper Saddle River.
3. Hines P, Rich N. 1997. The seven value stream mapping tools. *International Journal of Operations & Production Management* 17(1), 46-64.
4. Womack JP, Jones DT. 2003. *Lean thinking: Banish waste and create wealth in your Corporation*. 2nd ed., London, UK: Simon and Schuster Inc., 15-90.
5. Rother M, Shook J. 1999. Learning to See: Value Stream Mapping to Create Value and Eliminate Muda. Learning Enterprise Institute, Brookline.
6. Kumar BS, Thavaraj HS. 2015. Impact of Lean Manufacturing Practices on Clothing Industry Performance. *International Journal of Textile and Fashion Technology* 5(2), 1-14.
7. Brandt E, Tjärning A. 2015. Changing from a reactive to a proactive maintenance culture; Implementing of OEE. Lulea University of Technology Engineering Programme, Master Thesis.
8. Sudhakar S. 2015. Value stream mapping and value stream design in a complex diesel pump production flow: A case study. *Journal of Mechanical Engineering and Automation* 5(3B), 69-75.
9. Kumari R, Quazi TZ, Kumar R. 2015. Application of lean manufacturing tools in garment industry. *International Journal Of Mechanical Engineering And Information Technology* 3(1), 976-982.
10. Akçagün E, Dal V, Yılmaz A. 2012. Using value stream mapping at apparel industry: A case study. In Proceedings of the 6th International Textile, Clothing & Design Conference - Magic World of Textiles October 07-10 2012, Dubrovnik, Croatia.
11. Yıldız EZ, Güner M. 2013. Applying value stream mapping technique in apparel industry. *Tekstil ve Konfeksiyon* 23(4), 393-400.
12. Silva S. 2012. Applicability of value stream mapping (VSM) in the apparel industry in Sri Lanka. *International Journal of Lean Thinking* 3(1), 36-41.
13. Kumar BS. 2016. Value stream mapping-a lean manufacturing approach to reduce the process wastages in clothing industry. *International Journal of Advances in Management and Economics* V5(5), 23-33.
14. Bamber CJ, Castka P, Sharp JM, Motara Y. 2003. Cross-functional team working for overall equipment effectiveness(OEE). *Journal of Quality in Maintenance Engineering* 9(3), 223-238.



Development of Tubular Woven Preform Reinforced Composite Pipe and Comparison of Its Compression Behavior with Filament Wound Composite

Gulsah Pamuk¹, Ugur Kemiklioglu², Onur Sayman³¹ Department of Textile Technology, Emel Akin Vocation School, Ege University, Izmir, Turkey² Department of Mechanical Engineering, Dogus University, Kadikoy, Istanbul, Turkey³ Department of Mechanical Engineering, Faculty of Engineering, Dokuz Eylul University, Izmir, Turkey**Corresponding Author:** Gülşah Pamuk, gulsah.pamuk@ege.edu.tr

ABSTRACT

In this research a preform for the reinforcement of tubular composite structures has been developed to improve the mechanical properties of composite pipes. The mentioned preform was woven from para aramid yarn in the tubular form. A mandrel was passed through a certain amount of tubular woven preform layer then impregnated with resin, cured in an oven and the resulting composite pipe was removed from the mandrel. By using the same para aramid yarn, filament wound composite pipes were also manufactured with the same production parameters. Axial and transverse compression behaviors of tubular woven preform reinforced composite pipes were compared with the ones that are manufactured by conventional filament winding method. The test results indicated that under transverse and axial compression, composite pipes developed in this study showed superior strength values than filament wound ones.

1. INTRODUCTION

Tubes refer to any shape of hollow material of uniform wall thickness and defined by the outside diameter and wall thickness dimensions. On the other hand, a pipe is one type of tube with the specific circular shape [1] and composite technology has been utilized in pipes for more than 50 years [2] because of their light weight, high strength, stiffness and durability to corrosion. Composite pipes have been used in many engineering applications like wastewater treatment, transmission of gas, oil and chemicals [2-4]. They also found their way as structural elements in buildings, bridges, automotive and aerospace industries [1].

Filament winding is one of the most common method to produce composite pipes in which filament fibre is

impregnated with the resin, winded around a mandrel and then cured [6]. Some previous investigations about filament wound composite pipes are focused on their mechanical and thermal properties [4, 7-14] while the others focused on design and development [15-18] of these pipes. The filament winding process is an efficient and low cost technique that ensures high fibre volume fraction with unlimited number of repeatable and accurate fibre angles [19-20] but also has some disadvantages. Although the yarn winding angle can be adjusted, the filament fibre cannot be exactly oriented towards the lengthwise direction of the structure in respect of the process. Therefore, if filament wound pipes are exposed to transverse impact loads and destructive environmental conditions, having no fibres in the thickness direction causes problems during their installation, maintenance and service life [14]. Also, in

To cite this article: Pamuk G, Kemiklioglu U, Sayman O. 2019. Development of tubular woven preform reinforced composite pipe and comparison of its compression behavior with filament wound composite. *Tekstil ve Konfeksiyon* 29(3), 262-267.

filament wound composites, cracks easily propagate through fibre direction [21].

The main objective of this study was to design and manufacture a tubular woven preform that can be used as textile reinforcement in composite pipes and reduce the disadvantages of filament winding method mentioned above. Preforms manufactured by weaving technology, draw attention by their strength properties in reinforcement of composite structures. The advantages of woven preforms compared to non-woven surfaces, which are their greatest competitors, are that they can better adapt to complex shapes, exhibit better drapeability and resistance to impact [22]. As Pastore [23] stated, woven fabrics are by far the most commonly used textile system for composite applications. In literature woven preforms were restricted to the reinforcement of composite materials mostly in plate and laminated form [24-30]. With this regard, the novelty of this work lies in the utilization of tubular woven preform in reinforcement of composite pipes. Axial and transverse compression behaviors of the new developed pipe were compared with the filament wound ones. In addition, some instructions are also provided for further research and design of such structures.

2. MATERIAL AND METHOD

Carbon, glass and aramids are the most commonly used high performance fibres in composite production. In this study, para aramid fibres were chosen for preform production owing to their high degree of toughness, associated with the failure mechanism and damage tolerance performance. Another attractive feature of them in composite reinforcement is when they break; they do not fail by brittle cracking, as do glass or carbon fibres [31]. Instead, the aramid fibres fail by a series of small fibril failures, where the fibrils are molecular strands that make up each aramid fibre and are oriented in the same direction as the fibre itself. These many small failures absorb much energy and, therefore, result in very high toughness [31].

For composite tube configurations, (i) tubular woven preform reinforced composite pipe (TWP) and (ii) filament wound composite pipe (FWP) were considered and the production procedures of these pipes were explained as follows:

Production of tubular woven preform reinforced composite pipe

Woven fabrics are produced by the interlacing of warp (0°) yarns and weft (90°) yarns in a regular pattern. The types of woven fabrics can be identified by the pattern of repeat of the interlaced regions [32]. For weft and warp threads, different raw materials may be selected depending on the use of the composite pipe or both may be the same raw material. Similarly, according to the mechanical properties expected of the composite pipe, the fineness of the weft and warp yarn and the weft-warp frequency of the fabric can be modified.

Tubular woven preform was produced on fully automatic sampling loom with the double-layer woven fabric production technique and the layers were not connected in order to achieve a tubular gap between them. The tubular preform has a 2/2 twill woven structure with a count of 20 ends/cm in warp direction and 20 picks/cm in weft direction. In weft direction multifilament 83 tex para aramid yarn (146 cN/tex) was used. On the other hand, if multifilament yarn has been used as warp yarn, yarn breakages would occur during the weaving process. Thereby, in order to eliminate yarn breakages, twisted 20 tex para aramid yarn (108 cN/tex) was used in warp direction.

After the tubular woven preform is produced, a separator was applied on mandrel which is selected according to the desired composite pipe diameter and then the tubular preform was passed over the mandrel. After that, a coat of epoxy resin is applied on it, and this process is repeated for each layer of preform. Totally 3 layers of tubular woven preform was used. Once the fabric layers were completed, the shrink tape was wrapped on the top layer. Then the mandrel, with 3 layers of epoxy impregnated preform, heated in a slow motion rotary oven at 120°C for 4 hours to be cured. The pipe was kept rotating during the curing in order to avoid resin glow toward a particular bottom side of the cross section. After curing, specimens were extracted from the mandrel and cut to length. The fibre volume fraction of the composite pipe was %29.24.

Production of filament wound composite pipe

83 tex multifilament para aramid yarn which is also used in the production of tubular woven preform was used for the production of filament wound composites. Tows were wetted with EPR 828 EL epoxy resin and EPH 875 hardener. For thin walled cylindrical shaped structures an optimum winding angle of 55° was noted [9]. For this reason, in our study, wet fibres were wound on the mandrel 3 layers with $\pm 55^\circ$ angle by using a CNC winding machine. Then, the mandrel put in an oven, rotating around its axis and cured at 120°C for 4 hours. After all, the filament wound composite pipes were cut into desired test length.

Compression testing of composite pipes

Transverse and axial compression tests were conducted on tubular woven preform reinforced composite pipes (TWP) (Figure 1-a) and filament wound composite pipes (FWP) (Figure 1-b) to understand the mechanisms of compressive failure and to examine the influence of reinforcement type on these mechanisms. Transverse compression tests were conducted according to ASTM Standard Test Method for Determination of External Loading Characteristics of Plastic Pipe by Parallel-Plate Loading (D-2412) and axial compression tests were conducted according to ASTM Standard Test Method for Compressive Properties of Rigid Plastics (D-695). The dimensions of the specimens were the same for both composite pipe types and showed in Figure 2.

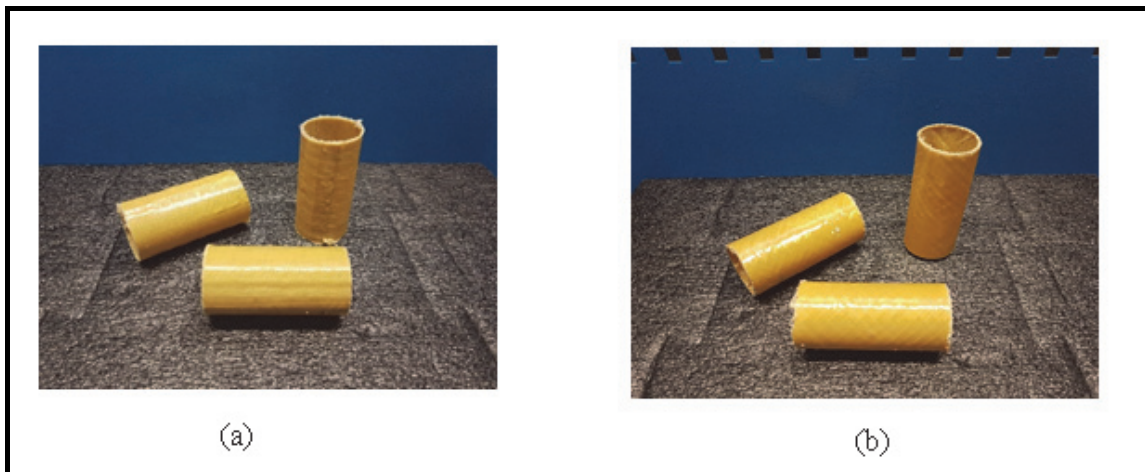


Figure 1. Compression test specimens; **a)** tubular woven preform reinforced composite pipes (TWP), **b)** filament wound composite pipe (FWP)

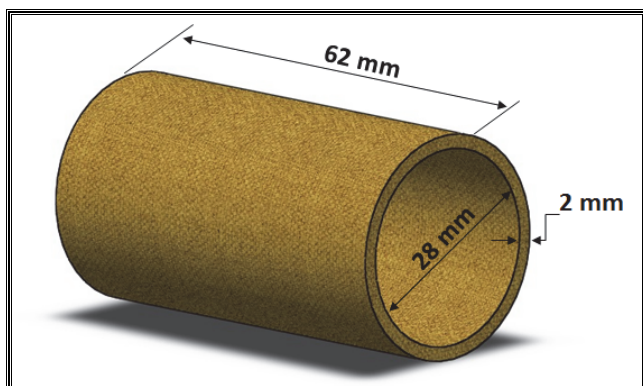


Figure 2. Test specimen dimensions

During pretrial tests when compression was applied to the (empty) pipes, buckling occurred and the pipes were damaged more quickly than the internal walls. In order to eliminate buckling the compression tests were conducted both with fine sand filled pipes and empty pipes. The compression tests were performed with the help of a Shimadzu 100kN tester at a progressive speed of 1mm/min. The load and displacement were recorded by standard coordinate (x-y) system. The specimens were tested at room temperature, which was about 20°C and the relative humidity was about 65%. The number of specimen of each set was three. The averages of values obtained from the test results were used to form force-displacement plot.

3. RESULTS AND DISCUSSION

The recent studies about the compressive behavior of tubular composites are mostly focused on their axial compression behaviors. However, a lateral compression test highlights the transverse behavior of the material, and even though this kind of tests is rather seldom, it is of high interest for the design of low-speed impact resistant structures [33]. The results of transverse compression tests (Figure 3) executed in this study showed that the maximum strength of the empty pipes reinforced by the tubular woven

preform method was about 800N, while the maximum strength of the empty pipes produced by the filament winding method was around 180N (Fig.3). These results proved that empty pipes produced with newly developed tubular woven preform can withstand forces with the prefactor 4.3 with compared to those of empty pipes produced with filament winding method.

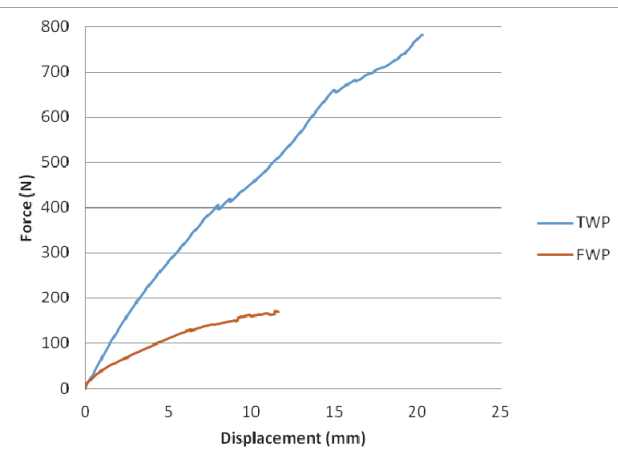


Figure 3. Force – displacement diagram of empty pipes subjected to transverse compression test

Moreover, the force-displacement curves for the compression test of the empty pipes in the axial direction are shown in Figure 4. The axial compressive strengths of both composite pipe types are ten times as much as their transverse compressive strengths. Also the amount of displacement in axial tests is far less than the ones observed in transverse tests. The empty pipes subjected to the axial compression tests show that the maximum strength of the pipes produced by the woven preform method is about 8000N, while the maximum strength of the pipes produced by the filament bending method is around 2800N. These results proves that empty pipes reinforced with novel tubular woven preform can withstand axial forces with the prefactor 2.8 when compared to those of empty pipes produced with filament winding method.

The damages seen in empty composite pipes during the transverse and axial compression tests are shown in Figure 5-6. From the images, it is clear that buckling occurs at empty pipes during the pressure tests. In order to prevent buckling during the compression tests, additional experiments were carried out with other pipe samples which were filled with sand.

The force-displacement curves of the sand-filled pipes which were subjected to the compression tests in the transverse direction are shown in Figure 7. As can be seen from the figure the damage propagation of sand filled pipes are quite slowly when compared to empty pipes and also the maximum strength of both pipes are much higher. The sand in the tubes increased the strength against lateral pressure so the experiment was terminated after the displacement exceeded 10 mm.

Figure 8 shows the force-displacement curves of the sand-filled pipes subjected to the compression tests in the axial direction. As can be seen from the figure, the maximum strength of the sand-filled pipes subjected to the axial compression test is around 6000N for the samples reinforced by the tubular woven preform while it is around 2300N for the samples produced by the filament winding method. The result proves that the sand filled TWP can withstand forces with the prefactor 2.48 when compared to

the sand filled FWP. This ratio is very close to the coefficient which was obtained in the compression test on empty pipes in axial direction. In filament wound composites, cracks easily propagate in the direction of the fibres. However, it is thought that the interlacement points of weft (90°) and warp yarns (0°) in tubular woven preforms are assumed to be a crack-stopping task. That is why the transverse and axial compression strengths of empty and sand filled TWP are higher than filament wound ones.

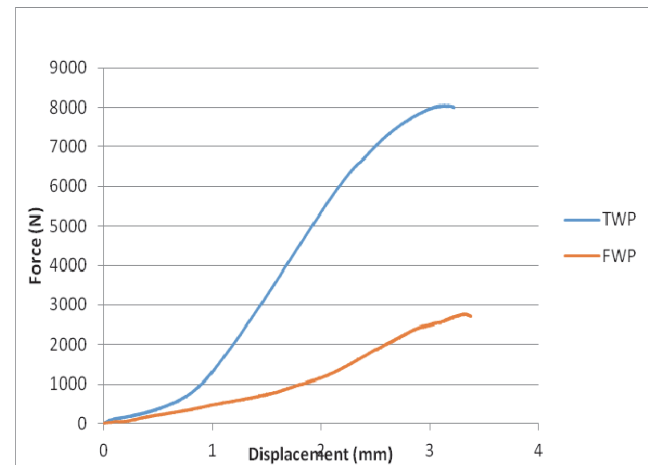


Figure 4. Force – displacement diagram of empty pipes subjected to axial compression test

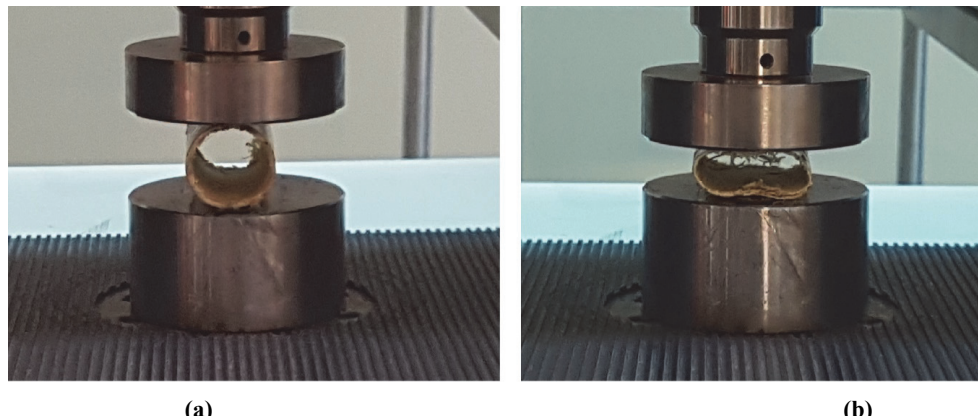


Figure 5. Transverse compression test of empty pipes; a) Before the test, b) After the test

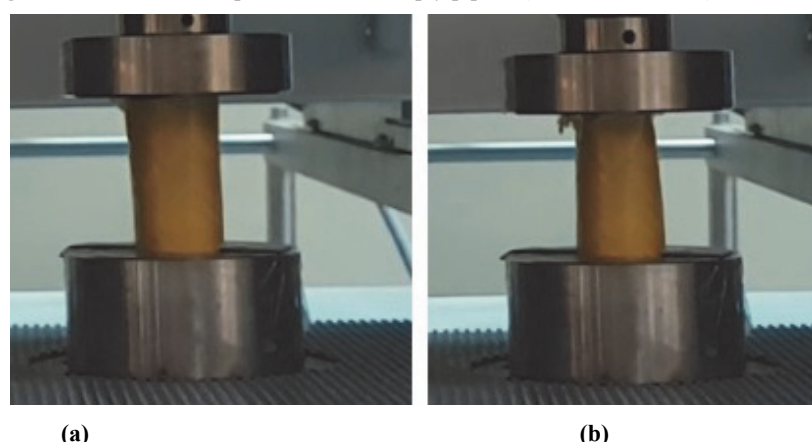


Figure 6. Axial compression test of empty pipes; a) Before the test, b) After the test

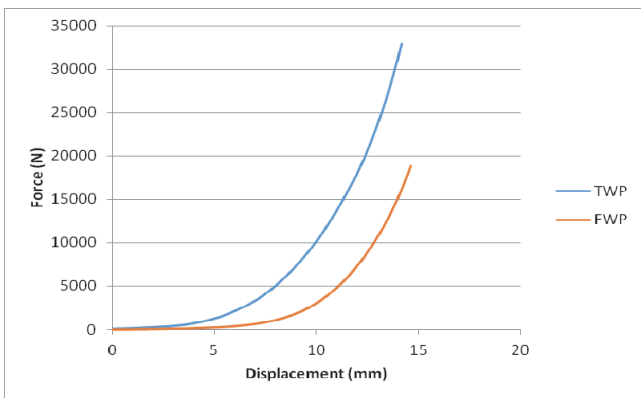


Figure 7. Force – displacement diagram of sand-filled pipes subjected to transverse compression test.

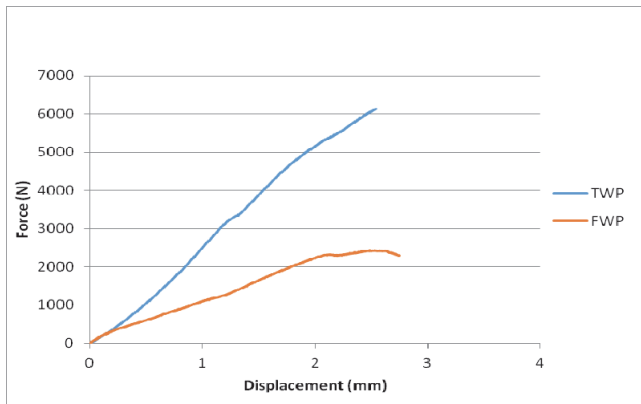


Figure 8. Force – displacement diagram of sand-filled pipes subjected to axial compression test

After the transverse tests, no visible damage to the naked eye was observed on the surface of the composite pipes while some apparent damages were occurred on the surfaces of pipes subjected to compression tests in the axial direction. Damages of the pipes after the axial compression tests are shown in Figure 9.

Figures 9a and 9c showed that buckling is formed on the internal walls of the pipes which were tested empty while the tearing occurred suddenly in the pipes which were filled with sand as seen in Figures 9b and 9d with the red marked.

4. CONCLUSION

Composite pipes have numerous end uses like pressure vessels, pipe lines, oxygen and other gas cylinders, rocket motor casings, helicopter blade and storage tanks. Filament

winding is one of the most common methods to produce composite pipes. However, filament winding have some advantages for instance the filament fibre cannot be exactly oriented towards the lengthwise direction of the structure in respect of the winding process. Because of having no fibres in the thickness direction makes filament wound pipes weak to transverse impact loads and destructive environmental conditions. The aim of this study was to design and manufacture a tubular woven preform that can be used as textile reinforcement in composite pipes and compare transverse and axial compression behaviors of this pipe with filament wound one.

Empty and sand filled tubular woven preform reinforced composite pipes withstood transverse compression forces 4.3 and 1.8 times higher than filament wound ones respectively. In axial compression tests, tubular woven composites showed almost 2.8 times better performance than filament wound ones. In filament wound composites, cracks easily propagated in the direction of the fibres. However, the interlacement points of weft (90°) and warp yarns (0°) in tubular woven preforms had a crack-stopping task. That is why the transverse and axial compression strengths of empty and sand filled tubular woven preform reinforced composite pipes were higher than filament wound ones.

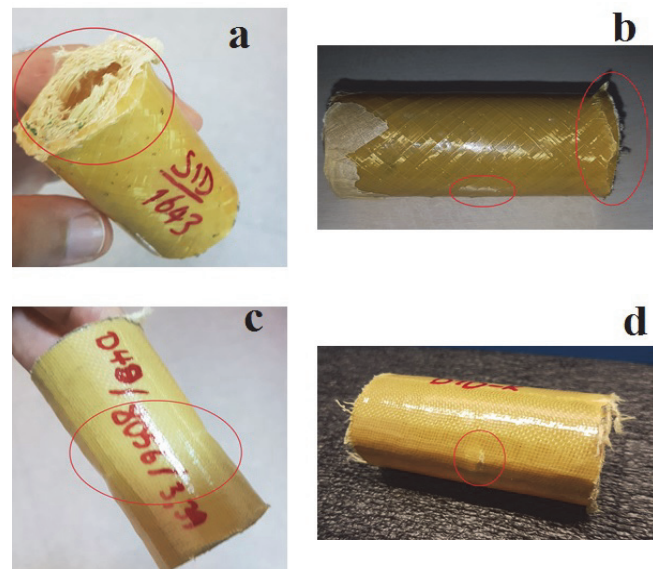


Figure 9. Failure of the specimens after axial compression tests;
a) empty FWP specimen, b) sand filled FWP specimen, c) empty TWP specimen, d) sand filled TWP specimen

REFERENCES

1. Hashmi MSJ, 2006. Aspects of tube and pipe manufacturing processes meter to nanometer diameter., *Journal of Materials Processing Technology* 179, 5-10.
2. Zou GP, Taheri F. 2006. Stress analysis of adhesively bonded sandwich pipe joints subjected to torsional loading. *International Journal of Solids and Structures* 43, 5953-5968.
3. Shen H, Wen J, Yu D, Wen X, 2009. The vibrational properties of a periodic composite pipe in 3D space. *Journal of Sound and Vibration* 328, 57-70.
4. Mertiny P, Ellyin F, Hothan A, 2004. An experimental investigation on the effect of multi angle filament winding on the strength of tubular composite structures. *Composites Science and Technology* 64, 1-9.

5. Use of Composite Pipe Materials in the Transportation of Natural Gas (2002) Available at:
<http://citeseerx.ist.psu.edu/viewdoc/download?doi=10.1.1.165.1163&ep=rep1&type=pdf> (accessed 12 march 2018).
6. Sari M, Karakuzu R, Deniz ME, Icten BM. 2011, Residual failure pressures and fatigue life of filament wound composite pipes subjected to lateral impact. *Journal of Composite Materials* 46(15), 1787-1794.
7. Xia M, Kemmochi K, Takayanagi H. 2002. Bending behavior of filament-wound fiber-reinforced sandwich pipes. *Composite Structures* 56, 201-210.
8. Ma Y, Sugahara T, Yang Y, Hamada H. 2015. A study on the energy absorption properties of carbon/aramid fiber filament winding composite tube. *Composite Structures* 123, 301-311.
9. Xia M, Kemmochi K, Takayanagi H. 2001. Analysis of filament wound fiber reinforced sandwich pipe under combined internal pressure and thermomechanical loading. *Composite Structures* 51(3), 273-283.
10. Deniz ME, Karakuzu R. 2012. Seawater effect on impact behavior of glass epoxy composite pipes. *Composites Part B* 43(13), 1130-1138.
11. Onder A, Sayman O, Dogan T, Tarakcioglu N. 2009. Burst failure load of composite pressure vessels. *Composite Structures* 89(1), 159-166.
12. Sayman O. 2005. Analysis of multi-layered composite cylinders under hygrothermal loading. *Composites Part A*, 36(7), 923-933.
13. Demir I, Sayman O, Dogan A, Arikan V, Arman Y. 2015. The effects of repeated transverse impact load on the burst pressure of composite pressure vessel. *Composites Part B* 68, 121-125.
14. Deniz ME, Ozdemir O, Ozen M, Karakuzu R. 2013. Failure pressure and impact response of glass epoxy pipes exposed to seawater. *Composites Part B* 53, 355-361.
15. Cohen D. 1997. Influence of filament winding parameters on composite vessel quality and strength. *Composites Part A* 28(12), 1035-1047.
16. Velosa JC, Nunes JP, Antunes PJ, Silva JF, Marques AT. 2009. Development of a new generation of filament wound composite pressure cylinders. *Composites Science and Technology* 69(9), 1348-1353.
17. Cohen D, Mantell S., Zhao L. 2001. The effect of fiber volume fraction on filament wound composite pressure vessel strength. *Composites Part B* 32(5), 413-429.
18. Sung J, Chang P, Chun SH, Cheol GK, Kim U. 2002. Analysis of filament wound composite structures considering the change of winding angles through the thickness direction. *Composite Structures* 55(1), 63-71.
19. Jia X, Chen G, Yu Y, Li G, Zhu J, Luo X, Duan C, Yang X, Hui D. 2013. Effect of geometric factor, winding angle and pre-crack angle on quasi-static crushing behavior of filament wound CFRP cylinder. *Composites Part B*, 45, 1336-1343.
20. Peters ST. 2011. Filament winding-introduction and overview. In: Peters ST. (ed.). *Composite Filament Winding*. USA: ASM International
21. Ahmadi MS, Johari MS, Sadighi M, Esfandeh M. 2009. An experimental study on mechanical properties of GFRP braid pultruded composite rods. *Polymer Letters* 3(9), 560-568.
22. Harrocks AR, Anand SC. 2000. *Handbook of Technical Textiles*. New York: Woodhead Publishing Limited.
23. Pastore C. 2000. Opportunities and challenges for textile reinforced composites. *Mechanics of Composite Materials* 36(2), 97-116.
24. Yang B, Kozey V, Adanur S, Kumar S. 2000. Bending, compression, and shear behavior of woven glass fiber epoxy composites. *Composites Part B* 31, 715-721.
25. Hosseinzadeh R, Shokrieh MM, Lessard L. 2006. Damage behavior of fiber reinforced composite plates subjected to drop weight impacts. *Composites Science and Technology* 66, 61-68.
26. Karakuzu R, Gulem T, Icten BM. 2006. Failure analysis of woven laminated glass-vinylester composites with pin-loaded hole. *Composite Structures* 72, 27-32.
27. Zhang J, Chaisombat K, He S, Wang CH. 2012. Hybrid composite laminates reinforced with glass/carbon woven fabrics for lightweight load bearing structures. *Materials and Design* 36, 75-80.
28. Baucom JN, Zikry MA. 2005. Low velocity impact damage progression in woven E-glass composite systems. *Composites Part A* 36, 658-664.
29. Icten BM, Karakuzu R. 2002. Progressive failure analysis of pin-loaded carbon-epoxy woven composite plates. *Composites Science and Technology* 62, 1259-1271.
30. Clark SR, Mouritz A., 2008. Tensile fatigue properties of a 3D orthogonal woven composite. *Composites Part A* 39, 1018-1024.
31. Reis PNB, Ferreira JAM, Santos P, Richardson MOW, Santos B. 2012. Impact response of Kevlar composites with filled epoxy matrix. *Composite Structures* 94, 3520-3528.
32. Ishikawa T, Chou T. 1982. Stiffness and strength behavior of woven fabric composites. *Journal of Materials Science* 17, 3211-3220.
33. Calme O, Bigaud D, Hamelin P. 2005. 3D braided composite rings under lateral compression. *Composites Science and Technology* 65, 95-106.



An Image Processing Research Consistent with Standard Photographs to Determine Pilling Grade of Woven Fabrics

Abdurrahman Telli

Cukurova University, Department of Textile Engineering, Adana, Turkey

Corresponding Author: Abdurrahman Telli, atelli@cu.edu.tr

ABSTRACT

In this study, MATLAB 2018a software was used to evaluate pilling grade of woven fabrics objectively. Experimental works were carried out on the EMPA W3 standard photographs and accordingly two woven fabrics. Equations were built based on the measurements of pill characteristics and textural parameters of these photographs with the help of curve fitting method after image processing steps. Intervals were generated for each fabric by using slope of these equations and quantitative parameters obtained from the original fabric. Furthermore, fabrics that were provided pilling formation at different test turns were evaluated subjectively by expert operators. Objective results corresponding to each parameter were analyzed comparatively with these subjective results. The developed method was successful by using mean of matrix elements from textural parameters and total area from pill characteristics.

ARTICLE HISTORY

Received: 29.03.2019

Accepted: 03.09.2019

KEYWORDS

Pilling, image processing, GLCM, texture analysis, MATLAB

1. INTRODUCTION

Pilling is one of the most important features that provide information about fabric performance and aesthetic properties. In recent years, the increase in the use of synthetic fibers and blends has more increased the importance of pilling. Pilling is affected by a wide range of parameters such as material type, spinning technology, fabric production technology, finishing technology. The evaluation of pilling grades is usually based on rubbing fabric to fabric surfaces up to a specific turns. The tested samples are given a pilling grade by a trained and experienced expert. Pilling grades of samples are evaluated by the eye. Furthermore, this evaluation should be supported by standard photos [1-5]. Most of the time in decision making, it is difficult to obtain same results because of differences in visual perception between experts.

These assessments have significant limitations because it greatly depends on the human factor [6]. Due to these reasons, there has been an increasing interest in the determination of pilling resistance objectively with the applications of the image processing technology for a long time. Furferi *et al.* presented an outstanding and chronological review of the most relevant methods for pilling measurement proposed so far [7]. In general, quantitative analysis of pilling evaluation consists of surface digitization, pills segmentation, pills quantization and pills classification [8]. In these studies, calculating the pilling grade depends upon a host of measurements including pill density, pill size, pill height, and fuzz loft. There is limited available publication based on textural parameters of images [9]. However, it was seen that the classification of pilling is a major problem with this kind of works. Regression models, discriminant analysis and

To cite this article: Telli A. 2019. An image processing research consistent with standard photographs to determine pilling grade of woven fabrics. *Tekstil ve Konfeksiyon* 29(1), 268-276.

artificial neural networks have been used comparing subjective methods for classification in the literature in recent years [10-12]. A significant number of studies are based on existing standard photographs. Because this system has been used for years and the new system must be compatible with them [13-20].

This paper seeks to remedy the mentioned problems by analyzing the deficiencies of literature with a new approach. This study takes into consideration both pills characteristics and texture features of the binary images among the quantization parameters. In different to earlier studies, the fabric was scanned before and after pilling. In this study, a system was tested based on the standard photographs (W3) corresponding to different pilling grades developed by EMPA according to Martindale method. Equations were built based on the measurements of pill and textural parameters of this photograph with the help of curve fitting method. Intervals were generated for each fabric by using slope of a distribution curve of these standard photographs and quantitative parameters obtained from the original fabric in the determination of the pilling grades of woven fabrics. Furthermore, fabrics that were provided pilling formation at different test turns were evaluated subjectively by expert operators. Objective results corresponding to each parameter were analyzed comparatively with these subjective results.

2. MATERIAL AND METHOD

Two different woven fabrics were used in this study as shown in Table 1.

“Nu-Martindale Test Instrument” was chosen to determine pilling resistance of these fabrics in compliance with TS EN ISO 12945-2. The images of fabric specimens with a diameter of 140 mm were obtained by digital scanner as 300 x 300 dpi (dots per inch) 24 bits before the process of placing in the rubbing area. The 300 dot/inch equals 11.811024 pixels/mm. The tests were carried out with three specimens for each type at 1000, 2000, 5000 and 7000 turns. After this process, fabric surfaces containing pills with a diameter of 90 mm were scanned again. To capture images with same method as standard every time, digital scanner was used. In this way, the test samples (diameter of 140 mm) corresponded to approximately 1650x1650 pixels and pilling area (diameter of 90 mm) in specimens corresponded to 1063x1063 pixels each time. Due to the lissajous movement, the pilling area on the fabric is

prominent. However, the boundary regions of the pilling area may be damaged depending on the fabric structure due to the additional loading mass used in woven fabrics or the improper placement of the sample. According to our experiences, this situation causes negative effects on image processing. To eliminate these problems, taken images before and after in pilling were resized as 900 x 900 pixels by cutting from width and length at the same size. After that, the digital image processing steps have started.

2.1 Image Quantization and Segmentation

MATLAB R2018a software was used to evaluate pilling of woven fabrics. Figure 1 provides the steps of image quantization and segmentation. Firstly, the RGB color images of fabrics are loaded to MATLAB package program. These images are three-dimensional matrices in "900x900x3 uint8" format. After that, matrices must be two-dimensional (900x900 uint8) in order to be able to operate on them. Thus, matrices expressing the different tone of the gray consisted values ranging from 0 to 256 were generated. These matrices are transformed into a form (900 x 900 double) that will have a value between 0 and 1. These forms of matrices were ready for texture analysis using GLCM from image processing techniques. Standard deviation filter was implemented on these matrices in the context of texture analysis [21, 22]. Histogram-fitting technique was used to compare a reasonable threshold for image segmentation [23]. In this way, all images were segmented with same thresholding value. Then, these images were segmented using Otsu's global thresholding algorithm (thresholding value=0.49804). Thus, the pills in the image were separated from the image background. Values below the specified radius were masked using close mask. This mask provides dilation followed by erosion. And, this removes pills smaller than the determined element. The same radius (shape=disk radius=4) was also used to mask fabric images after pilling to provide the possibility of comparing the fabrics. Furthermore, the fabric's own fuzz and structure are not regarded as discomfort. After this phase, the negatives of images were obtained applying "invert mask" to matrices. Image processing was finished by clearing the borders of the image. And so, matrices of images have reached to "900x900 logical" format. Several statistics were derived with feature extraction from these matrices. Fabric's surface digitization, pills detection and segmentation were carried out with these procedures.

Table 1. Specifications of fabrics

Code	Weight (g/m ²)	Material	Weave	Fabric type
01	208	50% Polyester 50% Cotton	Plain weave	Trouser fabric
02	408	50% Polyester 50% Viscose	Plain weave	Crepe dressmaking fabric

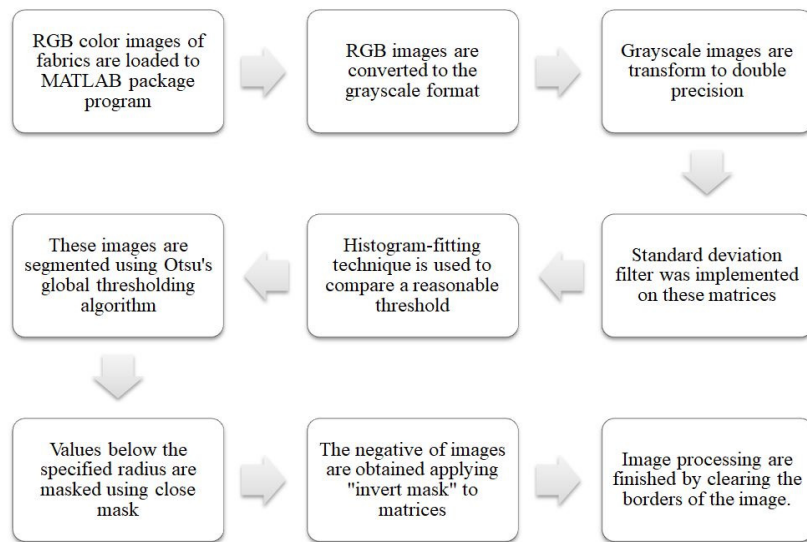


Figure 1. Steps of image quantization and segmentation

2.2 Pills Quantizations

Pill quantizations were made using images in matrix format obtained from image processing studies. Statistical measures were extracted from matrices. Texture analysis was performed with Gray Level Co-occurrence Matrix (GLCM). GLCM consist of contrast, correlation, energy and homogeneity. Mean of matrix elements (mean2), entropy of grayscale image (entropy) and standard deviation of matrix elements (std2) information can be obtained within texture analysis. Furthermore, it is possible to extract values from grayscale images such as pill number, area, convexArea, eccentricity, equivdiameter, Euler number, extent, filled area, major axis length, minor axis length, orientation, perimeter and solidity through image region analyzer.

2.3 Pills Classification

In this study, a system was tested based on the standard photographs corresponding to different pilling grades developed by EMPA. EMPA SN 198525 is an industrial standard for fabric pilling evaluation. This standard was developed for the evaluation of specimens worked in the Martindale pilling test tool. The EMPA standard contains

three separate categories, each consisting of four images. In total, there are 24 photographs for knitted (K1, K2, K3) and woven (W1, W2, W3) fabrics. In this study, experimental works were carried out on the W3 standard photograph and accordingly two woven fabrics. Equations were built based on the measurements of pill and textural parameters of these photographs with the help of curve fitting method. Intervals were generated for each fabric by using slope of a distribution curve of these standard photographs and quantitative parameters obtained from the original fabric in the determination of the pilling grades of woven fabrics. Furthermore, fabrics that were provided pilling formation at different test turns were evaluated subjectively by expert operators. Objective results corresponding to each parameter were analyzed comparatively with these subjective results.

3. RESULTS AND DISCUSSION

Figure 2 presents images of EMPA SN 198525 “W3” standard photographs before and after image processing. The pill quantization results obtained binary images can be compared in Table 1.

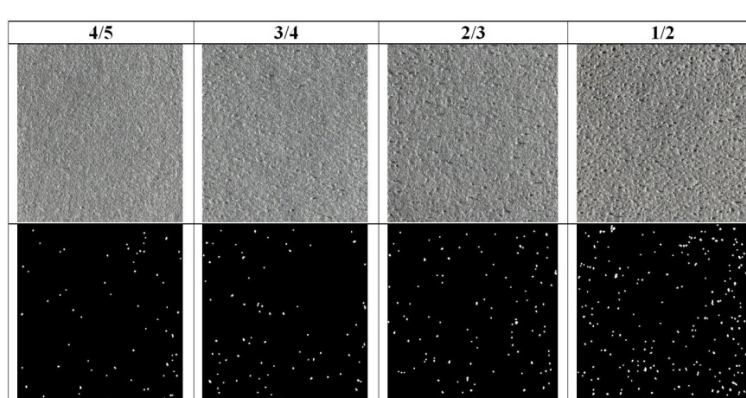


Figure 2. EMPA SN 1982555 “W3” standard photographs before and after image processing

From Table 2, it can be seen that six features (mean of matrix elements, standard deviation of matrix elements, entropy of grayscale image, contrast, number of pills and total area) have an increasing trend when the pilling grade worse. And, two statistics (energy and homogeneity) extraction from Gray-level Co-occurrence Matrix has a reducing trend with the decrease of pilling grade. There was no clear trend between pilling grades and other variables. In these eight properties, linear curve fitting is made for each property using measuring points. As shown in Figure 3 and 4, the coefficients of the determination (R^2) for selected features was found to be 82.7% and above. Thanks to these equations, the eight intervals (5, 4/5, 4, 3/4, 3, 2/3, 2, 1/2) of different pilling grades for standard photograph were generated as shown in Table 3.

The slopes of the lines obtained for each feature on the basis of these data were used for fabric samples to be tested. The extracted features from the untested fabric samples were written against the starting point of 5.25. Intervals have been generated for eight features in each fabric by using formula of the slope of the line. Then, it was investigated the intervals corresponding to values of the eight features obtained from fabrics that had pilling formation at different turns.

The results obtained from the image processing of two different woven fabrics are shown in Figure 5. Images of fabrics in 0 and 7000 turns were given in this figure.

Table 4 provides subjective evaluation results and the results of statistical measurements obtained from binary images of fabrics with feature extraction.

Table 2. The pill quantizations results obtained from “W3” standard photographs

Pilling Grade	4/5	3/4	2/3	1/2
Mean of matrix elements	0.00530	0.00698	0.00961	0.02072
Standard deviation of matrix elements	0.07258	0.08328	0.09758	0.14243
Entropy of grayscale image	0.04766	0.06006	0.07822	0.14544
Contrast	0.00167	0.00210	0.00296	0.00614
Correlation	0.84205	0.84904	0.84479	0.84883
Energy	0.98779	0.98402	0.97799	0.95328
Homogeneity	0.99917	0.99895	0.99852	0.99693
Number of Pills	62	75	108	217
Total Area	4290	5657	7787	16780
Major Axis Length	10.3299	10.9462	10.4451	11.0280
Minor Axis Length	8.6400	8.8453	8.7950	8.9456
Eccentricity	0.3572	0.4097	0.3611	0.3782
Orientation	20.5863	7.8236	20.8937	13.4818
EquivDiameter	9.2727	9.6460	9.4151	9.7091
Solidity	0.9294	0.9299	0.9311	0.9299
Extent	0.6227	0.6230	0.6342	0.6249
Perimeter	28.07	29.47	28.38	29.73

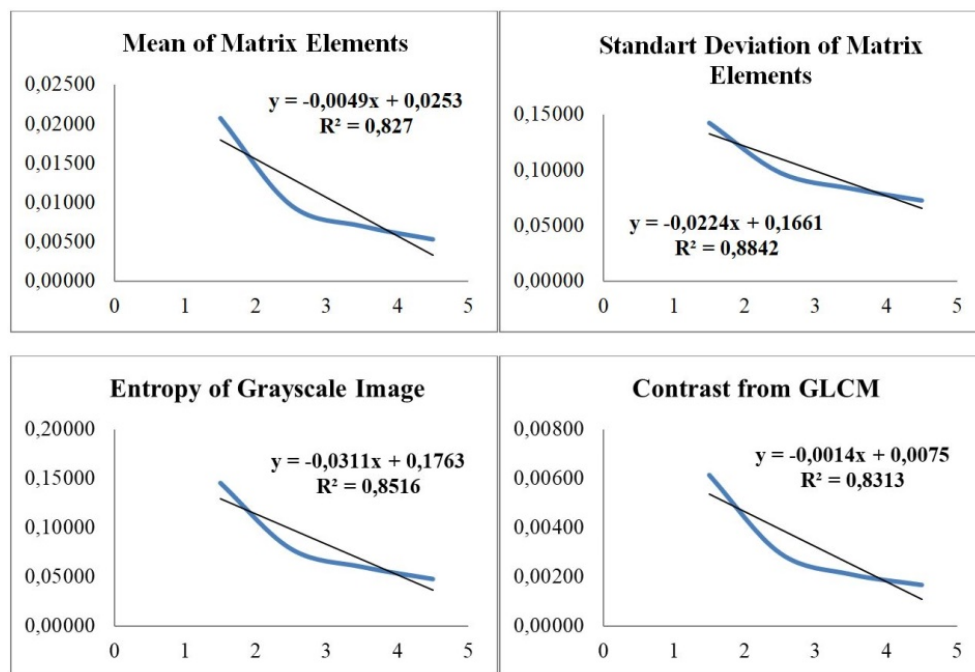


Figure 3. The obtained equations for mean, standard deviation, entropy and contrast

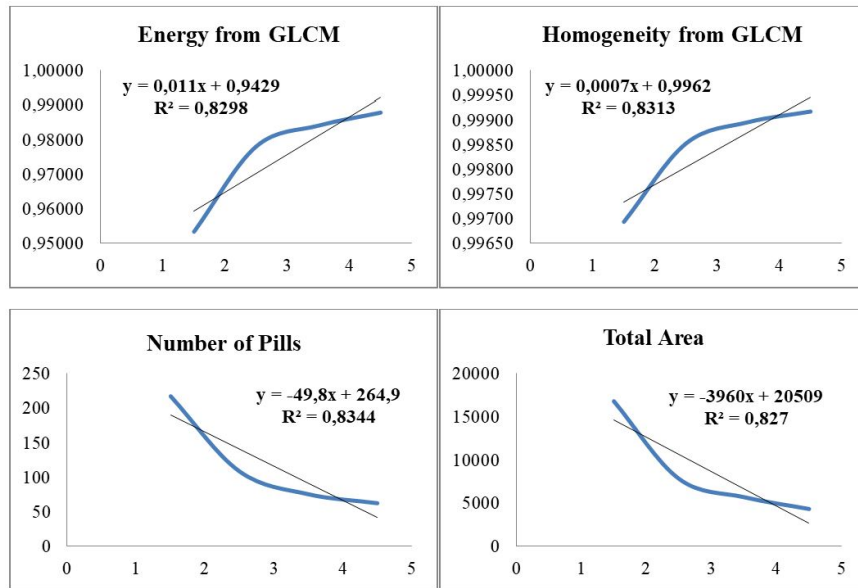


Figure 4. The obtained equations for energy, homogeneity, number of pills and total area

Table 3. The intervals of different pilling grades for standard photograph (EMPA W3)

	5.25	4.75	4.25	3.75	3.25	2.75	2.25	1.75	1.25
Mean	-0.0004	0.0020	0.0045	0.0069	0.0094	0.0118	0.0143	0.0167	0.0192
Std. Dev.	0.0485	0.0597	0.0709	0.0821	0.0933	0.1045	0.1157	0.1269	0.1381
Entropy	0.0130	0.0286	0.0441	0.0597	0.0752	0.0908	0.1063	0.1219	0.1374
Contrast	0.0002	0.0009	0.0016	0.0023	0.0030	0.0037	0.0044	0.0051	0.0058
Energy	1.0007	0.9952	0.9897	0.9842	0.9787	0.9732	0.9677	0.9622	0.9567
Homogeneity	0.9999	0.9995	0.9992	0.9988	0.9985	0.9981	0.9978	0.9974	0.9971
Number of Pills	3.45	28.35	53.25	78.15	103.05	127.95	152.85	177.75	202.65
Total Area	-281	1699	3679	5659	7639	9619	11599	13579	15559

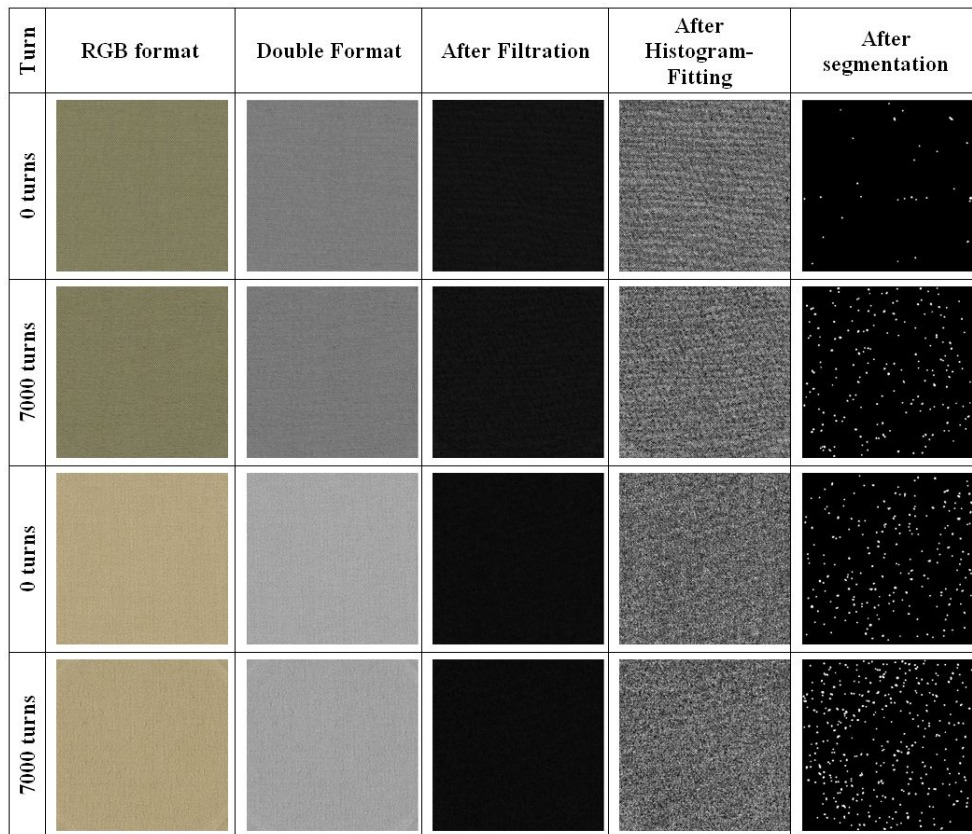


Figure 5. Images of analyzed two different fabrics in the steps of processing for 0 and 7000 turns

Table 4. Statistical measurements obtained from binary images of fabrics with feature extraction

Fabric Code	Test Turn	Mean	Std. Dev.	Entropy	Contrast	Energy	Homogeneity	Number of Pills	Total Area	Subjective Results
01	0	0.0038	0.0606	0.0358	0.0016	0.9879	0.9992	43	3088	-
	1000	0.0085	0.0918	0.0708	0.0025	0.9806	0.9987	96	6900	4/5
	2000	0.0111	0.1049	0.0882	0.0033	0.9747	0.9984	123	9016	4
	5000	0.0122	0.1096	0.0949	0.0036	0.9723	0.9982	139	9861	3/4
	7000	0.0142	0.1180	0.1072	0.0043	0.9678	0.9979	162	11485	3
02	0	0.0177	0.1318	0.1283	0.0054	0.9598	0.9973	204	14338	-
	1000	0.0228	0.1491	0.1567	0.0067	0.9488	0.9966	246	18451	4
	2000	0.0264	0.1601	0.1757	0.0078	0.9409	0.9961	284	21345	3/4
	5000	0.0314	0.1743	0.2012	0.0090	0.9302	0.9955	325	25415	2/3
	7000	0.0330	0.1787	0.2093	0.0094	0.9268	0.9953	334	26737	2

It is apparent from Table 4 that subjective pilling grades have a decreasing trend with the increase of turns for both fabrics. From the data in Table 4, it can be seen that six features (mean of matrix elements, standard deviation of matrix elements, entropy of grayscale image, contrast, number of pills and total area) have an increasing trend with the worse pilling grade and the increase of test turns. And, there was a clear trend of decreasing with the increase of turns and decrease of pilling grade in two statistics (energy and homogeneity) extraction from Gray-level Co-occurrence Matrix. Data from this table can be compared with the pill quantizations results obtained from "W3" standard photographs in Table 2 which show same trends for eight features. The results indicate that eight statistical values show similarity as direction with the relationship trend between variables and pilling grades in standard photographs. However, results of the pill quantizations obtained from statistical features of both fabrics and "W3" were different in the same subjective results. The subjective results of fabric coded as "01" after 2000 turns and fabric coded as "02" after 1000 turns were equal to "4". The subjective results of fabric coded as "01" after 5000 turns and fabric coded as "02" after 2000 turns were equal to "3/4". However, the obtained eight statistical results were completely different (Table 4). Furthermore, it can be seen from Figure 6 that binary images after segmentation corresponding to same subjective results were completely

different. Similar situations were observed when binary images were analyzed after segmentation in Figure 5. There were also significant increases in amounts of pills in 7000 turns according to 0 turns for both fabrics. The appearance of the fabric codes as "01" after 7000 turns were similar to the appearance of the fabric codes as "02" after 0 turns.

Very different images can be observed for the same subjective result although fabrics were used the same image processing steps and were segmented at the same diameter. In the literature, the results obtained from extracted from binary images were used directly for classification. As explained by the examples, this situation prevents reaching the correct result since the structure of each fabric is different from each other. Fabrics have different amounts of fuzz or surface properties. To eliminate this limitation of work, the data belongs to original fabrics (0 turns) were approved as reference point. The extracted features from the untested fabric samples were written against the starting point of 5.25. Intervals have been generated for eight features in each fabric by using formula of the slope of the line from the intervals of different pilling grades for standard photograph (EMPA W3) in Table 3. Tables 5 and 6 present the intervals of different pilling grades for fabric coded as "01" and "02". To give an example, let's examine how 3.75 and 3.25 intervals were generated for the 3.5 pilling grade value in statistics of number of pills from Table 5.

Subjective Results	4	4	3/4	3/4
Binary Images after segmentation				
Definition	"01" after 2000 turns	"02" after 1000 turns	"01" after 5000 turns	"02" after 2000 turns

Figure 6. Binary images after segmentation corresponding to "4" or "3/4"

Table 5. The intervals of different pilling grades for fabric coded as “01”

	5.25	4.75	4.25	3.75	3.25	2.75	2.25	1.75	1.25
Mean	0.0038	0.0063	0.0087	0.0112	0.0136	0.0161	0.0185	0.0210	0.0234
Std. Dev.	0.0606	0.0718	0.0830	0.0942	0.1054	0.1166	0.1278	0.1390	0.1502
Entropy	0.0358	0.0513	0.0669	0.0824	0.0980	0.1135	0.1291	0.1446	0.1602
Contrast	0.0016	0.0023	0.0030	0.0037	0.0044	0.0051	0.0058	0.0065	0.0072
Energy	0.9879	0.9824	0.9769	0.9714	0.9659	0.9604	0.9549	0.9494	0.9439
Homogeneity	0.9992	0.9989	0.9985	0.9982	0.9978	0.9975	0.9971	0.9968	0.9964
Number of Pills	43	68	93	118	143	168	193	218	243
Total Area	3088	5068	7048	9028	11008	12988	14968	16948	18928

Formula of slope of the line → $m = (y_2 - y_1) / (x_2 - x_1)$ (1)

The slope between the values of “5.25” and “3.75” in Table 3 has remained constant for Table 5.

The result of “5.25” for number of pills in Table 3 was “3.45”.

The result of “3.75” for number of pills in Table 3 was “78.15”.

The result of “3.25” for number of pills in Table 3 was “103.05”.

The results of original fabrics (0 turns) were used for the initial value of 5.25 in Table 5.

The result of original fabrics (0 turns) for number of pills in Table 4 was “43”.

In the light of this information, for “3.75” in statistics of number of pills from “Formula 1”:

$$(78.15 - 3.45) / (3.75 - 5.25) = (y_2 - 43) / (3.75 - 5.25)$$

$$y_2 = 118$$

For “3.25” in statistics of number of pills from “Formula 1”:

$$(103.05 - 3.45) / (3.75 - 5.25) = (y_2 - 43) / (3.75 - 5.25)$$

$$y_2 = 143$$

In this case, an interval for the 3.5 pilling grade value of number of pills was generated to 118-143 as shown in Table 5. The same operations were repeated for the other values and statistical properties.

Statistical measurements obtained from binary images of fabrics with feature extraction in Table 4 were processed on the intervals of different pilling grades for fabrics in Tables 5 and 6. These objective results can be compared in Table 7. The same results with subjective results were painted with bold. Furthermore, 0.5 unit differences have added in addition to the same grades with the decrease of sensitivity. These similar results with subjective results were shown in a sub-color (Table 7).

In general, the relationship of similar grades among test results was compatible except standard deviation of matrix elements in “5000” and “7000” turns for fabric coded as “02”. However, there were significant differences in same grades. The increase of sensitivity has provided significant decrease in similarities for most of statistical properties.

Table 6. The intervals of different pilling grades for fabric coded as “02”

	5.25	4.75	4.25	3.75	3.25	2.75	2.25	1.75	1.25
Mean	0.0177	0.0202	0.0226	0.0251	0.0275	0.0300	0.0324	0.0349	0.0373
Std. Dev.	0.1318	0.1430	0.1542	0.1654	0.1766	0.1878	0.1990	0.2102	0.2214
Entropy	0.1283	0.1438	0.1594	0.1749	0.1905	0.2060	0.2216	0.2371	0.2527
Contrast	0.0054	0.0061	0.0068	0.0075	0.0082	0.0089	0.0096	0.0103	0.0110
Energy	0.9598	0.9543	0.9488	0.9433	0.9378	0.9323	0.9268	0.9213	0.9158
Homogeneity	0.9973	0.9970	0.9966	0.9963	0.9959	0.9956	0.9952	0.9949	0.9945
Number of Pills	204	229	254	279	304	329	353	378	403
Total Area	14338	16318	18298	20278	22258	24238	26218	28198	30178

Table 7. The comparison of subjective and objective results

Fabrics Turns	01				02			
	1000	2000	5000	7000	1000	2000	5000	7000
Subjective Results	4.5	4	3.5	3	4	3.5	2.5	2
Mean	4.5	4	3.5	3	4	3.5	2.5	2
Std. Dev.	4	3.5	3	2.5	4.5	4	3.5	3
Entropy	4	3.5	3.5	3.5	4.5	3.5	3	2.5
Contrast	4.5	4	4	3.5	4.5	3.5	2.5	2.5
Energy	4.5	4	4	3.5	4.5	3.5	2.5	2
Homogeneity	4.5	4	3.5	3.5	4.5	3.5	2.5	2.5
Number of Pills	4	3.5	3.5	3	4.5	3.5	3	2.5
Total Area	4.5	4	3.5	3	4	3.5	2.5	2

The same grades between subjective results and the results of standard deviation of matrix elements were not obtained for any turns in two different fabrics. In entropy of grayscale image, same grades were only measured “5000” turns for fabric “01” and “2000” turns for fabric “02”. In number of pills, there were two same grades in “5000” and “7000” turns for fabric “01”. One same grade was observed in “2000” turns for fabric “02”. In contrast, four same grades as total were determined for two fabrics. In homogeneity and energy results, five same grades as total were observed for two fabrics. The best relationships were obtained in mean of matrix elements and total area. According to Table 6, there were same grades in all turns for two fabrics with respect to mean of matrix elements and total area. It can be seen from the data in Table 7 that no differences were found in mean and total area between subjective and objective pilling grades. The developed method in this study in order to determine the fabric pilling was successful by using mean of matrix elements and total area.

A strong relationship between total area and subjective results has been reported in the literature [13, 15, 16, 23]. This study confirms that total area from pilling characteristics is associated with subjective assessments. In reviewing previous studies, no data found on the association between mean of matrix elements from textural parameters and subjective results. In addition to earlier findings, a strong relationship was observed between

subjective assessments and mean of matrix elements obtained from textural parameters. There were no differences between subjective assessments and the obtained objective results by using mean of matrix elements and total area. Moreover, the developed method in this study was compatible with the current method used in the sector.

4. CONCLUSION

A common quality language is very important for the textile industry in the globalizing world. The most frequently fabric pilling evaluation systems are very subjective and have a broad quality interval. Differences in visual perception between operators make difficult to obtain same results. Disputes occur between some operators in the samples especially containing loosely entangled fuzz fibers. This situation often leads to disagreements in high costs in the supply chain. In this investigation, the purpose was to evaluate pilling grade of fabrics objectively with a new approach. The developed method was successful by using mean of matrix elements from textural parameters and total area from pill characteristics. The findings of the study were consistent with EMPA W3 standard photograph. In future works, the developed method should be carried out on the other EMPA or different standard photographs (BS, ASTM, IWS, M&S and etc.) in order to be made applicable to the whole sector.

REFERENCES

1. Ukpomwan JO, Mukhopadhyay A, Chatterjee KN. 1998. Pilling. *Textile progress* 28(3), 1-57.
2. Özdi N. 2003. *Kumaşlarda fiziksel kalite kontrol yöntemleri*, E.Ü. Tekstil ve Konfeksiyon Araştırma Uygulama Merkezi Yayınları Yayın No: 21, ISBN No: 975-483-579-9, Bornova-İzmir, 120s.
3. Özçelik G. 2009. Kumaş boncuklanma özelliğinin objektif olarak değerlendirilmesi ve tahminlenmesi üzerine bir araştırma, E.Ü. Fen Bilimleri Enstitüsü Doktora Tezi, Bornova-İzmir, 291s.
4. Kayseri GÖ, Kirtay E. 2015. Part 1. Predicting the pilling tendency of the cotton interlock knitted fabrics by regression analysis. *Journal of Engineered Fibers and Fabrics* 10(3), 155892501501000305.
5. Kayseri GÖ, Kirtay E. 2015. Part II. Predicting the pilling tendency of the cotton interlock knitted fabrics by artificial neural network. *Journal of Engineered Fibers and Fabrics* 10(4), 155892501501000417.
6. Telli A. 2015, April. The reliability of subjective assessment in the determination of pilling resistance of knitted fabrics, 4th International Mediterranean Science and Engineering Congress (IMSEC 2019), 420-422.
7. Furferi R, Governi L, Volpe Y. 2015. Machine vision-based pilling assessment: a review. *Journal of Engineered Fibers and Fabrics* 10(3), 155892501501000320.
8. Wong C. (Ed.). 2017. *Applications of Computer Vision in Fashion and Textiles*. Woodhead Publishing.
9. Eldessouki M, Hassan M. 2015. Adaptive neuro-fuzzy system for quantitative evaluation of woven fabrics pilling resistance. *Expert Systems with Applications* 42(4), 2098-2113.
10. Zhang J, Wang X, Palmer S. 2007. Objective grading of fabric pilling with wavelet texture analysis. *Textile Research Journal* 77(11), 871-879.
11. Eldessouki M, Bukhari HA, Hassan M, Qashqary K. 2014. Integrated computer vision and soft computing system for classifying the pilling resistance of knitted fabrics. *Fibres & Textiles in Eastern Europe*.
12. Techniková L, Tunák M, Janáček J. 2017. New objective system of pilling evaluation for various types of fabrics. *The Journal of The Textile Institute*, 108(1), 123-131.
13. Konda A, Xin LC, Takadera M, Okoshi Y, Toriumi K. 1990. Evaluation of pilling by computer image analysis. *Journal of the Textile Machinery Society of Japan*, 36(3), 96-107.
14. Xu B. 1997. Instrumental evaluation of fabric pilling. *The Journal of the Textile Institute*, 88(4), 488-500.
15. Hsi CH, Bresee RR, Annis PA. 1998. Characterizing fabric pilling by using image-analysis techniques. Part II: Comparison with visual pill ratings. *Journal of the Textile Institute*, 89(1), 96-105.
16. Abril HC, Garcia-Verela MSM, Moreno YMT, Navarro RF. 1998. Automatic method based on image analysis for pilling evaluation in fabrics. *Optical Engineering*, 37(11), 2937-2948.
17. Kang TJ, Cho DH, Kim SM. 2004. Objective evaluation of fabric pilling using stereovision. *Textile research journal* 74(11), 1013-1017.

-
- 18. Kim SC, Kang TJ. 2005. Image analysis of standard pilling photographs using wavelet reconstruction. *Textile Research Journal* 75(12), 801-811.
 - 19. Behera BK, Madan Mohan TE. 2005. Objective measurement of pilling by image processing technique. *International Journal of Clothing Science and Technology* 17(5), 279-291.
 - 20. Zhang J, Wang X, Palmer S. 2007. Objective pilling evaluation of wool fabrics. *Textile Research Journal* 77(12), 929-936.
 - 21. Telli A, Özkan İ. 2018, October. The Objective Evaluation of Pilling Tendency of Knitted Fabrics Through Digital Image Processing, ITTC- 7th International Technical Textiles Congress. 309-312.
 - 22. Telli A, Özkan İ. 2018. Objective Measurement of Pilling Resistance in Knitted Fabrics with Image Processing Techniques. *Journal of Textiles and Engineer* 25(112), 313-318.
 - 23. Xin B, Hu J, Yan H. 2002. Objective evaluation of fabric pilling using image analysis techniques. *Textile Research Journal* 72(12), 1057-1064.